CHARACTERIZING THE IMMUNOMODULATORY EFFECTS OF THE ANTIOXIDANT TEMPOL IN A MODEL OF MULTIPLE SCLEROSIS

by

Sarah Elizabeth Neil

B.Sc., The University of British Columbia, 2007

A THESIS SUBMITTED IN PARTIAL FULFILLMENT OF
THE REQUIREMENTS FOR THE DEGREE OF

MASTER OF SCIENCE

in

The Faculty of Graduate and Postdoctoral Studies

(Pathology and Laboratory Medicine)

THE UNIVERSITY OF BRITISH COLUMBIA
(Vancouver)

October 2013

Abstract

Background: Reactive oxygen and nitrogen species are implicated in inflammatory-mediated damage to the central nervous system in multiple sclerosis (MS) and an animal model of the disease, experimental autoimmune encephalomyelitis (EAE). We have shown that oral administration of the antioxidant TEMPOL (4-hydroxy-2,2,6,6-tetramethylpiperidine-N-oxyl), a stable nitroxide radical, lowers incidence and reduces severity of disease in EAE. We hypothesize that TEMPOL limits inflammatory demyelinating disease by regulating the development of pathogenic immune responses that influence immune cell activation, including T cell and antigen presenting cell phenotypes and function. **Methods:** Immune responses were compared between control and TEMPOL-fed EAE or healthy mice by examining differences in proliferation, population distribution, surface marker expression, and cytokine production in immune cells isolated from lymphoid organs. The effect of added TEMPOL on immune cell proliferation and phenotype was also studied *in vitro* using mixed lymphocyte reactions (MLR) with human or mouse cells, and in isolated murine lymphoid cell cultures stimulated with anti-CD3. **Results:** TEMPOL-fed animals exhibit comparable levels of myelin-reactive T cells versus controls, but show reduced production of the pro-inflammatory cytokines interferon gamma, tumor necrosis factor alpha, and transforming growth factor-beta 1. Flow cytometry showed enrichment of CD8+ over CD4+ T cells in lymphoid tissues of TEMPOL-fed EAE mice, as well as decreased MHC II and increased CD80 and CD86 expression in myeloid cells and myeloid dendritic cell (DC) populations. Enrichment of Foxp3+ regulatory T cells was also observed in lymph nodes with TEMPOL. *In vitro*,

TEMPOL was found to enhance proliferation of lymphoid cells in mouse MLR or when stimulated with anti-CD3 in a dose-dependent manner. Human MLR experiments also showed enhanced cell proliferation and enrichment of CD8 T cells in the presence of TEMPOL. Adding TEMPOL to cell cultures decreased expression of MHC II, CD80, and CD86 in splenic myeloid cells and myeloid DCs.

Conclusions: These studies suggest that TEMPOL is not globally immunosuppressive, but instead alters the phenotype of antigen-specific or autoreactive immune cells generated *in vivo*, reducing the pro-inflammatory nature of immune responses in EAE. These immunomodulatory properties contribute to TEMPOL's potential as an efficacious therapeutic in MS.

Preface

Animal data shown in Chapter 1 (Figure 1.3) represent experiments performed at the National Institutes of Health and are unpublished, but are included in a patent application held by Dr. Jacqueline Quandt and collaborators (PCT/US08/73007; filed Aug 13, 2008 [priority to USPPA 60/955,731], entitled "Method of Treating Disease Involving Myelin and/or Axonal Loss." Inventors: Lead: Jacqueline Quandt, James Mitchell, Anastasia Sowers, Murali Krishna). This patent is also listed as a relevant interest of Dr. J Quandt. All experiments were carried out in compliance with the Guide for the Care and Use of Laboratory Animals and approved by the National Institute of Neurological Disorders and Stroke at the National Institutes of Health.

Dr. Quandt performed all work involving live mice that is described in Chapters 3 and 4, including EAE induction, scoring, and euthanasia. Once euthanized, spleens and lymph nodes were collected by either Dr. Quandt, the author, or other members of the Quandt laboratory (Dr. Lixin Zhou, Dr. Daphne de Launay, Ms. Elena Cavazzi, Mr. Andrew Leung). Dr. Quandt and other lab members also provided assistance with tissue processing and cell culture setup during some of these experiments. All animal work was approved by the UBC Animal Care Committee (certificate #A09-0453). Cell culture work with biohazardous materials was performed with approval from the UBC Biosafety Committee (certificate #B09-017) and radioactivity with approval from the UBC Radiation Safety Committee (certificate #PATH-3226-15).

MOG IgG ELISA experiments described in Chapter 3 were performed entirely by Ms. Victoria Baronas. Figure 3.6 was modified from a figure that Ms. Baronas previously created from her own data. Statistical analysis was done by the author. Ms. Baronas also performed some replicates of cytokine ELISA experiments, but data analysis was done by the author.

Live/dead cell assays described in Chapter 4 were performed by both Ms. Cavazzi and the author. The representative graphs shown in Figure 4.1 are modified from a figure that was originally prepared by Ms. Cavazzi.

Human mixed lymphocyte reaction experiments described in Chapter 4 were performed in the laboratory of Dr. Mark Scott, with the supervision and guidance of Dr. Dan Wang. Dr. Wang arranged for the collection of blood from consenting volunteer donors, and experiments were completed by both Dr. Wang and the author working together. Subsequent data analysis was done entirely by the author. Work with human blood samples in Dr. Scott's laboratory was approved by the UBC Clinical Ethics Research Board (certificate #H02-70215) and the UBC Biosafety Committee (certificate #B10-0026).

Otherwise, this thesis represents original, unpublished work performed by the author, Ms. Sarah Elizabeth Neil.

Table of Contents

List of Tables

List of Figures

List of Abbreviations

ANOVA	Analysis of variance
APC	Antigen presenting cell
BBB	Blood-brain barrier
BCA	Bicinchoninic acid
BSA	Bovine serum albumin
CD	Cluster of differentiation
CFSE	Carboxyfluorescein succinimidyl ester
CNS	Central nervous system
ConA	Concanavalin A
CTLA-4	Cytotoxic T-Lymphocyte Antigen 4
DC	Dendritic cell
DMT	Disease-modifying therapy
EAE	Experimental autoimmune encephalomyelitis
ELISA	Enzyme-linked immunosorbent assay
FACS	Fluorescence-activated cell sorting
FBS	Fetal bovine serum
FDA	Food and Drug Administration
GM-CSF	Granulocyte-macrophage colony-stimulating factor
HC	Health Canada
HLA	Human leukocyte antigen
IFNγ	Interferon gamma
IL	Interleukin
IM	Intramuscular
IV	Intravenous
MFI	Median fluorescence intensity
MHC	Major histocompatability complex
MLR	Mixed lymphocyte reaction
MOG	Myelin oligodendrocyte glycoprotein
MS	Multiple sclerosis
MWRS	Mann-Whitney Rank Sum test
PBMC	Peripheral blood mononuclear cell
PBS	Phosphate-buffered saline
PML	Progressive multifocal leukoencephalopathy
PPMS	Primary-progressive multiple sclerosis
PRMS	Progressive-relapsing multiple sclerosis
RNS	Reactive nitrogen species

ROS	Reactive oxygen species
RPMI	Roswell Park Memorial Institute
RRMS	Relapsing-remitting multiple sclerosis
SDS	Sodium dodecyl sulfate
SDS-PAGE	Sodium dodecyl sulfate polyacrylamide gel electrophoresis
SI	Stimulation index
SPMS	Secondary-progressive multiple sclerosis
SQ	Subcutaneous
TBS	Tris buffered saline
TBS-T	Tris buffered saline with Tween 20
TCR	T cell receptor
TEMPOL	4-hydroxy-2,2,6,6-tetramethylpiperidine-N-oxyl
TGF-β1	Transforming growth factor beta 1
TMB	3,3',5,5'-Tetramethylbenzidine
TNFα	Tumor necrosis factor alpha
T_{reg}	Regulatory T lymphocyte

Acknowledgements

First and foremost, I would like to thank my supervisor, Dr. Jacqueline Quandt for her guidance and support over the last few years. I greatly appreciate her dedication to her lab, as well as her patience and sense of humour. As well, I would like to thank the other members of the Quandt lab, past and present, for their ongoing support – both technical and moral.

Many thanks are also owed to Dr. Mark Scott, the chair of my supervisory committee, for providing valuable feedback and allowing me to make use of his laboratory for some experiments. I would also like to thank Dr. Dan Wang in Dr. Scott's laboratory for his technical expertise and eagerness to help make those experiments a success. Thank you also to my supervisory committee – Dr. Cheryl Wellington and Dr. Marc Horwitz – for their helpful suggestions and input throughout this project.

Thank you also to the Department of Pathology and Laboratory Medicine, and the Faculty of Medicine for providing much-appreciated scholarship awards. Much of the research described in this thesis was supported by the Alistair M. Fraser Studentship award, which was generously provided by the Multiple Sclerosis Society of Canada.

Last but not least, my thanks to the endMS Research and Training Network for providing me with a travel award, as well as countless valuable training and networking opportunities.

For Leila.

Chapter 1: Introduction

1.1 Multiple sclerosis

1.1.1 Overview and history

Multiple sclerosis (MS) is a chronic inflammatory-mediated demyelinating and neurodegenerative disease of the central nervous system (CNS) [1]. Primarily diagnosed in early adulthood, MS is one of the most common and debilitating neurological diseases of young adults in North America [2]. While historical evidence suggests that MS may have been observed as early as the 14th century, Jean Cruveilhier is credited as being the first to document the clinical features of the disease in 1841 [3]. Around the same time, Robert Carswell provided illustrations of sclerotic lesions and atrophied tissue in the CNS, but neither Cruveilhier nor Carswell attributed their observations to a unique disease [3]. Eventually, in 1868, Jean-Martin Charcot correlated the clinical presentation of the disease with his observations of pathological changes in the CNS, identifying the illness as a distinct disease that he named “la sclérose en plaques” [4].

1.1.2 Symptoms and disease course

In MS, localized episodes of demyelination and axonal loss lead to the development of what are called “plaques” or “lesions” in the CNS [5]. The symptoms of MS vary greatly between patients, as they are largely dependent on the location of CNS damage, and lesions may also be asymptomatic [5]. Symptoms often occur suddenly and with no warning. Lesions in the cerebrum can cause cognitive dysfunction and depression; damage to the cerebellum results in tremor and poor

balance; spinal cord damage may cause weakness, muscle spasms, bladder dysfunction, and constipation; and brainstem lesions produce double vision and impaired speech [5]. Generalized symptoms of pain, weakness, and fatigue are also common [5], with severe fatigue often described by patients as their most debilitating symptom [6].

The course of disease in MS is highly variable and unpredictable, but can be characterized by four clinical subtypes (Figure 1.1). 85% of patients first exhibit a relapsing-remitting (RRMS) disease course, which is characterized by repeating episodes of disability (relapses), followed by total or partial recovery [7]. The majority of patients with RRMS ultimately progress to a secondary-progressive (SPMS) disease course, where recovery from relapses is limited and permanent disability increases [7]. A smaller percentage (10%) of patients have a primary-progressive (PPMS) disease, where a steady increase in disability occurs from onset without recovery [7]. An even smaller number (~5%) of patients exhibit progressive-relapsing (PRMS) disease, where steadily increasing disability is combined with distinct acute relapses [7].

1.1.3 Epidemiology

MS affects more than 2.5 million people worldwide [8]. MS is generally more common in the northern hemisphere, but prevalence is observed to increase with latitude both north and south of the equator [9].The prevalence of MS in Canada is estimated to be in the range of 55 to 240 people per 100,000, one of the highest rates of MS in the world [10]. The MS Society of Canada estimates that three more

Canadians are diagnosed with MS every day. Within Canada, geographical differences in prevalence of MS have been observed, with one study observing a lower prevalence (180 per 100,000) in Quebec and a higher prevalence in British Columbia (240 per 100,000) and the Prairie provinces (340 per 100,000) [10]. Increasingly more females are diagnosed with MS than males, with the sex ratio in Canada currently exceeding 3.2:1 [11]. The MS Society of Canada estimates that the cost of MS to the Canadian economy is over $1 billion per year.

1.1.4 Etiology

The precise cause of MS is unknown, but it is widely regarded to be an immune-mediated disease that develops from a combination of genetic susceptibility and environmental factors. While MS is not completely hereditary, there is significant evidence that genetics plays a key role. For someone who has a first-degree relative with MS, the risk that they will develop the disease themselves is increased over 20 fold compared to the general population [12]. However, this elevated risk is not present for individuals who are adopted into a family with an affected relative [13]. Further, monozygotic twins show concordance rates of 25 to 30%, versus a 4% rate found in dizygotic twins [12].

Rather than being caused by mutations, MS appears to be polygenic, stemming from a particular combination of normal polymorphisms [13]. Studies suggest an association between the major histocompatability complex (MHC) class II alleles (known in humans as the human leukocyte antigen, or HLA) HLA-DR15 and -DQ6, with the genotypes -DRB1*1501, -DRB5*0101, -DQA1*0102, and -

DQB2*0602 [5]. The HLA system is an immune-associated gene family that encodes antigen-presenting proteins, and also plays a role in recognition of self-antigens. This link is observed in most populations, but is strongest in northern European groups [5]. A different linkage is seen within some Mediterranean groups, where the allele -DR4 is most strongly associated with MS [5]. More recent genome screening studies also suggest that increased susceptibility may be associated with single nucleotide polymorphic markers for interleukin (IL)-2 and IL-7 receptor alpha chains, and that there may be a protective effect given by the MHC class I alleles HLA-A*02, HLA-B*44, and HLA-C*05 [14] [5] [15]. However, the specific manner in which these MHC genes contribute to disease susceptibility remains unknown.

Because genetics do not fully explain how a person develops MS, some particular combination of environmental triggers may also be at play. This is supported by data from migration studies, which suggest that immigrants from areas with low rates of MS who move to areas with a high prevalence of MS retain the lower risk of their country of origin [16]. Conversely, people who move from lower risk areas to higher risk areas maintain a risk of disease that is generally intermediate. Age may also be a factor in this observation – some studies suggest that younger immigrants (under 15 years) are more likely to experience decreased risk when moving to countries where MS rates are lower, which older immigrants experience less risk reduction [16].

Numerous environmental factors have been studied for their influence on MS risk, including diet, climate, stress, occupation, vaccination, and history of infections – yet few have provided definitive results. The fact that MS is most common in

countries with colder climates has made sunlight exposure, and subsequently vitamin D intake, particularly popular areas of research. Pre-2000s research on sun exposure had varying results, with separate studies showing an inverse relationship, a correlation, or no effect at all of sun exposure on MS risk [16]. More recent studies, performed in several different countries, more consistently suggest that the risk of MS is increased in people who have less exposure to sun [16]. The issue of age of exposure is highlighted in one Australian study, which found a connection between increased sun exposure during childhood and a decreased risk of MS [17]. In Canada, a month of birth effect was observed on MS incidence – significantly fewer RRMS patients are born in November while significantly more are born in May [18]. This suggests that environmental effects during gestation may play a role, with May babies developing during winter months when mothers have limited sun exposure [18].

Relevant properties of ultraviolet light exposure include its immunosuppressive effects, and increased production of vitamin D in the skin [16]. The effects of vitamin D – and specifically, 1,25-dihydroxyvitamin D3, its active metabolite – on MS risk have also been investigated in depth. While vitamin D is largely associated with bone health, it has also been shown to play a key role in immune system function. Lymphocytes, particularly CD8+ T cells, have been found to have high amounts of vitamin D receptors [19]. Vitamin D compounds have also been shown to be effective in blocking development of autoimmune diseases in animal models, though only in conjunction with high calcium intake [19].

One study determined that vitamin D regulates expression of the MS-associated MHC class II allele HLA-DRB1*1501, by way of a vitamin D response element in its promoter region [20]. The authors suggest that vitamin D deficiency early in development could lead to autoreactive T cells escaping deletion in the thymus, increasing the risk of autoimmune disease in individuals with the HLA-DRB1*1501 allele. Studies so far support the idea that vitamin D has a protective effect on the risk of MS. One study in the United States observed a 40% reduction in MS risk in women who took a vitamin D supplement or multivitamin [21]. Another study found that higher levels of circulating vitamin D was associated with a lower risk of MS, though only in Caucasians – no effect was observed in African-American or Hispanic participants [22].

Researchers have studied the link between MS and numerous childhood or adolescent infections, including measles, mumps, rubella, and chickenpox. One of the more commonly cited potential risk factors is infection with Epstein-Barr virus (EBV). EBV affects 90% of the general population, with a similar global distribution to that of MS [23]. While it is usually asymptomatic in children, it often causes infectious mononucleosis in adolescents and adults [23]. Upon infection with EBV, virus/antigen-specific T cells are expanded, persisting at high levels for several years. Long-term, EBV infection establishes a lifelong latent infection of B cells [23]. Studies have shown that people with MS are significantly more likely to report a previous infection with infectious mononucleosis than healthy controls [24]. Additionally, nearly 100% of MS patients are found to be seropositive for EBV-

specific antibodies, compared to 90-95% of controls [25]. However, the role that EBV infection plays in the development of MS remains unclear.

There is significant evidence that MS is an immune-mediated disease. As described above, there is a demonstrated link between MS and HLA alleles, with over 50% of the risk of developing MS being attributed to HLA genes [16]. In addition, MS can be effectively treated by immunomodulatory or immunosuppressive therapies, though the fact that these therapies do not completely stop disease progression suggests that there is also a role for non-immune mechanisms [26]. MS also shares many similarities with experimental autoimmune encephalomyelitis (EAE), which is an inducible animal model of autoimmune disease where clinical disease is specifically attributed to myelin-specific autoreactive T cells [16] [27].

1.1.5 Experimental autoimmune encephalomyelitis

Much of what we believe about the pathogenesis of MS stems from research that utilizes the animal model of the disease, EAE. EAE is an inducible inflammatory demyelinating disease with symptoms that are similar to MS. Upon induction of disease, activated T cells travel to the CNS, where they encounter myelin and initiate an inflammatory response [28]. There are many variants of EAE, involving different animal species (typically rodents, but studies have also extended to non-human primates), genetic backgrounds, target auto-antigen, and methods of disease induction. By altering these factors, numerous EAE models have been created able to mimic different presentations and aspects of MS, but currently no single model perfectly imitates the disease [29].

In the classic rodent EAE model, the disease presents as an ascending paralysis that begins with a limp tail and spreads to hind and forelimbs [30]. Lesions in this model are typically localized to the spinal cord, in contrast to MS where lesions are located in both the brain and spinal cord [30]. Atypical forms of EAE also exist, which can involve rotatory or other symptoms that develop largely from lesions in the brain or brainstem [31]. Researchers will usually assess the severity of disease in EAE using a scoring system, generally a 5- or 10-point scale where 0 is equated with no disease symptoms.

The many types of EAE generally fall into one of three categories: actively-induced, passively-induced/adoptive-transfer, and spontaneous/transgenic models [32]. Active EAE is induced by direct injection of self-antigens. The earliest models of active EAE involved injection of crude CNS homogenates, later supplemented by Freund's adjuvant to boost the humoral immune response [33]. More recent evolutions of this method make use of specific antigens, from myelin proteins (myelin basic protein [MBP], myelin oligodendrocyte glycoprotein [MOG], proteolipid protein) to neuronal membrane proteins, and the addition of pertussis toxin to open the blood-brain barrier (BBB) [33]. This has given rise to active EAE variants that can model a range of MS components, from relapsing-remitting cycles to specifically-located CNS lesions [33]. The experiments described in this thesis utilize an active EAE model, induced in C57BL/6J mice by immunization with amino acids 35-55 of MOG peptide (MOG 35-55) and mycobacterium H37Ra in incomplete Freund's adjuvant, with pertussis toxin in phosphate buffered saline (PBS) given

intraperitoneally on the first day and two days later. This results in a chronic-progressive model of disease, observable 10 to 14 days post-induction.

Passive or adoptive-transfer EAE models were first created by transferring activated total lymph node cells, and later pathogenic antigen-specific T cell lines, into naïve rats or mice [34]. This model allows researchers to more closely study the effector stage of disease by monitoring the cells involved – for example, T cells can be labelled *in vitro* before being transferred into the naïve animal, to track their activity *in vivo* [30]. More recently, models of EAE where disease develops spontaneously have been created using transgenic animals, more closely mimicking how MS develops in humans [29]. These include transgenic mice expressing T cell receptors that are specific for MOG 35-55 [35] or an immunoglobulin chain specific for MOG [36], and even humanized transgenic mice that have been generated to express HLA-DR15 alleles with an MBP-specific T cell receptor isolated from an MS patient [37]. The disease that develops replicates numerous features of MS, including demyelination and axonal degeneration [29].

EAE was first discovered in the 1930s, first originating as a model for acute disseminated encephalomyelitis rather than MS [38]. Since then, EAE has evolved considerably, and has served as a valuable model for thousands of studies in MS [38]. Three MS therapies have been successfully brought to market after first showing promise in MS (glatiramer acetate, mitoxantrone, and natalizumab), and more are currently showing promise in clinical trials [1] [38]. However, the use of EAE as a model for MS is not without controversy. A number of drugs that ameliorate EAE have no effect on MS, and some are even observed to exacerbate

disease [1]. Still, research in EAE has led to numerous advances in our understanding and treatment of MS, and the model remains a valuable resource when used in conjunction with human-based studies [38].

1.1.6 Pathogenesis

The mechanism that has been proposed for MS pathogenesis is largely modeled on what is observed in EAE [26]. It is suggested that MS first begins with activation of myelin-reactive T cells in the periphery, as activated myelin-reactive T cells have been found in the blood and cerebrospinal fluid of patients with MS, and have been observed in all four MS subtypes [39]. These cells then cross the BBB to enter the CNS, where they become reactivated and initiate an inflammatory immune response [26]. Other immune cells are recruited, producing cytokines, reactive oxygen species, and other mediators of inflammation, initiating processes that lead to demyelination, axonal damage, and ultimately loss of neurons [26]. Macrophages are thought to play an important role in this process, as they phagocytose myelin, act as antigen-presenting cells (APCs), and are known to produce a number of inflammatory mediators [40].

The BBB is the interface between blood and brain tissue, composed of the specialized endothelial cells of cerebral blood vessels [41]. These endothelial cells lack the fenestrations that are typical of non-brain endothelial cells, instead expressing tight junction complexes and specialized transport proteins [41]. This creates a highly restrictive barrier that carefully regulates the passage of substances in and out of the CNS. The BBB is also supported by the basal lamina, along with

astrocytes, and pericytes [41]. The BBB is not ubiquitous throughout the brain – circumventricular organs are specialized areas within the brain that are characterized by their lack of a BBB, and are localized to the surface of the ventricles [42]. These regions are permeable to peptides and hormones, allowing an exchange of signals between the blood and the brain, and play an important role in neuroendocrine functions and the maintenance of homeostasis [43].

Normally, the BBB limits the entry of immune mediators into the CNS, and is not supportive of the leukocyte homing and trafficking that are characteristic of immune organs or other parts of the body. However, research has suggested that the microvasculature forming this barrier becomes compromised in MS, allowing for increased access of cells and mediators to the CNS. Proposed mechanisms for increased BBB permeability in people with MS include chemokine gradients, infection-induced upregulation of adhesion molecule expression, and loss of tight junction proteins [41].

T cell activation in the periphery requires the contributions of two activation signals. The first signal occurs when a T cell receptor (TCR) recognizes a cognate antigen that is bound to an MHC molecule on the surface of an APC [39]. The MHC class I (MHC I) complex is used in activation of cluster of differentiation (CD)8+ T cells, while the MHC class II (MHC II) complex activates CD4+ T cells. APCs can be characterized as professional or non-professional, where professional APCs constitutively express MHC II, while non-professional APCs only express MHC II when stimulated by certain cytokines [31]. Professional APCs include myeloid and

lymphoid dendritic cells (DCs), macrophages, and B cells. Non-professional APCs include endothelial cells and glial cells.

The second signal is provided when additional surface molecules on the T cell interact with molecules on the APC to provide co-stimulatory signals [39]. Together, these signals can induce a cascade of events that may drive the T cell to proliferate and differentiate, secreting cytokines and other effector molecules to activate additional components of the adaptive immune system [26]. Without the second signal, interaction between the TCR and the antigen-MHC complex induces the T cell to enter a non-responsive (anergic) state, or perhaps even to die, effectively inhibiting an immune response. Further, the action of co-stimulatory molecules themselves can be either positive or negative, inducing or inhibiting activation [39].

This key role for co-stimulatory molecules makes them an important subject of research, both for their function in disease development and their potential as drug targets. A particularly well-studied interaction is the B7-1/2-CD28/ Cytotoxic T-Lymphocyte Antigen 4 (CTLA-4) co-stimulatory pathway. B7-1 (CD80) and B7-2 (CD86) are expressed on the surface of B cells, macrophages, and APCs, and interact with CD28 and CTLA-4 expressed by T cells. CD28 is expressed by naïve T cells, and produces a positive signal to induce IL-2 production, activate T cell proliferation, and regulate cytokine production. In contrast, CTLA-4 is expressed by activated T cells and invokes an inhibitory signal to stop the immune response [39]. Three particular polymorphisms of the *CTLA4* gene have been observed in MS patients, but not in healthy controls [44]. Further, studies have showed that CD80

expression on T and B cells is increased in progressive disease and during relapses [39]. However, the specific role of this pathway in MS remains unknown.

The co-stimulatory molecule CD40, which is expressed on DCs, macrophages, astrocytes, and endothelial cells, interacts with CD154 (CD40L) on the surface of activated T cells [39]. The interaction of CD40 and CD40L plays a key role in induction of B cell proliferation by T cells, but has also been implicated in a number of inflammatory diseases [45]. In MS, it has been suggested that CD40 plays a role in increasing BBB permeability, being expressed by inflamed endothelium and increasing expression of adhesion molecules upon ligation [45]. CD40 may also be involved in the production of auto-antibodies in the CNS, or in macrophage activity [45]. However, like the CTLA-4 pathway, the specific function of CD40 in MS pathogenesis is still not clear.

When T cells are activated, the immune response profile that is generated can be specifically tailored to the situation at hand, by the release of signalling cytokines by APCs. This has been referred to as a third signal in the lymphocyte activation pathway [46]. CD4+ T cells can differentiate into T helper (T_H) cells, which further shape the immune response by releasing their own cytokines to activate and direct other immune cells. In the presence of IL-12 and IL-32, CD4+ T cells will become T_H1 cells, which produce interferon gamma (IFNγ), IL-2, and tumor necrosis factor alpha (TNFα), and initiate an inflammatory response [47]. T_H1 cells play a key role in cell-mediated immunity and the response to viral infections, by activating macrophages and cytotoxic CD8+ T cells. When IL-12 and IL-32 are absent and IL-4 is present, CD4+ T cells will differentiate into T_H2 cells, which produce IL-4 and IL-5

[47]. T_H2 cells assist B cells in the response to extracellular pathogens such as parasites. IL-6 and transforming growth factor beta 1 (TGF-β1) induce CD4+ T cells to differentiate into T_H17 cells, which produce IL-17. T_H17 cells help to defend against extracellular bacteria and fungi, but can also mediate autoimmune disease [48].

In addition to the T_H cell family, CD4+ T cells can also differentiate into regulatory T (T_{reg}) cells. This occurs in the presence of TGF-β1. T_{reg} cells, which are characterized by expression of the transcription factor forkhead box P3 (Foxp3) and the IL-2 receptor molecule CD25, produce TGF-β1 and IL-10 [49]. IL-10 has numerous immunosuppressive properties, and is a major contributor to the regulatory function of another class of regulatory cells, Tr1, which produce significant amounts of IL-10 [50]. As their name suggests, T_{reg} cells have an immunosuppressive function, regulating the immune response. T_{reg} cells also play a key role in tolerance to self-antigens, and help to prevent autoimmune disease [51].

Abnormal regulation of T_H1 and T_H17 responses have been shown to be pathogenic in EAE and MS [26]. It has also been suggested that a T_H1 or T_H17 response in MS could be pro-inflammatory, and therefore damaging, while a T_H2 response could be protective [26]. Therefore, therapies that shift the immune response towards a T_H2 type, or promote a T_{reg} response, would potentially be effective in limiting disease. This is one potential mechanism of action for the drugs glatiramer acetate and interferon-beta, which are both therapeutics that have been approved for use in MS [26].

1.1.7 Oxidative damage

Reactive oxygen (ROS) and nitrogen (RNS) species are highly reactive molecules with unpaired elections, and are regularly generated as by-products of the body's normal metabolic processes [52]. Normally, these free radicals are neutralized by antioxidant enzymes and do not cause significant harm, and minor damage is easily repaired [53]. However, when ROS and RNS are produced in excess, they can interact with lipids, proteins, and DNA in a process called oxidative damage or oxidative stress [52]. Oxidative damage is known to occur during an inflammatory response, where ROS and RNS such as hydrogen peroxide, nitric oxide, and superoxide are produced in excess by macrophages and microglia [54].

The CNS is particularly susceptible to oxidative damage. The brain is active in oxidative metabolism, which generates high levels of superoxides, and antioxidant defences are low [55]. As well, the brain contains high levels of readily peroxidizable fatty acids, and localized high levels of iron that can react with ascorbate to create a strong pro-oxidant [55]. Beyond these localized factors, some protection to the CNS is afforded by the BBB, which largely restricts entry of immune mediators and is not supportive of immune surveillance of other organs such as lymph nodes. However, ROS are capable of activating signalling pathways that can permeabilize the BBB, promoting trafficking of leukocytes into the CNS [56]. Once leukocytes enter the CNS, their production of ROS and RNS induces myelin phagocytosis by macrophages, oligodendrocyte damage, damage to axons, and loss of neurons [57] [58] [59].

There is significant evidence that oxidative stress in the CNS is one of the major contributors to ongoing tissue damage in MS [52]. Within active lesions in the CNS, markers of oxidative damage to proteins, nucleotides, and lipids can be observed [60] [61]. As well, there is increased expression of antioxidant enzymes, suggesting an effort to control oxidative damage [60] [62] [63]. While much of the oxidative damage in MS is attributed to inflammation, it is notable that disease progression occurs even when inflammation is suppressed (for example, by the administration of monoclonal antibody therapies) [64]. Mitochondrial dysfunction has been suspected as a key contributor to neurodegeneration in MS, as mitochondria are significant producers of ROS by oxidative phosphorylation, and considerable evidence for this has been shown [64]. The demyelination and axonal injury that are observed in MS lesions bear much similarity to white matter lesions that occur after stroke, suggesting that cells may be deprived of energy in a manner similar to what occurs when blood flow to cells is occluded [65]. As well, immunohistochemical studies of respiratory chain proteins in active MS lesions have indicated the presence of significant mitochondrial injury [65].

1.1.8 Current therapies

Currently, no cure for MS exists, but increasingly more therapeutic agents are becoming available to patients. In 1993, the only approved MS drug available to patients was interferon beta-1b (Betaseron) [66]. As of 2013, there are now ten major disease-modifying therapies (DMTs) approved by the United States Food and

Drug Administration (FDA) for use in treating MS (Table 1.1) [67]. Health Canada (HC) also approves eight of these DMTs for use in Canada.

All approved DMTs are variably effective in reducing relapse rates and slowing disease progression in relapsing forms of MS. At this time, no effective therapy is available for the treatment of PPMS [67]. Since DMTs do not alleviate pre-existing MS symptoms, medications and other therapies are also available to patients to treat fatigue, pain, spasticity, walking difficulties, tremor, depression, and other symptoms [67]. During an MS relapse, high doses of IV corticosteroids have been shown to speed recovery, but they do not affect the degree to which the patients recovers [67].

Despite the steadily increasing availability of MS DMTs, no “perfect drug” has yet been approved – a drug that is maximally effective, safe, and easy for patients to take. All current MS therapies have unpleasant and often unsafe side effects, and most are very expensive, with the MS Society of Canada estimating the cost of DMTs to range from $20,000 to $40,000 per year. Further, patients are currently faced with compromises between efficacy, safety, and ease of administration. For example, interferon-beta formulations and glatiramer acetate are widely used as first-line therapies for MS, but while they are usually well-tolerated with generally manageable side effects, they all require self-injection at least once per week, and reduce relapse rates by only 30% [66]. In comparison, natalizumab is observed to reduce relapse rates by almost 70% and is administered monthly by IV, but it is linked to an increased risk of progressive multifocal leukoencephalopathy (PML), an opportunistic viral disease that is usually fatal in immunocompromised patients [66].

While people with MS have increasingly more treatment options available to them, all current treatment options and the majority of those in development are immunomodulatory or immunosuppressive, focusing on limiting inflammation early in disease [66]. These DMTs are most useful early in relapsing-remitting disease, when inflammation is most intense, becoming ineffective when disease progresses into SPMS [68]. Ideally, future therapies would include neuroprotective agents that limit neurodegeneration, and ultimately enable repair to damaged neurons [66] [68].

1.2 TEMPOL

TEMPOL (4-hydroxy-2,2,6,6-tetramethylpiperidine-N-oxyl) is a stable, water-soluble cyclic nitroxide radical [69] (Figure 1.2). TEMPOL was originally used as a biophysical probe in electron paramagnetic resonance spectroscopy, when it was discovered that many such nitroxide probes had anti-oxidant properties *in vitro* [69]. This led to studies on nitroxides as protectants against radiation, and the finding that TEMPOL was capable of protecting cells against aerobic radiation cytotoxicity [69]. With a low molecular weight of 172.24, TEMPOL is membrane-permeable and capable of crossing an intact BBB into the CNS [70]. TEMPOL is a superoxide dismutase mimetic, and is capable of scavenging both intracellular and extracellular superoxide anions [71]. TEMPOL also inhibits the Fenton reaction by reducing intracellular concentrations of Fe^{2+}, thereby limiting the formation of hydroxyl radicals [71]. Studies with TEMPOL have shown that it has beneficial effects in a variety of disease models, including animal models of shock, pancreatitis, hypertension, diabetes, and traumatic brain injury [70] [72]. TEMPOL has also been

shown to limit weight gain and prevent tumour formation in mice, both of which may contribute to their observed longer life spans [73].

TEMPOL, delivered by intraperitoneal injection, was previously found to ameliorate disease [74]. Within this study, preservation of the BBB and a reduction in infiltration of macrophages into the CNS were observed in mice given TEMPOL. As well, these researchers demonstrated decreased tissue levels of markers of inflammation, including transcription of TNFα and IFNγ. However, the mechanisms by which these anti-inflammatory and neuroprotective properties occur were not elucidated.

A number of studies on TEMPOL have been performed using animal and *in vitro* models, but research on TEMPOL in humans is comparatively limited. In 2000, a Phase I efficacy study was done to determine the effect of a TEMPOL/ethanol solution on alopecia during whole-brain radiation therapy. TEMPOL was found to be well-tolerated by patients with no adverse effects, and significantly limited radiation-induced hair loss [75]. Following the success of this study, the same research group initiated a Phase II study using a 7% TEMPOL topical gel formulation, but results have yet to be published.

The Quandt lab has shown that TEMPOL-based feed lowers the incidence and reduces the severity of disease in a murine EAE model (unpublished data, Figure 1.3). TEMPOL is capable of limiting disease when given prophylactically, before induction of EAE (Figure 1.3 A); and therapeutically, after the onset of EAE symptoms (Figure 1.3 B). In our studies, TEMPOL is administered orally, incorporated into chow at 10 g/kg, as this dosage was previously demonstrated to

be well-tolerated by mice [73]. An interest in non-injectable MS therapies was a driving factor in the decision to employ orally-delivered TEMPOL in these studies. Levels of TEMPOL in the blood of TEMPOL-fed EAE mice range from 10 to 60 μM, measured using electron spin resonance (unpublished results). *In vivo*, TEMPOL exists almost exclusively in its reduced (hydroxylamine) form, TEMPOL-H. TEMPOL-H itself is also an efficacious antioxidant, and can be rapidly oxidized back to TEMPOL *in vivo* under the appropriate conditions [76]. The different forms of TEMPOL allow it to reversibly interact with a wide range of biologically diverse oxidants and reductants both *in vivo* and *in vitro* [77].

Taken together, the research on TEMPOL suggests that it has the potential to be an effective and desirable therapeutic in MS. Administered orally, TEMPOL would help to fill the need for an MS therapy that is safe, effective, and easy for patients to take.

1.3 Hypothesis

We hypothesize that TEMPOL limits inflammatory demyelinating disease by regulating the development of pathogenic immune responses that influence immune cell activation and pathogenicity. Specifically, the work described in this thesis was performed to address the following three specific aims:

1. To determine the effect of TEMPOL on T cell activation and proliferation.
2. To determine TEMPOL's influence on the generation of immune cell populations *in vivo.*

3. To study the effect of TEMPOL on co-stimulatory molecule expression as an indicator of antigen presenting capacity and immune cell activation.

Brand name	Chemical name	Mechanism	Adverse Effects	Dosage	Approval
Avonex	Interferon beta-1a	Limits inflammatory immune cell activity	Injection site reactions, flu-like symptoms, depression, liver and thyroid problems	IM, once weekly	FDA/HC
Rebif				SQ, 3 times weekly	
Betaseron	Interferon beta-1b			SQ, every other day	
Extavia					
Copaxone	Glatiramer acetate	Simulates myelin basic protein, suppresses inflammatory response	Injection site reactions, lipoatrophy, heart palpitations, anxiety	SQ, daily	FDA/HC
Gilenya	Fingolimod	Sphingosine 1-phosphate receptor modulator, retains lymphocytes in lymph nodes	Headache, diarrhea, back pain, infections, macular edema, harm to fetus	Oral, daily	FDA/HC
Tecfidera (BG12)	Dimethyl fumarate	Anti-inflammatory and neuroprotective properties	Flushing, diarrhea, stomach cramps, reduced white blood cell counts	Oral, twice daily	FDA/HC
Tysabri	Natalizumab	Blocks α4 integrins, prevents entry of T cells into CNS	Infections, allergic reactions, fatigue, PML	IV, every 4 weeks	FDA/HC
Novantrone	Mitoxantrone	Inhibits T cell, B cell, and macrophage proliferation	Alopecia, leukemia, infertility, infections, heart damage, nausea	IV, every 3 months	FDA
Aubagio	Teriflunomide	Pyrimidine synthesis inhibitor; inhibits an enzyme required for T and B cell proliferation	Liver damage, birth defects, alopecia, nausea, influenza	Oral, daily	FDA

Table 1.1: Therapies currently approved in the United States and/or Canada for treatment of MS. Adapted from publications by the National MS Society and the MS Society of Canada. (IM: Intramuscular; SQ: Subcutaneous; IV: Intravenous; FDA: Food and Drug Administration; HC: Health Canada)

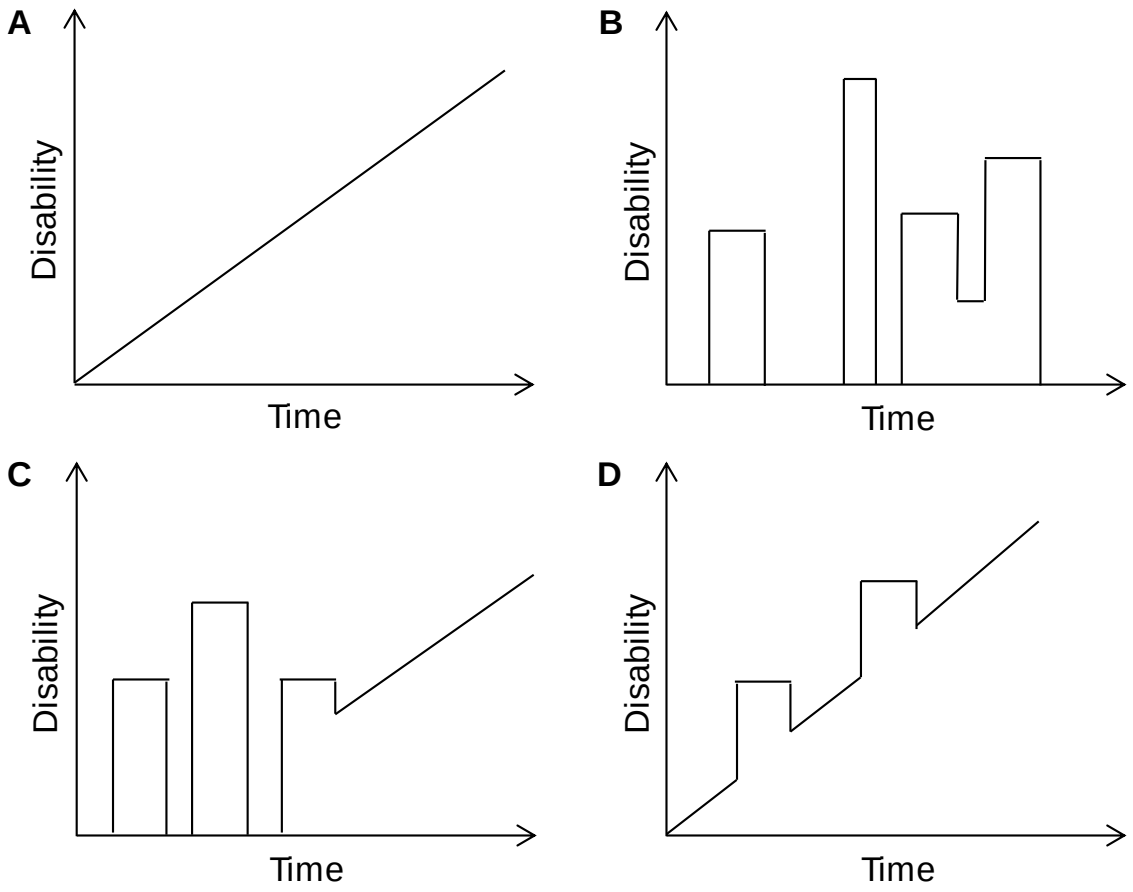

Figure 1.1: The course of disease in MS can be classified as one of four clinical subtypes. People with MS experience one of four general disease courses: primary progressive (A), relapsing-remitting (B), secondary progressive (C), or progressive-relapsing (D). Adapted from Lublin *et al.* [78].

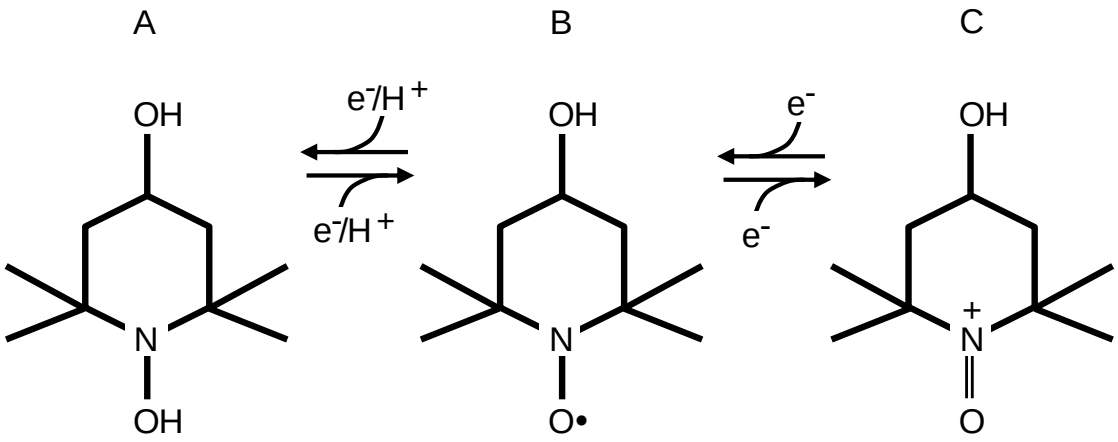

Figure 1.2: TEMPOL is capable of reversible oxidative and reductive reactions. *In vivo*, TEMPOL (B) exists largely in its reduced form, TEMPOL-H (A). TEMPOL can also be oxidized to an oxoammonium cation form (C).

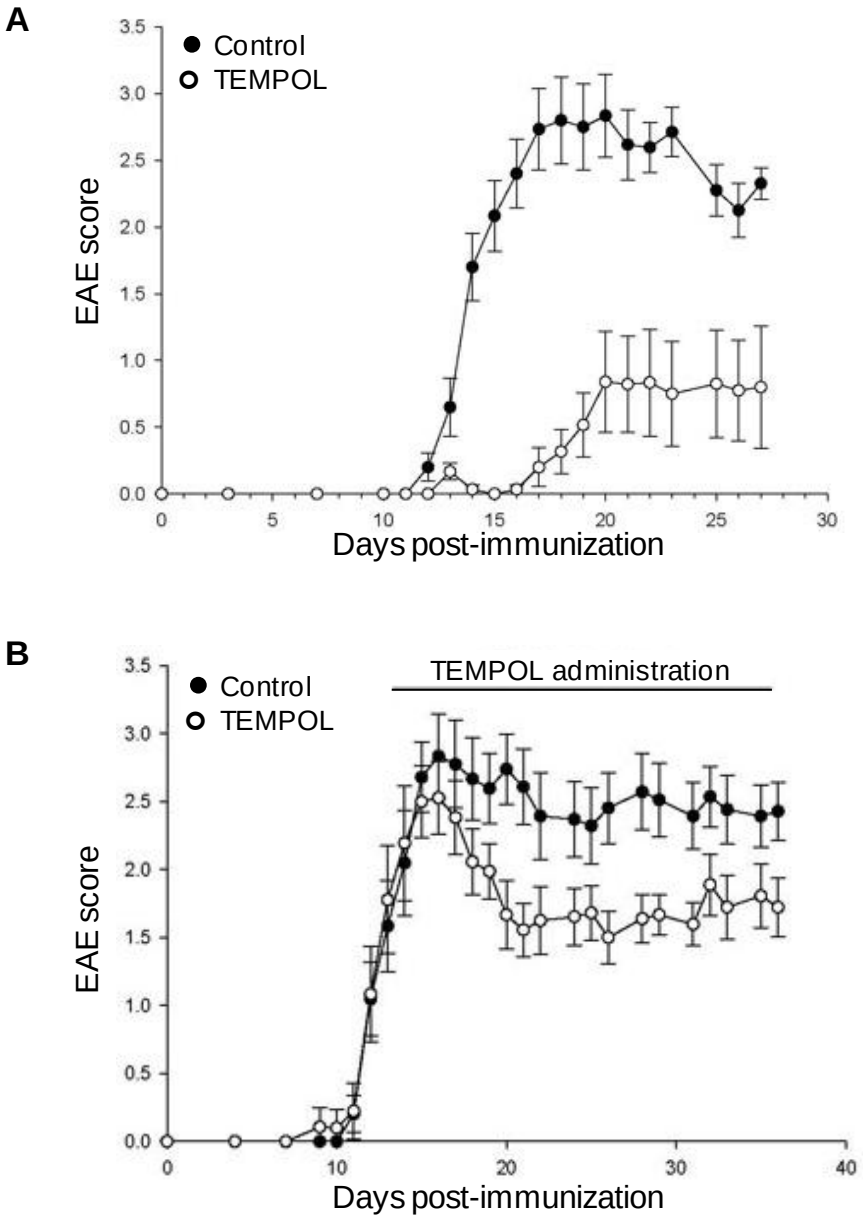

Figure 1.3: TEMPOL lowers the incidence and reduces the severity of disease in a mouse model of multiple sclerosis. Previous studies have demonstrated that orally-delivered TEMPOL is capable of ameliorating EAE when given 14 days before disease induction (prophylactic; A) and when given after 14 days after disease onset (therapeutic, B). EAE severity is quantified by a score based on physical symptoms, where an EAE score of 3.5 indicates paralysis of both hindlimbs. Figure courtesy of Dr. Jacqueline Quandt (unpublished data).

Chapter 2: Materials and Methods

2.1 EAE induction

Active EAE was induced using previously-described protocols [79]. In accordance with Canadian Council on Animal Care (CCAC) and UBC guidelines, female 6-8 week old CL57BL/6 mice (UBC Centre for Disease Modeling, Vancouver, Canada) were acclimatized to the Animal Resource Unit (ARU) prior to EAE induction. Animals were fed either control or TEMPOL chow (Bioserv Diet product #F6094 with 10 g/kg TEMPOL [Pharmasyn, Libertyville, IL]; provided by James Mitchell, National Institutes of Health, USA) *ad libitum* for 14 days. To induce EAE, mice were immunized subcutaneously with 200 µg MOG 35-55 peptide (MEVGWYRSPFSRVVHLYRNGK, 95% pure by high-performance liquid chromatography; Stanford Pan Facility, Stanford, CA) delivered in 4 mg/mL Mycobacterium H37Ra in incomplete Freund's adjuvant (Difco Laboratories, Detroit, MI). 200 ng Pertussis toxin (List Biologicals, Campbell, CA) was delivered intraperitoneally at immunization and two days later. Animals were weighed and monitored daily by a blinded examiner, and clinical signs were assessed according to the following scale: 0 - no disease; 1 - limp tail; 2 - mild hindlimb paresis; 2.5 - severe paresis; 3 - single hindlimb paralysis; 3.5 - two limbs paralyzed; 4 - hindlimb paralysis and forelimb paresis; and 5 - no mobility/moribund. Mice exhibiting clinical symptoms received moistened chow on the cage floor to enable access. Mice were euthanized on Day 14, and spleens, lymph nodes, brains, and spinal cords were collected. In some experiments, animals were fed TEMPOL or control feed in

parallel without induction of EAE and tissues were processed in a similar manner to test the effect of feed alone.

2.2 Removal and processing of immune tissue

Animals were anesthetized using carbon dioxide (CO_2) followed by cervical dislocation. Spleens and inguinal, brachial and axillary lymph nodes were removed from non-immunized/naïve C57BL/6J or EAE mice 14 days after immunization or in both cases, 28 days after feeding start. Organs were mashed through 40 µM strainers over 50 mL tubes using the plunger of a 3 mL syringe, rinsing with X-VIVO 15 media (Lonza, Walkersville, MD) to create a single cell suspension. Cell suspensions were washed by centrifugation for 8 minutes at 250x*g*, and supernatants were aspirated. Splenic red blood cells were lysed by resuspending the cell pellet in 5 mL of Ammonium-Chloride-Potassium (ACK) Lysing Buffer (Gibco by Life Technologies, Carlsbad, CA) for 5 minutes at room temperature (RT), followed by the addition of 10 mL of 2% fetal bovine serum (FBS; GE Healthcare Bio-Sciences, Piscataway, NJ) in Roswell Park Memorial Institute medium (RPMI; Gibco). Cells were washed twice and resuspended in 2 mL X-VIVO 15. Cells were diluted 1/10 in Trypan blue (Gibco). 10 µL of stained cells were applied to a hemocytometer and counted on an inverted phase microscope (Leica Microsystems, Wetzlar, Germany).

2.3 Lymphoid organ cell culture

Leukocytes isolated from spleens or lymph nodes were seeded on 96-well round-bottom plates (Corning Incorporated Life Sciences, Tewksbury, MA) at densities of $2x10^5$ or $4x10^5$ cells/well in X-VIVO 15 media. Cells from EAE mice were either left unstimulated or cultured with MOG 35-55 at doses of 0.8, 4, and 20 µg/mL; anti-CD3 at 0.125 µg/mL (clone 2C11, purified from mouse ascites; NCI, Frederick, MD); or the T cell mitogen Concanavalin-A (ConA; Sigma-Aldrich, Oakville, ON) at 0.2 µg/mL. Cells from naïve mice were either left unstimulated or cultured with anti-CD3 at doses ranging from 0.125 to 1.0 µg/mL; and with TEMPOL (Sigma-Aldrich), TEMPOL-H (GVK Biosciences, Hyderabad, India), or ascorbic acid (Sigma-Aldrich) at 0, 50, 100, 200, 400, and 800 µM. After seeding, cells were incubated at 37°C for 48 hours. Cell proliferation was measured by adding 0.5 µCi of tritiated thymidine, ([^{3}H]-T; Perkin Elmer, Waltham, MA) in 50 µL X-VIVO 15 per well for an additional 16 hours. Plates were then harvested on a Tomtec IIIM harvester (Tomtec, Hamden, CT) and incorporated radioactivity was measured on a Wallac Trilux Microbeta Scintillation Counter (Perkin Elmer).

2.4 Enzyme-linked Immunosorbant Assay (ELISA)

2.4.1 Cytokine ELISA

Immune cells were seeded as above at $2x10^5$ cells/well, either unstimulated or with the addition of 20 µg/mL MOG 35-55, 0.125 µg/mL anti-CD3, or 0.2 µg/mL ConA. Supernatants were collected at 65 hours and stored at -20°C. The cytokine content of the supernatants was quantified using DuoSet ELISA Development kits

(R&D Systems, Minneapolis, MN) for IL-2, IL-4, IL-10, IL-17, granulocyte macrophage colony-stimulating factor (GM-CSF), TGF-β1, and IFNγ according to the manufacturer's instructions. TNFα content was measured using a Ready-SET-Go!® ELISA reagent set (eBioscience, San Diego, California), again according to the manufacturer's instructions. Briefly, 96-well plates (Greiner Bio-One, Monroe, NC) were coated with capture antibody diluted in PBS (Sigma-Aldrich) and incubated overnight at RT or at 4°C (TNFα kit only). Wells were washed 3-5 times with 0.05% Tween-20 [Sigma-Aldrich] in PBS (PBS-T) wash buffer and blocked with blocking buffer at RT for one hour. Plates were again washed 3-5 times with PBS-T before application of supernatant samples diluted in reagent diluent (0.1 – 1.4% bovine serum albumin [BSA; MP Biomedicals, Solon, OH] in PBS with 0 – 0.05% Tween-20). A set of cytokine standards was prepared as serial dilutions from kit stocks and included on each plate. Detection antibody was added in reagent diluents at RT for 1-2 hours, then plates were washed and streptavidin-horseradish peroxidase (HRP) was added to the wells. Plates were incubated at RT in the dark for 20 minutes, followed by a final wash in PBS-T. Following a 20 min incubation with the chromogenic substrate 3,3',5,5'-Tetramethylbenzidine (TMB; eBioscience), a 2N H_2SO_4 stop solution was added to each well and optical density (OD) was detected at 450 nm on a EnVision Multilabel plate reader (Perkin Elmer). A 570 nm background reading was also collected for each plate and the values subtracted from those of the 450 nm reads. Cytokine concentrations were calculated using a standard curve with GraphPad Prism 5 software (version 5.04; GraphPad Software, La Jolla, CA).

2.4.2 MOG-specific antibody ELISA

Blood from EAE mice was collected following lancing of the submandibular vein and the processed serum [80] stored at -20°C until use. Flat-bottomed 96-well high-binding ELISA plates (Greiner) were coated with 2 µg/mL MOG 35-55 in 100 µL carbonate buffer per well, then sealed and incubated overnight at 4°C. Plates were washed 3 times with PBS-T, then incubated with blocking buffer for 1 hour. Mouse sera and positive controls were diluted in blocking buffer at 1:10, 1:20, 1:40 and 1:300, 1:600, 1:1200 respectively. Samples and controls were added in 50 µL per well, then incubated at RT for 1 hour. Plates were washed 3 times, followed by the addition of antibody diluted in blocking buffer and incubation for 1 hour at RT. The antibodies that were used are described in Table 2.1, and were supplied by Sigma-Aldrich or Jackson ImmunoResearch Laboratories Inc. (West Grove, PA) as indicated. Plates were then washed 3 times with wash buffer. For isotype-specific (IgG1, IgG2a, and IgG2c) assays, 100 µL of streptavidin-HRP (diluted 1:1000) was added to wells and incubated at RT for 20 minutes, then washed 3 times with wash buffer. The IgG ELISA does not require this extra streptavidin-HRP step. 50 µL of TMB was then added to each well, and plates were incubated in the dark at RT for 20 minutes. Following the addition of 50 µL of 2N H_2SO_4 stop solution per well, OD was read and results were calculated as described previously for cytokine ELISA experiments.

2.5 Mixed lymphocyte reaction (MLR)

2.5.1 Mouse MLR

Spleens from FVB mice (generously provided by Dr. Lynn Raymond at the University of British Columbia, Vancouver, Canada) were processed to produce a single-cell suspension as described previously. Cells were seeded to a 96-well flat bottom plate at 1 million cells per well in 50 µL X-VIVO 15 and incubated for at least 1 hour at 37°C to enable macrophage adherence. After incubation, wells were washed multiple times with X-VIVO 15 to remove non-adherent cells. A spleen from a histoincompatible C57BL/6 mouse was processed and the splenocytes were seeded to the macrophage-coated plate at densities of $2x10^5$, $4x10^5$, or $8x10^5$ cells/well. Either TEMPOL or TEMPOL-H was added to achieve final concentrations of 0, 50, 100, 200, 400, or 800 µM. Plates were then incubated at 37°C for 72 hours and proliferation was assessed with [^{3}H]-T as described above.

2.5.2 Human MLR

Human MLR experiments were performed in the laboratory of Dr. Mark Scott (University of British Columbia, Vancouver, Canada) using established protocols [81]. Specifically, blood from healthy donors was diluted 1:1 with 1× Hank's Balanced Salt Solution (HBSS; Gibco). Aliquots of 20 mL of diluted blood were layered over 15 mL of Ficoll-Paque (GE Healthcare) and centrifuged for 35 minutes at 400x*g*. Peripheral blood mononuclear cells (PBMCs) were collected and washed twice with HBSS. Cells were resuspended in 15 mL RPMI and counted using a hemocytometer. Cells were then stained with carboxyfluorescein succinimidyl ester

(CFSE; Invitrogen by Life Technologies, Carlsbad, CA) at $2x10^6$ cells/mL in RPMI by addition of a 5 mM CFSE stock prepared in dimethyl sulfoxide (DMSO; Invitrogen) for a final concentration of 2.5 µM. Cells were incubated at 37°C for 10 minutes, followed by the addition of 5 volumes of ice-cold RPMI. Cells were washed twice to remove excess dye and resuspended in AIM-V serum-free culture media (Invitrogen) at 2 million cells per mL. For the MLR, 48-well plates were seeded with 500,000 cells from each donor with treatment (TEMPOL or TEMPOL-H at 50 µM or 200 µM) or plain AIM-V. Control wells of single-donor PBMC were seeded with 200 µM TEMPOL or plain AIM-V. Single-donor PBMCs were also seeded with 2 µg/mL of the mitogen phytohemagglutinin (PHA, Sigma-Aldritch) as a positive proliferative control, with treatments as described for MLR wells. All treatments were tested in triplicate and harvested on days 10 and 14 for flow cytometric analysis.

2.6 Flow cytometry

For surface staining, cells were resuspended in staining buffer (1% FBS plus 0.05% sodium azide in PBS) at $1x10^6$ cells/well on a 96 well V-bottom plate (Corning) in 100 µL. Plates were centrifuged (8 minutes at 250x*g*) and inverted to discard buffer, then washed again. For mouse samples, 0.5 µL Fc block (Pharmingen by BD Biosciences, San Diego, CA) in 50 µL staining buffer was added to each well and incubated on ice for 10 minutes prior to the addition of primary antibodies. The primary antibodies used are outlined in Table 2.2, and were provided by eBioscience, Pharmingen by BD Biosciences, or BioLegend (San Diego, CA) as indicated. Antibody solutions were then added in 50 µL and incubated

on ice for 30 minutes. Human leukocyte cell pellets were resuspended in 100 µL of staining buffer containing primary antibodies, covered, and incubated on ice for 30 minutes. After staining, wells were topped up with staining buffer and washed twice.

If applicable, intracellular staining with Foxp3 and IgG2a isotype control antibodies was performed following surface staining using kits from eBioscience (Mouse Regulatory T Cell Staining Kit #2 and Human Regulatory T cell Staining Kit #2). Following the manufacturer's protocol, surface-stained cells were washed with staining buffer and resuspended in 150 µL of Fixation/Permeabilization working solution (eBioscience), then incubated on ice for 30 minutes (or overnight). Cells were washed twice in Permeabilization buffer (eBioscience), then resuspended in 100 µL of Permeabilization buffer containing primary antibody. Cells were incubated on ice for 30 minutes, washed twice in Permeabilization buffer, and resuspended in 150 µL staining buffer. Flow cytometry analysis was done using either a FACSCalibur (human samples; BD Biosciences, San Jose, CA) or a MACSQuant (mouse samples; Miltenyi, Auburn, CA) flow cytometer and analyzed using FlowJo software (version 7.6.5; Treestar, Ashland, OR).

2.7 Live/dead cell assay

A LIVE/DEAD® Viability/Cytotoxicity Kit (Invitrogen) was used to assess cell death in the presence of TEMPOL. Spleen cells isolated from health C57BL/6J mice were processed as described, and seeded to 96-well round-bottomed plates (Corning) at $2.5x10^5$ cells/well in 100 µL X-VIVO 15 media. Either 50 µL plain X-VIVO 15 was added to each well, or 50 µL of anti-CD3 in X-VIVO 15 to a final

concentration of 0.125 µg/mL. TEMPOL was added in 50 µL X-VIVO 15 to final concentrations of 0, 1, 3, 10, 30, 100, 300, 1000, 3000, 10000, and 30000 µM per well. All treatments were set in quadruplicate, followed by incubation of the plates for 48 hours at 37°C.

After incubation, media was aspirated from all wells. To create "dead" controls, 100 µL of 70% ethanol (Commercial Alcohols, Brampton, ON) was added to 4 wells of 0 µM TEMPOL unstimulated cells and 4 wells of 0 µM TEMPOL anti-CD3 treated wells. 100 µL of X-VIVO 15 media was added to all other wells. Cells were incubated at 37°C for 15 minutes, and centrifuged for 8 minutes at 250x*g*. Cells were then washed once with X-VIVO 15 and centrifuged again, followed by aspiration of media from all wells. Calcein AM (live cell stain) and ethidium homodimer-1 (dead cell stain) were mixed with PBS as per the manufacturer's instructions and added to cells 150 µL per well. Cells were transferred using a multichannel pipette to a flat-bottomed black-walled 96-well plate (Greiner Bio-One). Plates were incubated at RT for 30 minutes. Fluorescence was read using a SpectraMax M2 microplate reader (Molecular Devices, Sunnyvale, CA) with excitation/emission settings at 485/530 nm and 530/645 nm.

2.8 Statistical analysis

All statistical analysis was performed using SigmaPlot (version 11.0, Systat Software, San Jose, CA), and graphs were prepared in GraphPad Prism 5. Analyses comparing multiple treatment groups used Kruskall-Wallace one-way analysis of variance (ANOVA) on ranks, followed by Dunn's multiple comparison tests.

Analyses comparing two treatment groups used Mann-Whitney Rank Sum tests. All data are reported as mean +/- standard deviation (SD) or +/- standard error (SE) as indicated.

Antibody	Host/ specificity	Conjugate	Source	Catalogue #	Dilution
IgG	Goat anti-mouse	Peroxidase	Sigma-Aldrich	A-0168	1:30,000
IgG1	Goat anti-mouse	Biotin	Jackson	115-065-205	1:80,000
IgG2a	Goat anti-mouse	Biotin	Jackson	115-065-206	1:40,000
IgG2c	Goat anti-mouse	Biotin	Jackson	115-065-208	1:40,000

Table 2.1: Antibodies used in MOG-specific antibody ELISA. All antibodies were stored at -20°C and thawed before use.

Anti-Mouse	Conjugate	Source	Catalogue #	µg per test
CD11b	APC	eBioscience	17-0112-82	0.2
CD11c	APC Cy7	BioLegend	117323	0.5
CD11c	PE Cy7	eBioscience	25-0114-81	0.1875
CD19	PE	BD Pharmingen	553786	0.05
CD25	PE Cy7	eBioscience	25-0251-81	0.125
CD25	PE	eBioscience	12-0251-81	0.06
CD3	FITC	BD Pharmingen	553062	0.5
CD4	APC-eFluor 780	eBioscience	47-0041-80	0.15
CD4	eFluor-450	eBioscience	48-0041-80	0.2
CD40	PE Cy7	BioLegend	124621	0.2
CD45	eFluor-450	eBioscience	48-0451-82	0.1
CD8	APC	BD Pharmingen	553035	0.2
CD8	FITC	BD Pharmingen	553031	0.5
CD80 (B7.1)	FITC	BD Pharmingen	553768	0.5
CD86 (B7.2)	PE	BD Pharmingen	09275b	0.05
MHC I (H-2Db)	FITC	eBioscience	11-5999-81	0.25
Foxp3	APC	eBioscience	17-5773-82	0.5
MHC II (I-A/I-E)	PE	BD Pharmingen	557000	0.2
IgG2a	APC	eBioscience	17-4321-81	0.5
NK1.1	APC-eFluor 780	eBioscience	47-5941-80	0.15
Anti-Human	**Conjugate**	**Source**	**Catalogue #**	**µg per test**
CD25	PE	eBioscience	12-0259-42	0.125
CD3	PE Cy5	BD Pharmingen	555341	(5 µL)
CD4	PB	eBioscience	48-0048-42	0.125
CD4	PE	BD Pharmingen	555347	(5 µL)
CD8a	PE Cy7	eBioscience	25-0087-42	0.06
Foxp3	APC	eBioscience	17-4776-42	0.5
IgG2a	APC	eBioscience	17-4321-41	1

Table 2.2: Antibodies used in flow cytometry. All antibodies were stored at 4°C and were titrated before use to determine optimal staining concentrations.

Chapter 3: *Ex vivo* Results

3.1 Autoreactive and polyclonal T cell proliferation is not reduced in TEMPOL-fed animals

The development of EAE relies upon the generation of autoreactive or MOG-specific T cells [27]. Interventions that limit or influence the generation of autoreactive responses therefore have the ability to influence the pathogenesis and severity of disease. To determine if TEMPOL may alter EAE by influencing the generation of autoreactive T cells in the course of disease, cells isolated from spleens and lymph nodes of EAE mice on control or TEMPOL feed were analyzed *ex vivo*. The addition of MOG 35-55 serves to re-activate memory T cells generated after exposure to MOG during EAE induction, testing the relative magnitude of the antigen-specific T cell response that occurred in animals on control versus TEMPOL feed. The anti-CD3 clone 2C11, a monoclonal antibody that binds to the CD3 T cell co-receptor to induce T cell proliferation [23]; as well as ConA, a T cell mitogen [82], were used to assess the influence of TEMPOL on *ex vivo* polyclonal T cell responses.

In both spleens and lymph nodes of TEMPOL-fed EAE mice, *ex vivo* proliferative responses to MOG (Figure 3.1 A,C) and anti-CD3 or ConA (Figure 3.1 B,D) were comparable to controls. While there was a trend towards increased polyclonal proliferative responses from TEMPOL-fed animals *ex vivo* in most experiments, this effect did not reach statistical significance. Proliferation was also examined using cells isolated from age-matched healthy mice administered control or TEMPOL feed for 28 days, spanning the pre-immunization and post-immunization

time points of the EAE mice. Since animals were not immunized with MOG, proliferative responses were only tested in spleen cells with 0.125 µg/mL anti-CD3 and 0.1 µg/mL ConA. Similar to findings in the EAE mice, polyclonal responses to ConA or anti-CD3 measured *ex vivo* were not reduced by the earlier oral administration of TEMPOL compared to animals on control feed (Figure 3.2).

3.2 TEMPOL administration alters the cytokine profiles of autoreactive and polyclonal responses measured *ex vivo*.

In addition to examining proliferation, the influence of TEMPOL on cytokine production by immune cells in EAE was also studied. Since the magnitude of the immune response did not appear to be altered by TEMPOL, we were interested in examining the characteristics of responding immune cells. Using supernatants collected from cells cultured for proliferation experiments, sandwich ELISAs were used to assess differences in production of IL-2, IL-4, IL-10, IL-17, IFNγ, GM-CSF, TGF-β1, and TNFα between control and TEMPOL-fed EAE mice.

Differences in cytokine production between control and TEMPOL-fed animals were most commonly observed in cells isolated from the draining lymph nodes. Within lymph node samples, production of IL-2 and IL-10 by ConA-stimulated cells from TEMPOL-fed animals were found to be significantly decreased compared to controls. IFNγ and TNFα production by anti-CD3-stimulated cells was also significantly reduced by TEMPOL, with ConA-stimulated cells showing a similar trend for IFNγ (Figure 3.3). Production of GM-CSF by Anti-CD3- and ConA-stimulated lymph node cells tended to be decreased by TEMPOL in all experiments,

but this trend did not reach statistical significance. Generally, MOG-stimulated lymph node cells did not show significant differences in cytokine production between control and TEMPOL samples, though production of IFNγ and GM-CSF tended to be reduced in TEMPOL fed animals. IL-17 levels were similar between lymph node samples from both feed groups. IL-4 and TGF-β1 were also similar between groups, but below the limit of detection (data not shown).

Within spleen samples, IL-2 production by MOG-stimulated cells was significantly reduced (P = 0.035) by TEMPOL, while anti-CD3- and ConA-stimulated cells showed a similar trend. A trend towards decreased TGF-β1 production was observed with TEMPOL in anti-CD3-stimulated cells from spleens, though results were not statistically significant (P = 0.090; Figure 3.4). No differences in IL-4, IL-10, IL-17, GM-CSF, IFNγ, or TNFα were observed between the two feed groups in spleen samples (data not shown).

Cytokine production was also examined in spleens from healthy mice fed a control or TEMPOL diet, as described previously in this chapter for *ex vivo* cell proliferation studies. In these supernatants, TGF-β1 production was reduced with TEMPOL (*P = 0.018 for ConA-stimulated cells; Figure 3.5). Trends towards decreased production of IL-2, IFNγ, GM-CSF, and TNFα with TEMPOL were also observed. No differences in production of IL-4, IL-10, or IL-17 were detected (data not shown).

3.3 TEMPOL administration enhances autoreactive IgG responses associated with an immunosuppressive rather than inflammatory isotype.

The generation of MOG-specific antibodies is thought to contribute to EAE pathogenesis in rodent models of MS [83], and to a greater extent the disease process in MS [84]. TEMPOL-fed EAE mice showed significantly increased levels of MOG-specific serum IgG antibodies (Figure 3.6 A). This increase was predominantly in the IgG1 isotype group, the isotype typically associated with a T_H2 response (Figure 3.6 B) [85]. Similarly, the IgG2c levels associated with more pro-inflammatory T_H1 responses tended to be reduced in TEMPOL-fed animals (Figure 3.6 C), and contributed to a significant and dramatic increase in the ratio of antibodies associated with immunosuppressive rather than inflammatory responses (IgG1:IgG2c ratio, Figure 3.6 D).

3.4 TEMPOL administration alters proportions of T lymphocyte subsets

To further examine how TEMPOL influences the immune response in EAE mice, spleen and lymph node cells were isolated from control or TEMPOL-fed animals and analyzed by flow cytometry. Panels were designed to examine B cell and T cell subset populations, as well as myeloid cell, DC, and natural killer (NK) cell populations. Cells were either stained and analyzed immediately after isolation, or thawed after being frozen from previous experiments. Frozen samples generally exhibited trends similar to fresh cells, but results were less robust and therefore these samples were not included in analyses (data not shown). Live cells were selected based on forward and side scatter, and then CD45+ leukocytes were

selected. CD3+ (T cell) and CD19+ (B cell) populations were gated, and the CD3+ population was further gated for CD4+ vs. CD8+ T cells. T_{reg} cell populations were gated from CD4+ and CD8+ groups by selecting cells that dually express CD25 and Foxp3. CD45+ cells were also gated for CD11b+CD11c- (myeloid), CD11b-CD11c+ (dendritic), and CD11b+CD11c+ (myeloid dendritic) cells. NK cells were selected as NK1.1+ cells from the CD45+ population.

Pooled results from two experiments (n = 13 mice per group of control vs. TEMPOL-fed) showed that CD19+ B cells in each organ were comparable between control and TEMPOL-fed mice, while NK cells were slightly enriched in lymph nodes (Table 3.1). The percentage of CD3+ T cells did not differ significantly between control and TEMPOL-fed animals. However, analysis of cells within the CD3+ family showed that both spleens and lymph nodes of TEMPOL-fed mice had significantly reduced percentages of CD4+ T cell populations, which corresponded with a 15% increase in CD8+ T cell percentages in both organs (Table 3.2), demonstrating a shift in T cell subset proportions without a change in overall T cell population size. CD4+ T_{reg} cell (CD4+CD25+Foxp3+) populations were also compared between control and TEMPOL-fed EAE mice. Pooled results showed that these T_{reg} cells were significantly enriched in lymph nodes of TEMPOL-fed mice compared to controls (Figure 3.7 A,B). Conversely, T_{reg} cells were significantly decreased in spleens of TEMPOL-fed mice (Figure 3.7 C,D). CD8+ T_{reg} cells were also enriched in lymph nodes, but still composed less than 1% of the CD8+ T cell population (data not shown).

Analyses also compared the frequencies of myeloid cell (CD11b+CD11c-), myeloid DC (CD11b+CD11c+), and lymphoid DC (CD11b-CD11c+) populations. In spleens from EAE mice, these populations were not significantly different between control and TEMPOL-fed groups (Table 3.1). In lymph nodes, however, TEMPOL-fed animals showed enrichment of CD11b+ myeloid cells, with a significant increase in CD11b+CD11c+ myeloid DCs, and a trend towards an increase in CD11b+CD11c- myeloid cells.

T and B cell distributions were also studied in healthy animals on control or TEMPOL feed, and results from two experiments (n = 12 mice per feed group) were pooled. CD19+ B cells were similar between groups in lymph nodes, but significantly decreased in spleens from the TEMPOL-fed group (55.5 ±2.2% versus 48.2 ±3.8%, $P < 0.001$). Overall, the CD3+ T cell population was not altered in lymph nodes of TEMPOL-fed healthy mice, but was significantly increased in spleens (34.4 ±2.4% versus 39.9 ±3.6%, $P < 0.001$). Within the CD3+ T cell group, a significant decrease in CD4+ T cells was again observed with TEMPOL, along with a 10% increase in CD8+ T cells in both organs (Table 3.3). As with EAE animals, a significant increase in T_{reg} cells was also observed in lymph nodes of healthy animals on TEMPOL feed (Figure 3.8 A,B). Similarly, T_{reg} cells were also significantly decreased in spleens from TEMPOL-fed animals (Figure 3.8 C,D).

3.5 TEMPOL influences antigen presenting and co-stimulatory molecule expression by lymphoid organ cells *in vivo*

Altered expression of antigen presenting molecules or co-stimulatory molecules at the time of antigen presentation may influence the magnitude and nature of an inflammatory response. They may also reflect the ability of immune cells, such as T_H cells of different effector functions, to prime or activate APC in a particular organ. Expression of MHC class I and II, CD40, CD80, and CD86 was therefore examined in myeloid cells, lymphoid DCs, and myeloid DCs in spleens and lymph nodes of EAE mice on control or TEMPOL feed. Expression levels were quantified using the median fluorescence intensity (MFI) of each marker, and results were pooled from two experiments (13 mice per group of control or TEMPOL-fed EAE animals).

Overall, changes in surface marker expression were observed to be most robust in draining lymph nodes. No changes in surface molecule expression were observed in CD11b-CD11c+ lymphoid DC populations with TEMPOL in either organ (data not shown). In draining lymph nodes of TEMPOL-fed EAE mice, CD11b+CD11c- myeloid cells showed significantly decreased expression of MHC II and increased expression of CD80 and CD86 (Figure 3.9 A). Myeloid cells in spleens also showed decreased MHC II and increased CD86, as well as decreased CD40 expression, in TEMPOL-fed animals (Figure 3.10 A). CD11b+CD11c+ myeloid DC had significantly decreased MHC II expression in both lymph nodes and spleens of TEMPOL-fed mice (Figure 3.9 B; Figure 3.10 B). In lymph nodes, CD80 expression was significantly increased with TEMPOL in myeloid DC (Figure 3.9 B).

In splenic myeloid DC, CD40 expression was significantly decreased in TEMPOL-fed animals (Figure 3.10 B). MHC I expression was also studied, but was not found to be altered in either spleens or lymph nodes in any cell population (data not shown).

Surface molecule expression based on MFI was also studied in healthy mice on control or TEMPOL feed, and results were pooled from two experiments (12 mice per feed group; Table 3.4). Both spleens and lymph nodes were examined, but results averaged from both experiments showed no conclusive influence of TEMPOL in lymph nodes (data not shown). In CD11b-CD11c+ lymphoid DC, MHC II expression showed a trend towards a decrease with TEMPOL in spleens (MFI of 2880.2 ±285.83 versus 2672.7 ±360.55; P = 0.069). CD80 expression was significantly increased with TEMPOL in this population in spleens, while MHC I expression was significantly decreased with TEMPO. CD40 and CD86 expression in lymphoid DC were not affected by TEMPOL (data not shown).

In CD11b+CD11c- myeloid cells, expression of MHC I and MHC II was significantly decreased with TEMPOL in spleens (Table 3.4). CD40, CD80, and CD86 expression were not altered in spleens. CD11b+CD11c+ myeloid DC showed significantly decreased expression of MHC I, MHC II, CD80, and CD86 with TEMPOL in spleens. CD40 expression in this population was not altered with TEMPOL (data not shown).

Lymph node	Control Average %	TEMPOL Average %	P value
T cells (CD3+)	37.9 ±4.4	38.2 ±2.9	0.538
B cells (CD19+)	55.6 ±3.4	54.6 ±4.1	0.441
Myeloid cells (CD11b+CD11c-)	1.1 ±0.6	1.8 ±0.8	0.051
Dendritic cells (CD11c+CD11b-)	1.3 ±0.2	1.3 ±0.2	0.681
Myeloid DCs (CD11b+CD11c+)	2.0 ±0.5	2.3 ±0.3	0.045*
NK cells (NK1.1+)	4.0 ±0.7	4.5 ±0.5	0.043*
Spleen			
T cells (CD3+)	19.7 ±8.0	17.6 ±4.3	0.918
B cells (CD19+)	36.3 ±7.3	34.2 ±6.3	0.719
Myeloid cells (CD11b+CD11c-)	26.1 ±8.0	29.4 ±5.0	0.442
Dendritic cells (CD11c+CD11b-)	1.5 ±0.3	1.4 ±0.3	0.259
Myeloid DCs (CD11b+CD11c+)	3.1 ±1.4	2.9 ±0.4	0.858
NK cells (NK1.1+)	4.92 ±1.5	4.71 ±2.4	0.305

Table 3.1: Composition of lymphoid organ populations in control vs. TEMPOL-fed EAE animals. Cells were isolated 10 days after EAE induction in animals on control or TEMPOL feed for 14 days prior to immunization. Analyses were performed on flow cytometry data by selecting the live cells based on forward and side scatter, then selecting the CD45+ leukocyte population, then subsequently gating the described populations as a percentage of CD45+ cells. Values represent average results of 2 pooled experiments (13 mice per feed group), ±SD. *P < 0.050, Mann-Whitney Rank Sum test, control vs. TEMPOL.

Lymph node	Control Average	TEMPOL Average	P value
% CD4+ T cells	53.3 ±3.3	46.7 ±2.3	<0.001*
% CD8+ T cells	40.1 ±2.1	46.4 ±2.2	<0.001*
CD4/CD8	1.3 ±0.2	1.0 ±0.1	<0.001*
Spleen			
% CD4+ T cells	56.6 ±3.6	50.7 ±4.2	0.001*
% CD8+ T cells	32.1 ±3.2	37.7 ±4.0	0.001*
CD4/CD8	1.8 ±0.3	1.4 ±0.3	<0.001*

Table 3.2: CD8+ T cells are enriched in spleens and lymph nodes of TEMPOL-fed EAE mice compared to controls. Cells were isolated 10 days after EAE induction in animals on control or TEMPOL feed for 14 days prior to immunization. Analyses were performed on flow cytometry data by selecting the live cells based on forward and side scatter, then selecting the CD45+ leukocyte population, then analyzing CD45+CD3+ T cells for CD4 and CD8 expression. CD4/CD8 represents the ratio of CD4+ to CD8+ T cells. Values represent average results of 2 pooled experiments (13 mice per feed group), ±SD. *P < 0.050, Mann-Whitney Rank Sum test, control vs. TEMPOL.

Lymph node	Control Average	TEMPOL Average	P value
% CD4+ T cells	49.9 ±1.6	45.1 ±3.2	0.001*
% CD8+ T cells	42.1 ±1.1	47.1 ±2.6	<0.001*
CD4/CD8	1.2 ±0.1	1.0 ±0.1	<0.001*
Spleen			
% CD4+ T cells	52.9 ±3.2	47.7 ±3.0	0.001*
% CD8+ T cells	40.9 ±2.9	46.5 ±2.9	<0.001*
CD4/CD8	1.3 ±0.2	1.0 ±0.1	<0.001*

Table 3.3: CD8+ T cells are enriched in spleens and lymph nodes of TEMPOL-fed healthy mice compared to controls. Cells were isolated at Day 28 after start of TEMPOL or control diet. Analyses were performed on flow cytometry data by selecting the live cells based on forward and side scatter, then selecting the CD45+ leukocyte population, then analyzing CD45+CD3+ T cells for CD4 and CD8 expression. CD4/CD8 represents the ratio of CD4+ to CD8+ T cells. Values represent average results of 2 pooled experiments (12 mice per feed group), ±SD. *P < 0.050, Mann-Whitney Rank Sum test, control vs. TEMPOL.

Spleen	Control Average MFI	TEMPOL Average MFI	P value
CD11b-CD11c+			
MHC I	1254.6 ±73.4	1114.9 ±104.7	0.002*
CD80	120.2 ±6.3	129.25 ±7.4	0.008*
CD11b+CD11c-			
MHC I	1006.5 ±125.9	883.5 ±147.0	0.030*
MHC II	133.75 ±15.0	108.5 ±21.1	0.010*
CD11b+CD11c+			
MHC I	2138.0 ±265.7	1879.3 ±223.8	0.026*
MHC II	5746.4 ±715.3	4843.8 ±1118.8	0.035*
CD80	286.8 ±14.4	256.0 ±18.4	0.002*
CD86	132.0 ±8.1	120.2 ±12.1	0.026*

Table 3.4: Markers associated with co-stimulation are altered in TEMPOL-fed healthy mice. Cells were isolated at Day 28 after start of TEMPOL or control diet. Analyses were performed on flow cytometry data by selecting the live cells based on forward and side scatter, then selecting the CD45+ leukocyte population, then gating CD11b-CD11c+, CD11b+CD11c-, or CD11b+CD11c+ cells. The MFI was calculated for each surface marker, and values from 2 experiments (12 mice per group) were pooled for statistical analysis. *P < 0.050, Mann-Whitney Rank Sum test, control vs. TEMPOL.

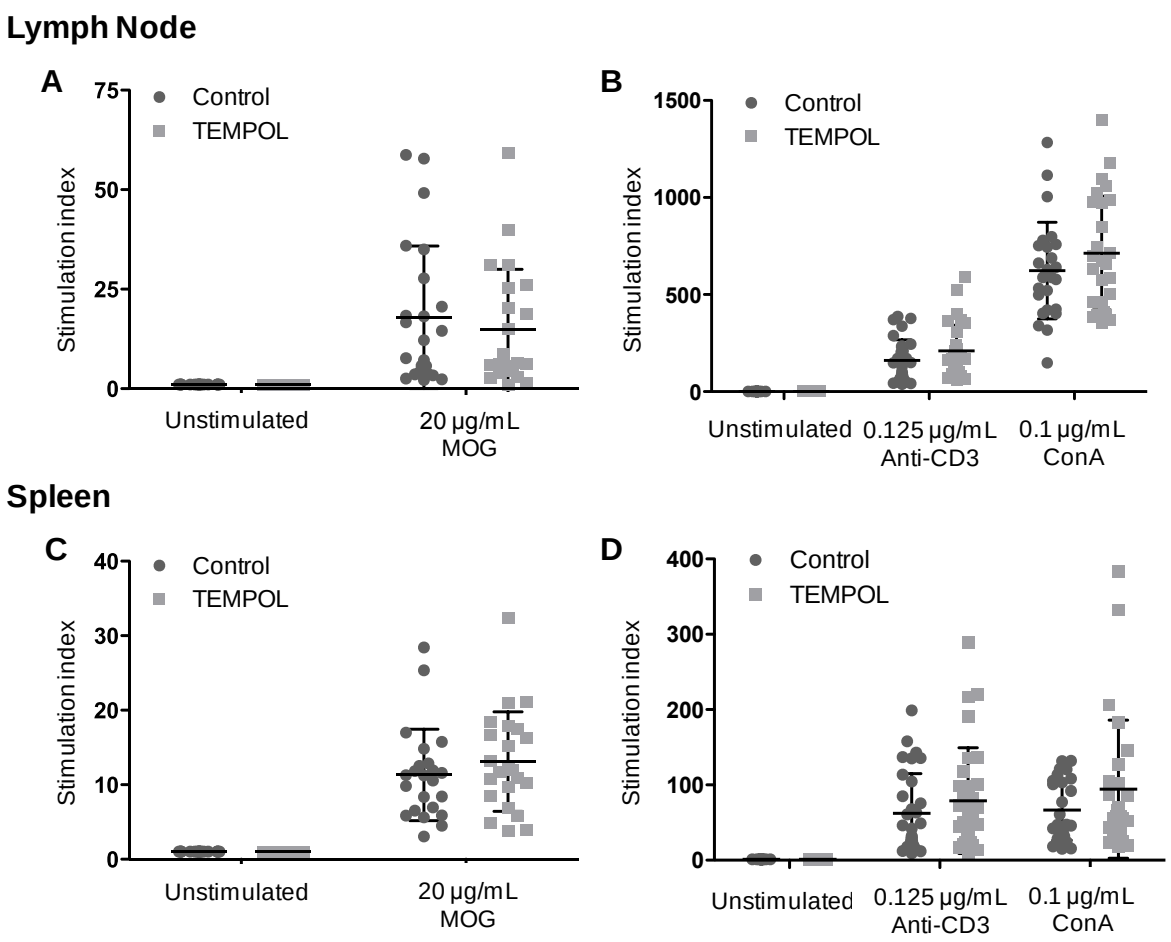

Figure 3.1: Autoreactive and polyclonal T cell responses measured *ex vivo* are similar in control and TEMPOL-fed EAE animals. Draining lymph nodes (A,B) and spleen cells (C,D) were isolated from control (circles) or TEMPOL-fed (squares) EAE mice and compared for proliferative responses after 48 hours in culture. Graphs show pooled results of 5 experiments, 31 mice per feed group. Proliferation was normalized to proliferation of unstimulated cells (the stimulation index, or SI) for each mouse before pooling. Bars represent the mean SI with error bars ± standard deviation (SD).

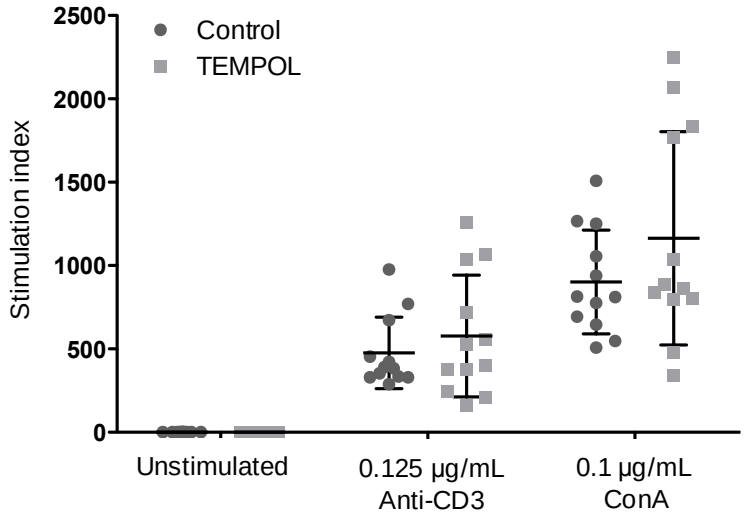

Figure 3.2: *Ex vivo* proliferation in response to polyclonal stimuli is not influenced by TEMPOL in healthy mice. Spleens were isolated from control or TEMPOL-fed healthy animals and compared for proliferative responses after 48 hours in culture. Graphs show pooled results of 2 experiments, 12 mice per feed group. Proliferation was normalized to proliferation of unstimulated cells for each mouse before pooling. Bars represent the mean SI with error bars ±SD.

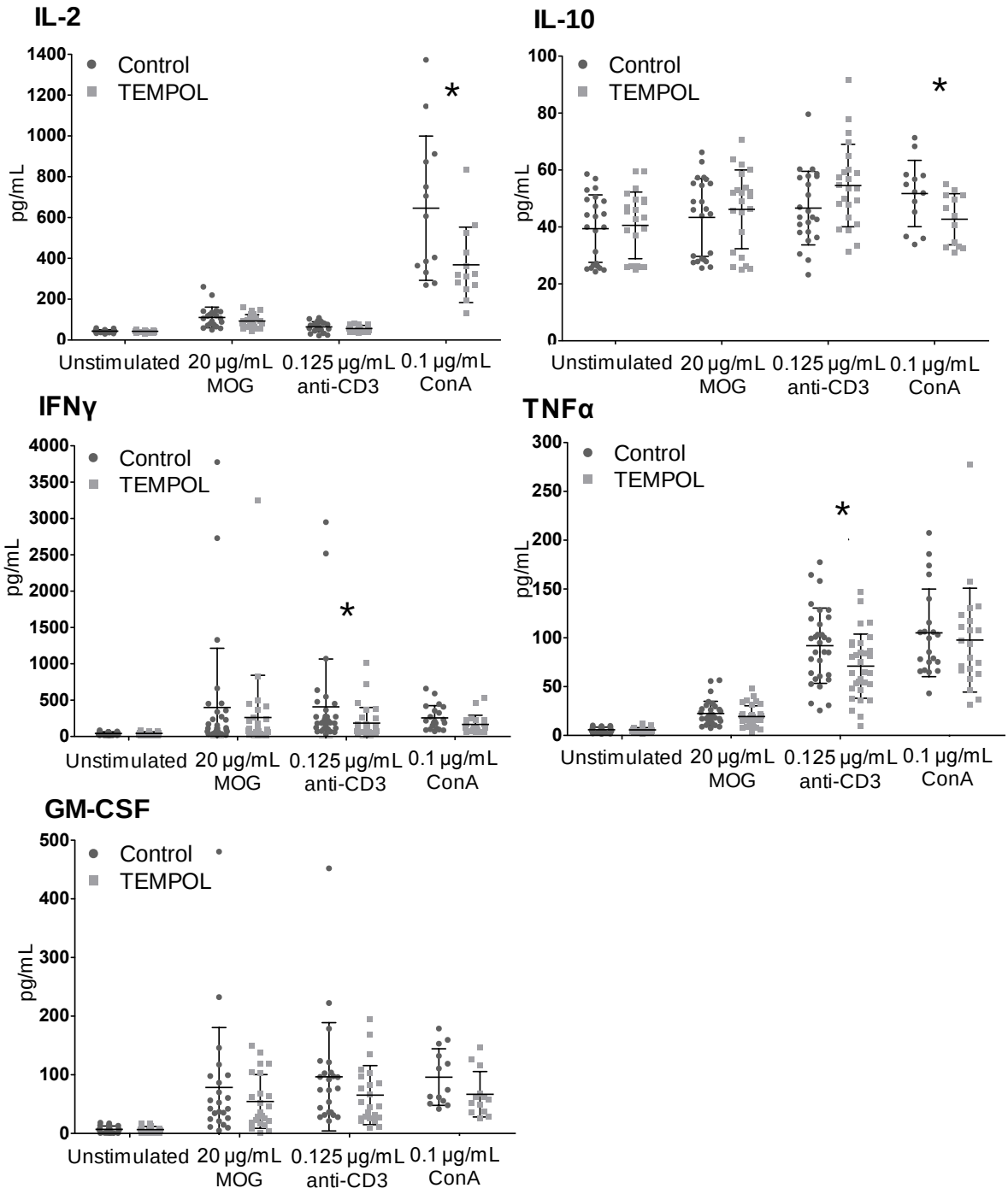

Figure 3.3: Cytokine production is altered by TEMPOL in lymph node cells isolated from EAE mice. Draining lymph nodes were isolated from control or TEMPOL-fed EAE mice and put into culture with the indicated stimuli, and supernatents were collected at 65 hours. Cytokine content was measured using ELISA kits. Data is pooled from 5 experiments of 5-8 mice each; each point represents a single mouse, with bars ±SD. *P < 0.05, Mann-Whitney rank sum test.

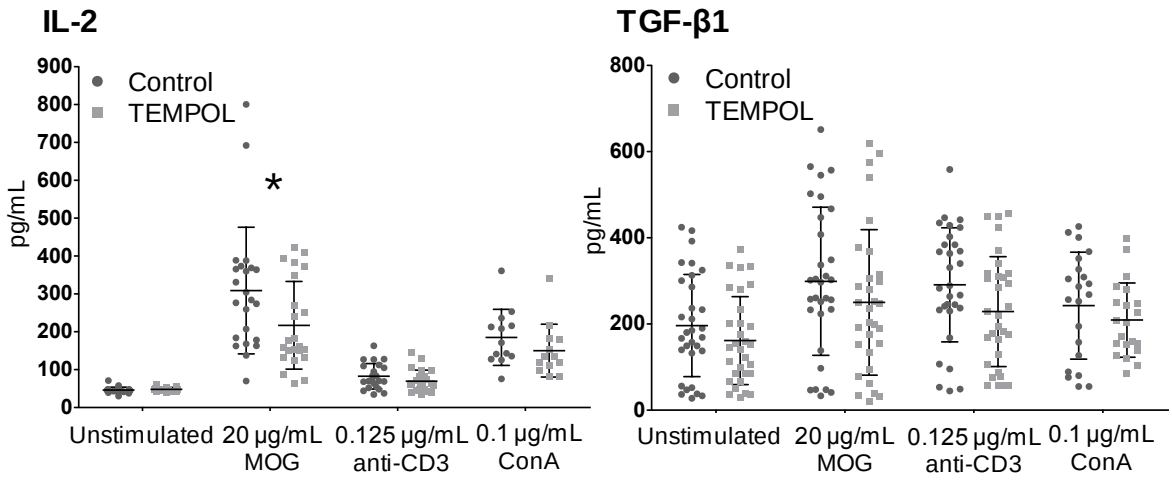

Figure 3.4: Cytokine production is altered by TEMPOL in spleen cells isolated from EAE mice. Spleens were isolated from control or TEMPOL-fed EAE mice and put into culture with the indicated stimuli, then supernatents were collected at 65 hours. Cytokine content was measured using ELISA kits. Data is pooled from 5 experiments of 5-8 mice each; each point represents a single mouse, with bars ±SD. *P < 0.05, Mann-Whitney rank sum test, control vs. TEMPOL.

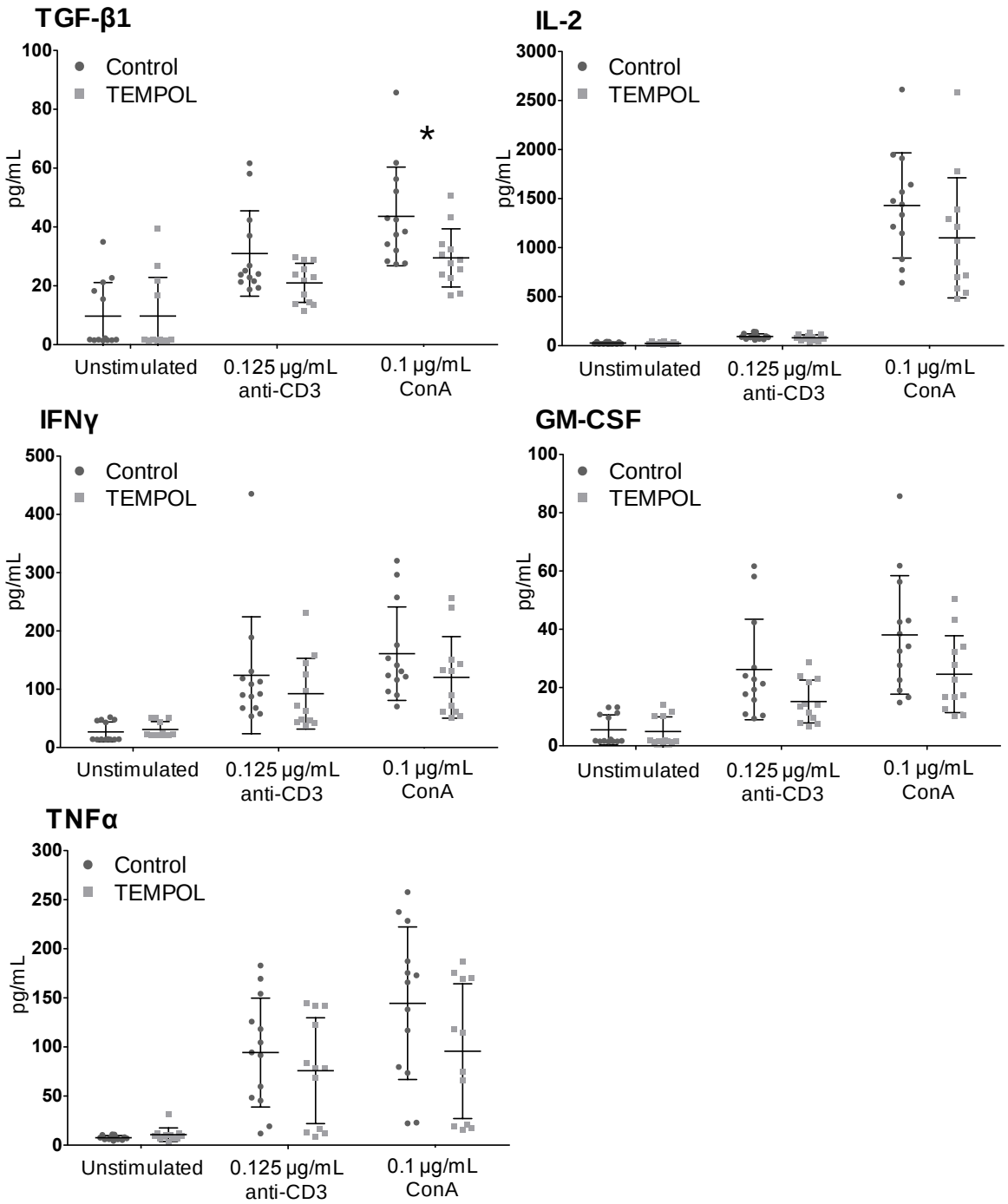

Figure 3.5: Cytokine production is altered by TEMPOL in spleen cells isolated from healthy mice. Spleens were isolated from control or TEMPOL-fed EAE mice and put into culture with the indicated stimuli, then supernatents were collected at 65 hours. Cytokine content was measured using ELISA kits. Data is pooled from 2 experiments with 5 and 8 mice; each point represents a single mouse, with bars ±SD.*P < 0.05, Mann-Whitney rank sum test, control vs. TEMPOL.

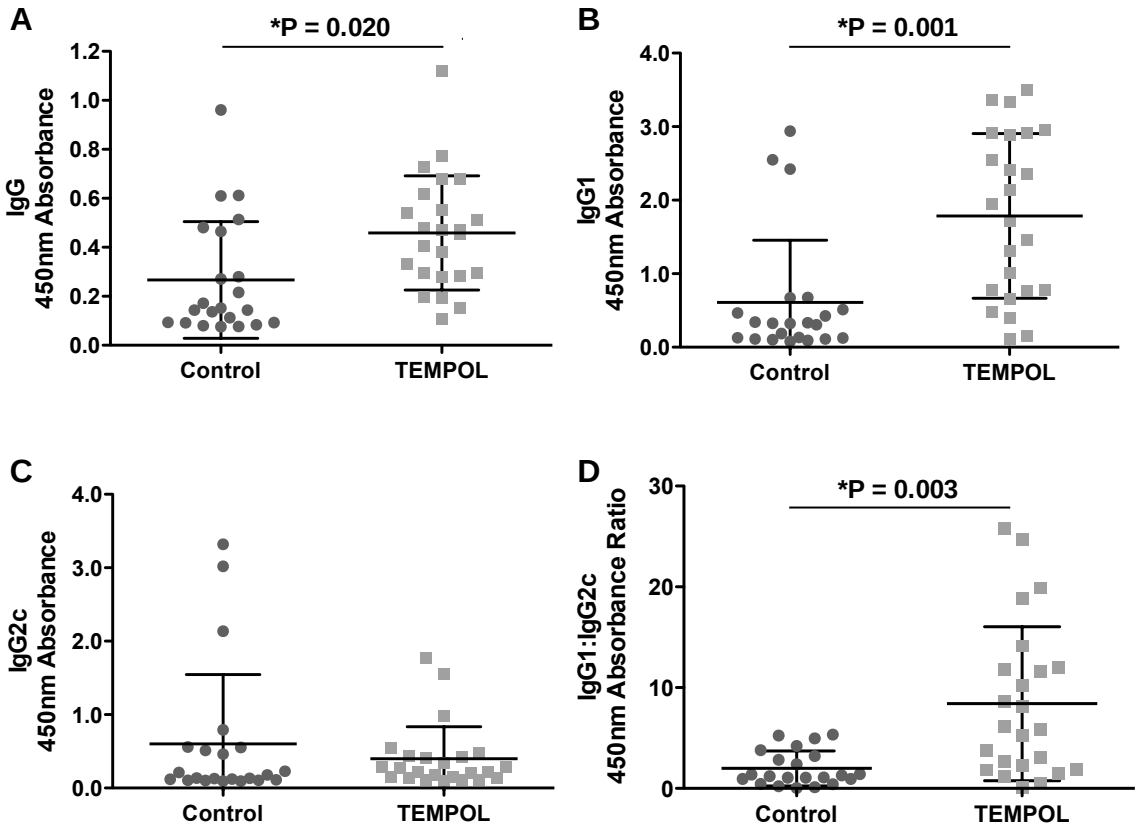

Figure 3.6: TEMPOL administration enhances MOG-specific antibody responses that are immunosuppressive rather than pro-inflammatory in nature. Sera were prepared from blood drawn from EAE animals at Day 24 – 28 and compared for overall IgG response (A) as well as isotype-specific responses (B – D). Results were pooled from 3 experiments, 22 mice per feed group. Bars represent the mean 450 nm absorbance with error bars ±SD. *P < 0.050, Mann-Whitney Rank Sum test, control vs. TEMPOL

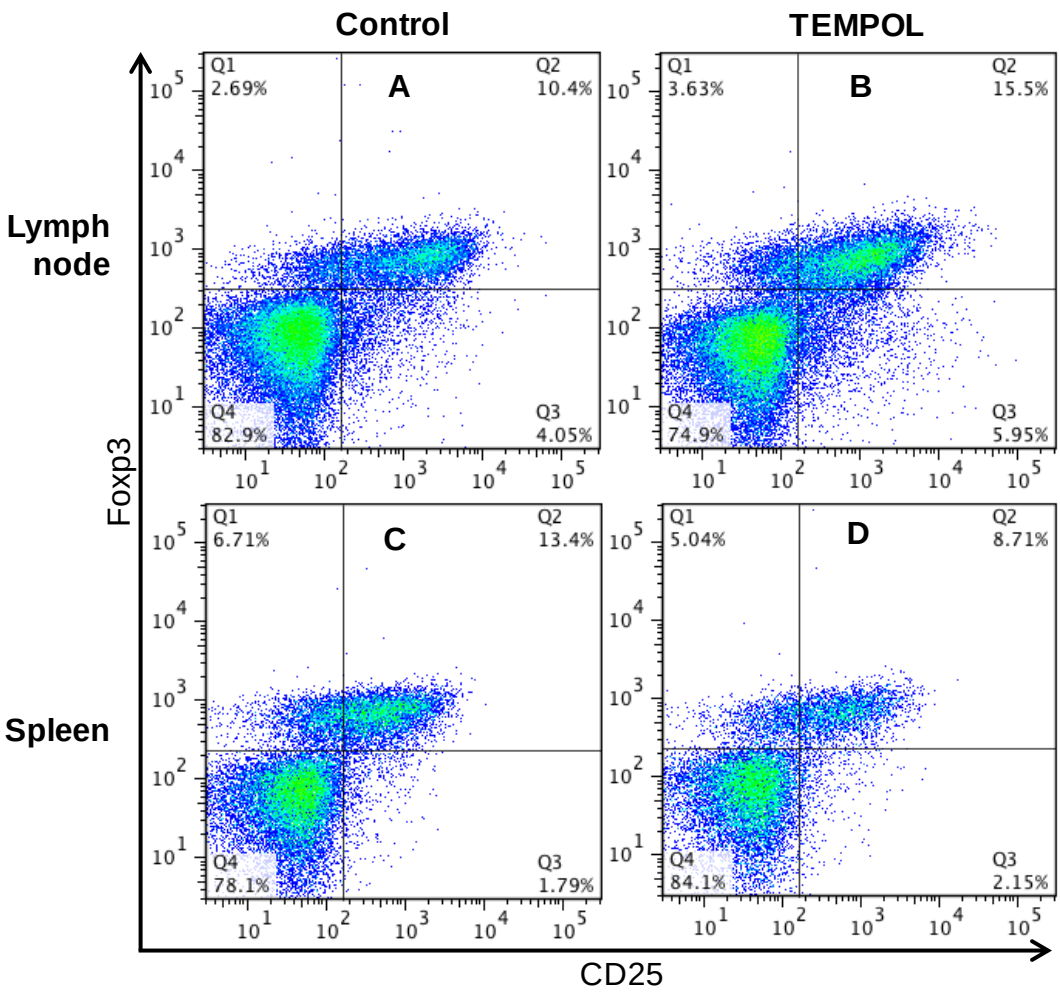

E

% of CD4+ T cells that are CD25+Foxp3+	Control Average %	TEMPOL Average %	P value
Lymph node	9.7 ±2.6	12.3 ±2.5	0.027*
Spleen	10.2 ±2.2	8.8 ±1.1	0.045*

Figure 3.7: TEMPOL-fed EAE mice show altered CD4+CD25+Foxp3+ T_{reg} cell populations compared to controls. The T_{reg} population (upper right quadrant) was found to be enriched in lymph nodes in TEMPOL-fed animals (A,B), but decreased in spleens (C,D). Cells were isolated 10 days after EAE induction in animals on control or TEMPOL feed for 14 days prior to immunization. Analyses were performed on flow cytometry data by gating the live cell population based on forward and side scatter, gating for CD4+CD8- T cells, then selecting CD25+Foxp3+ T_{reg} cells as a percentage of the CD4+ population. Representative flow cytometry dot plots are shown. Values (E) represent pooled results from 2 experiments, ±SD, with 13 mice per feed group. *P < 0.050, Mann-Whitney Rank Sum test, control vs. TEMPOL.

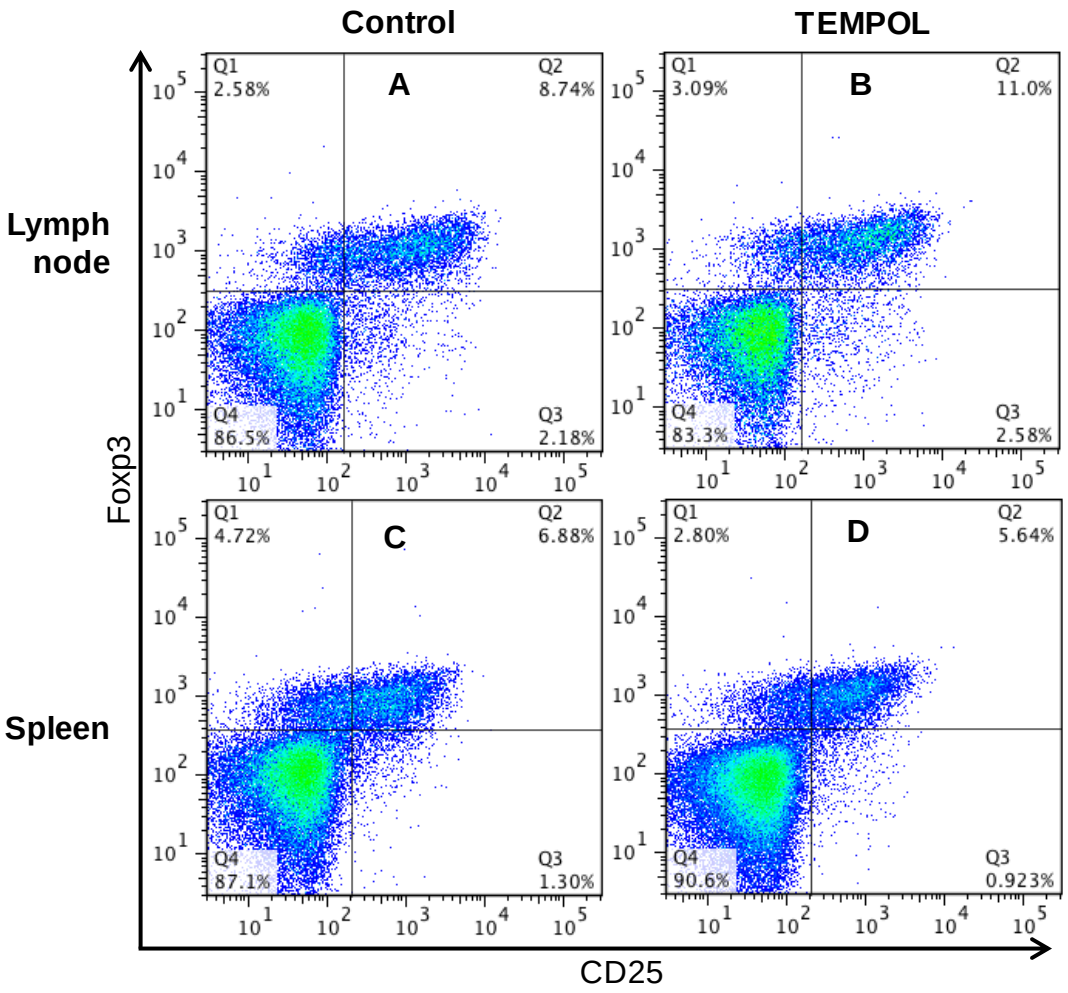

E

% of CD4+ T cells that are CD25+Foxp3+	Control Average %	TEMPOL Average %	P value
Lymph node	8.9 ±0.9	11.7 ±1.2	<0.001*
Spleen	7.0 ±0.6	6.1 ±0.6	0.003*

Figure 3.8: TEMPOL-fed <u>healthy</u> mice show altered CD4+CD25+Foxp3+ T_{reg} cell populations compared to controls. The T_{reg} population (upper right quadrant) was found to be enriched in lymph nodes in TEMPOL-fed animals (A,C), but decreased in spleens (B,D). Cells were isolated at Day 28 after start of TEMPOL or control diet. Analyses were performed on flow cytometry data by gating the live cell population based on forward and side scatter, gating for CD4+CD8- T cells, then selecting CD25+Foxp3+ T_{reg} cells as a percentage of the CD4+ population. Representative flow cytometry dot plots are shown. Values (E) represent pooled results from 2 experiments, ±SD, with 13 mice per feed group. *P < 0.050, Mann-Whitney Rank Sum test, control vs. TEMPOL.

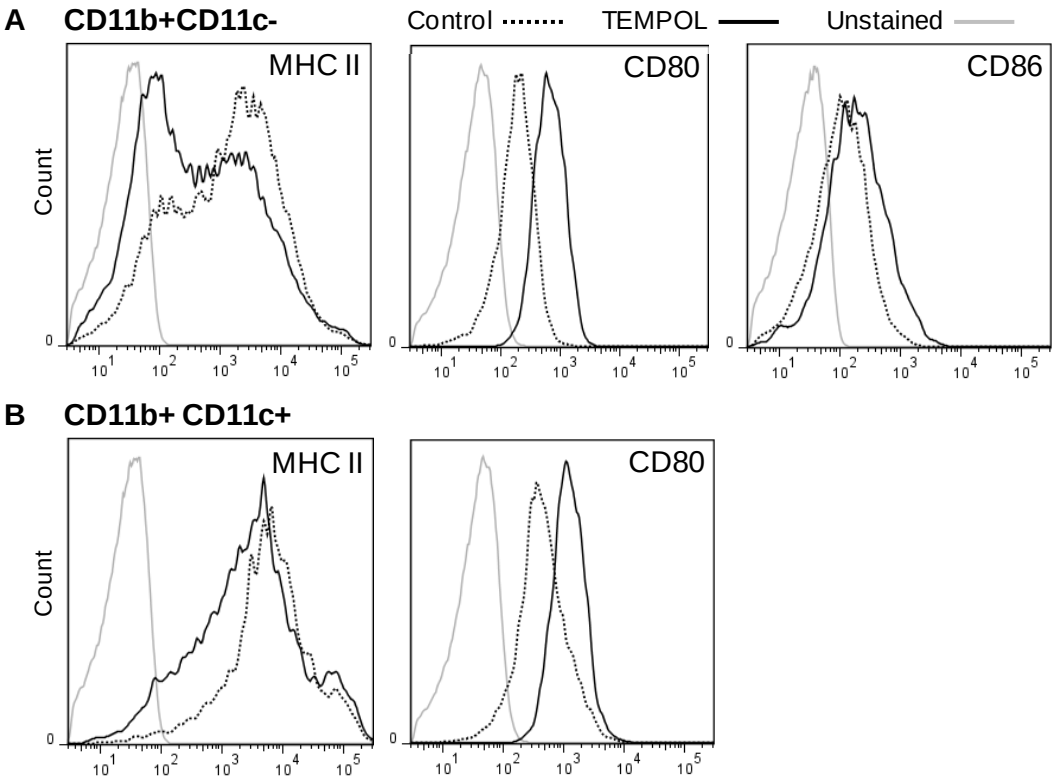

C

CD11b+CD11c-	Control Average MFI	TEMPOL Average MFI	P value
MHC II	1113.6 ±289.5	821.8 ±298.3	0.021*
CD80	211.1 ±24.0	295.5 ±126.3	<0.001*
CD86	130.5 ±38.7	176.1 ±60.3	0.033*
CD11b+CD11c+			
MHC II	5817.0 ±1334.9	4523.0 ±748.0	0.021*
CD80	441.2 ±43.6	544.7 ±212.9	0.024*

Figure 3.9: Markers associated with co-stimulation are altered in <u>lymph nodes</u> of TEMPOL-fed EAE mice. Analyses were performed 10 days after EAE induction in animals on control or TEMPOL feed for 14 days prior to immunization. Analyses were performed on flow cytometry data by selecting the live cells based on forward and side scatter, then selecting the CD45+ leukocyte population, then gating CD11b+CD11c- (A) or CD11b+CD11c+ (B) cells. The MFI was then calculated for each surface marker, and values from 2 experiments (13 mice per feed group) were pooled for statistical analysis (C). Representative histograms are shown. *P < 0.050, Mann-Whitney Rank Sum test, control vs. TEMPOL.

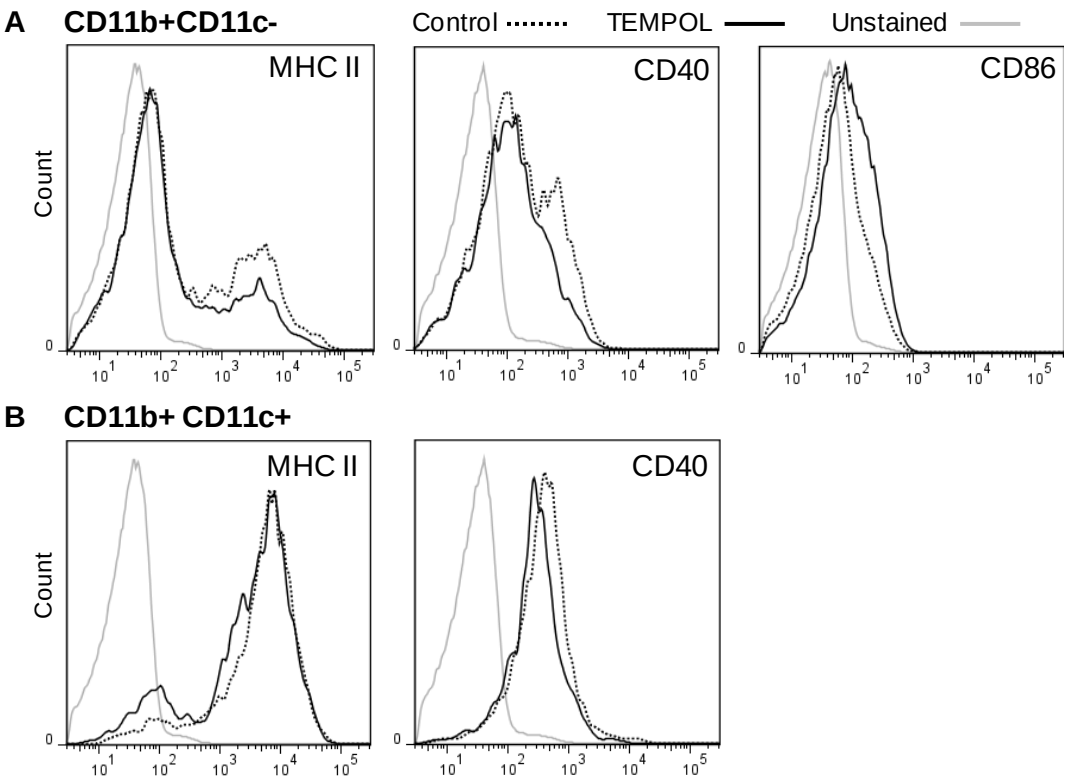

C

CD11b+CD11c-	Control Average MFI	TEMPOL Average MFI	P value
MHC II	122.4 ±60.4	87.9 ±8.5	<0.001*
CD40	119.6 ±14.4	103.8 ±7.8	0.008*
CD86	69.5 ±19.6	88.4 ±28.3	0.040*
CD11b+CD11c+			
MHC II	4660.6 ±1552.4	3188.6 ±1471.9	0.005*
CD40	455.1 ±80.0	352.7 ±61.4	0.002*

Figure 3.10: Markers associated with co-stimulation are altered in <u>spleens</u> of TEMPOL-fed EAE mice. Analyses were performed 10 days after EAE induction in animals on control or TEMPOL feed for 14 days prior to immunization. Analyses were performed on flow cytometry data by selecting the live cells based on forward and side scatter, then selecting the CD45+ leukocyte population, then gating CD11b+CD11c- (A) or CD11b+CD11c+ (B) cells. The MFI was then calculated for each surface marker, and values from 2 experiments (13 mice per feed group) were pooled for statistical analysis (C). Representative histograms are shown. *P < 0.050, Mann-Whitney Rank Sum test, control vs. TEMPOL.

Chapter 4: *In vitro* Results

4.1 TEMPOL enhances T cell proliferation at biologically relevant doses *in vitro*

Since proliferation and expansion of activated cells is an important part of the initiation and subsequent development of an immune response, the influence of TEMPOL on cell proliferation was studied *in vitro*. To first rule out toxicity as a means by which TEMPOL may influence T cells responses, unstimulated or anti-CD3 stimulated mouse spleen cultures were tested for viability following 48 hours of exposure to a wide range of TEMPOL doses (Figure 4.1). No reduction in viable cell staining or increase in dead cell staining was observed until doses of 1000 µM TEMPOL or greater were applied.

To determine the effect of added TEMPOL on cell proliferation *in vitro*, splenocytes were isolated from healthy C57BL/6J mice. Cells were either left unstimulated, or cultured with varying doses of anti-CD3. Anti-CD3 was titrated to determine an optimal dose for proliferation, and 0.125 µg/mL was chosen because it achieved better than half-maximal stimulation (Figure 4.2). Other doses were selected as two-fold increases above this value. TEMPOL was found to enhance cell proliferation at doses of 50 to 100 µM (Figure 4.3 A), which overlap with the values (10 to 60 µM) that are measured in the blood of animals on a prophylactically efficacious dose of TEMPOL. Co-incubation with doses of 200 µM TEMPOL or greater reduced proliferation to below baseline (0 µM TEMPOL) activity, with all doses of anti-CD3.

TEMPOL's influence on cell proliferation was compared to that of its reduced form, TEMPOL-H, and to another common antioxidant, ascorbic acid. TEMPOL-H also increased cell proliferation with doses up to 100 µM, but less so than TEMPOL (Figure 4.3 B). The positive effect of TEMPOL-H on proliferation peaked at 100 µM, though TEMPOL-H did not begin to decrease proliferation below baseline levels (0 µM TEMPOL-H) until a 400 µM dose was applied. In contrast to TEMPOL and TEMPOL-H, ascorbic acid decreased cell proliferation steadily in a dose-dependent manner, reaching statistical significance with an 800 µM dose (Figure 4.3 C).

Similar experiments to examine proliferation *in vitro* were also performed using both lymph node (Figure 4.4) and spleen (Figure 4.5) cells isolated from EAE mice. Cells were either left unstimulated, or cultured with MOG 35-55 or anti-CD3. Similar to experiments with healthy mice, cell proliferation in all conditions was increased with TEMPOL up to the 100 µM dose. 200 µM TEMPOL decreased proliferation compared to 100 µM in all conditions, but only in spleen cells did 200 µM TEMPOL decrease proliferation to levels at or below those observed with 0 µM TEMPOL (Figure 4.5).

4.2 TEMPOL enhances mixed lymphocyte reactions *in vitro*

In vitro experiments with anti-CD3 allow us to study the effect of TEMPOL on a somewhat artificially expanded cell population. In contrast, a mixed lymphocyte reaction (MLR) serves as a more representative model of an immune response *in situ*, similar to what would occur in the recognition of non-self cells by self. Both mouse and human MLR models were used.

A one-way MLR model was used for studies with mice, where adherent macrophages from FVB mice served as the stimulus for non-matched co-cultured C57BL/6J splenocytes to proliferate as they recognize non-self. C57BL/6J cells were seeded at three different densities: 2, 4, and 8 x 10^5 cells per well. The response was found to be most robust with 4 x 10^5 cells per well, though trends were similar across all seeding densities. 100 µM TEMPOL significantly enhanced proliferation compared to 0 µM TEMPOL, while proliferation levels with 200 µM TEMPOL tended to be comparatively decreased (Figure 4.6 A). Mouse MLR experiments were also performed using TEMPOL-H, and a trend towards a similar dose-dependent increase in proliferation was observed. However, peak proliferation with TEMPOL-H was observed at 200 µM, rather than at 100 µM as seen with TEMPOL (Figure 4.6 B). Similar to findings with TEMPOL, proliferation was generally decreased with TEMPOL-H at doses above 200 µM.

Two-way MLR experiments using healthy human donors did not distinguish between responding cell populations. Human MLR experiments were analyzed using flow cytometry and focused on expansion of specific cell populations, with antibody stains chosen to measure cell proliferation specifically in CD3+, CD4+, CD8+, and T_{reg} cell populations rather than global proliferation measured via incorporated thymidine. Trends were similar over both the Day 10 and Day 14 collection times, but more robust responses were observed at Day 14, and this data was therefore used for further analysis. Instead of tritiated thymidine incorporation, CFSE dilution was used as a measurement of cell proliferation in human MLR experiments. CFSE is a cell-permeable fluorescent dye that can be retained within

cells for long periods of time. When these cells divide, their daughter cells also contain CFSE, but a more dilute amount, which becomes more dilute with each subsequent division. Flow cytometry can then be used to visualize rounds of proliferation by plotting the cells of interest against an axis of CFSE intensity – more cells with low CFSE levels indicates that the parent cells have proliferated further.

TEMPOL was found to enhance the number of cells with diluted CFSE in a dose-dependent manner (Figure 4.7 A), with 200 µM TEMPOL significantly increasing proliferation and expansion of both CD4+ and CD8+ T cells (Figure 4.7 B). While both CD4+ and CD8+ T cell populations proliferated to a greater extent in the presence of TEMPOL, the CD8+ population became a greater proportion of the cell population by Day 14 (Figure 4.8). This suggests either increased proliferation, or augmented viability in the presence of 200 µM TEMPOL. Because regulatory T (T_{reg}) cells are thought to influence immune responses, we examined whether or not the proportion of CD25+Foxp3+ T_{reg} cells within the CD4+ compartment was altered by the presence of TEMPOL. Indeed, CD25+Foxp3+ T_{reg} cells within the CD4+ T cell compartment were reduced with TEMPOL at both given doses (Figure 4.9). CD25+Foxp3+ cells within the CD8+ T cell population were slightly enriched with 200 µM TEMPOL, but are less than 1% of all CD8+ T cells.

Human MLR experiments also tested the effect of TEMPOL-H at 50 and 200 µM. Results showed that TEMPOL-H enhanced proliferation of both CD4+ and CD8+ T cells (Figure 4.10), but again specifically and significantly enriched CD8+ T cells with a 200 µM dose (Figure 4.11). CD4+CD25+Foxp3+ T_{reg} cells were also reduced with TEMPOL-H at 200 µM (Figure 4.12). For all human MLR experiments,

single-donor PBMCs alone were used as controls, and showed low levels of proliferation that were not enhanced by 200 µM TEMPOL or TEMPOL-H (Figure 4.13).

4.3 TEMPOL influences antigen presenting and co-stimulatory molecule expression on splenic subpopulations *in vitro*

Because TEMPOL-fed mice demonstrated altered antigen presenting and co-stimulatory molecule expression compared to controls, we examined whether or not similar changes may be occurring *in vitro* and influencing immune cell proliferative responses. To determine the effect of added TEMPOL on *in vitro* spleen cell surface marker expression, spleen cells were isolated from healthy C57BL/6J mice and either left unstimulated or co-cultured with TEMPOL or TEMPOL-H at the indicated doses. The cells were collected after 48 hours and stained for analysis by flow cytometry. The MFI of each stain was used as a measure of surface marker expression level.

Within the CD11b+CD11c- myeloid cell population, expression of both CD80 and CD86 was significantly reduced on cells treated with 200 µM TEMPOL or TEMPOL-H (Figure 4.14). Lower concentrations of TEMPOL or TEMPOL-H had more variable results. CD80 expression was also reduced with 100 µM TEMPOL (Figure 4.14 A), while CD86 expression was reduced with 100 µM TEMPOL-H (Figure 4.14 B). While not significant, a trend towards decreased MHC II expression with both TEMPOL and TEMPOL-H at 200 µM was observed. Expression levels of

MHC I and CD40 were also studied, but no significant differences were observed in the myeloid cell population.

Within the CD11b+CD11c+ myeloid DC population, expression levels of CD80 and CD86 were significantly decreased with 50 µM TEMPOL and 200 µM TEMPOL-H (Figure 4.15). MHC II was also significantly decreased with 200 µM TEMPOL-H in this population (Figure 4.15 B), while only a trend towards decreased MHC II expression was observed with TEMPOL (Figure 4.15 A). Again, no change in MHC I or CD40 was observed in myeloid DCs. The CD11b-CD11c+ lymphoid DC compartment of the spleen cultures was also examined, but no significant changes in surface marker expression were observed (data not shown).

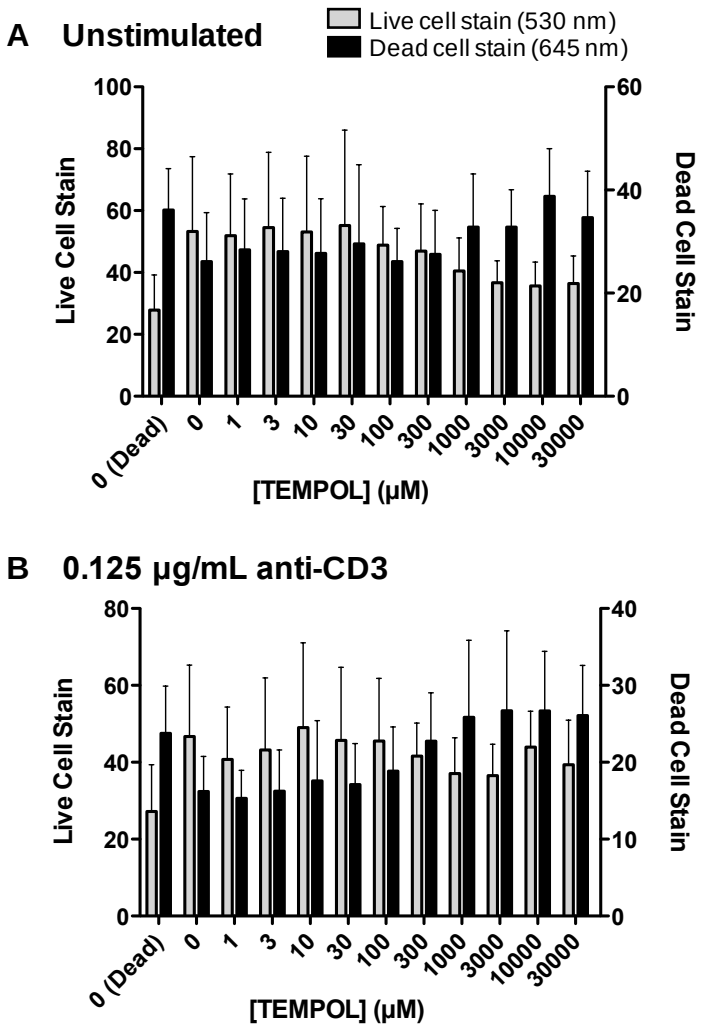

Figure 4.1: TEMPOL is not toxic to immune cells at physiologically relevant doses of 10 – 60 µM. TEMPOL was tested at doses from 1 - 30,000 µM on (A) resting and (B) anti-CD3 stimulated splenocytes isolated from healthy mice. Following 48 hours of incubation with TEMPOL and the addition of Invitrogen Live/Dead Cell kit dyes, cell viability was determined from fluorescence measurements. For a positive (dead) control, cells were exposed to 70% methanol for 15 minutes. Bars represent the average fluorescence readings of triplicate wells, ±SD. Representative figures from 1 of 3 experiments are shown.

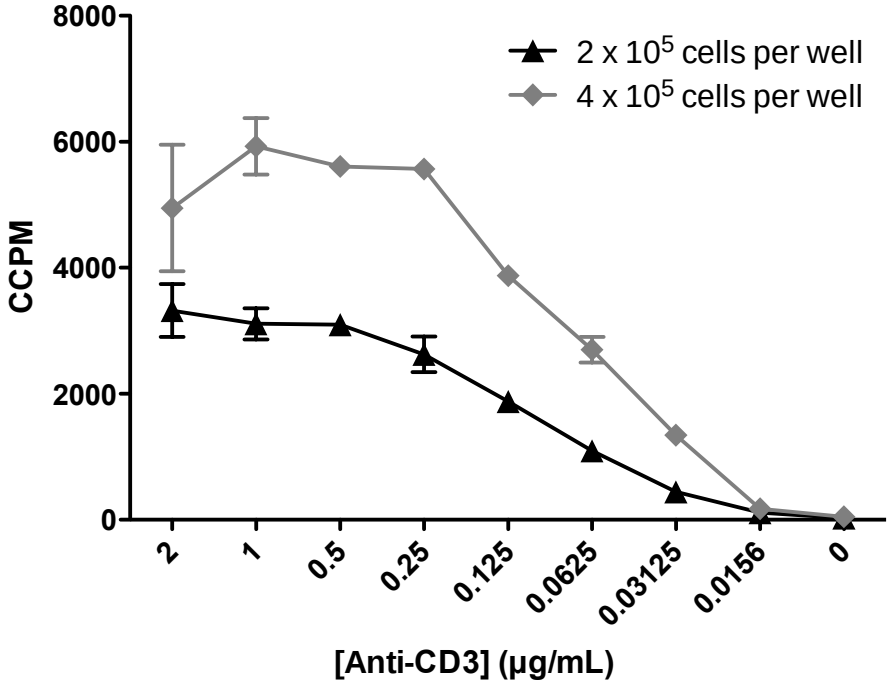

Figure 4.2: Titration of anti-CD3 shows 0.125 µg/mL to be the desired dose for cell proliferation experiments. Under these culture conditions, this dose achieved better than half-maximal stimulation. Cells isolated from healthy mouse spleens were seeded in triplicate at the indicated concentrations with soluble anti-CD3 (clone 2C11) for 48 hours, and thymidine incorporation was measured over the next 16 hours. Points represent average cell counts per minute (CCPM) from 3 wells (n = 1 experiment), ±SD.

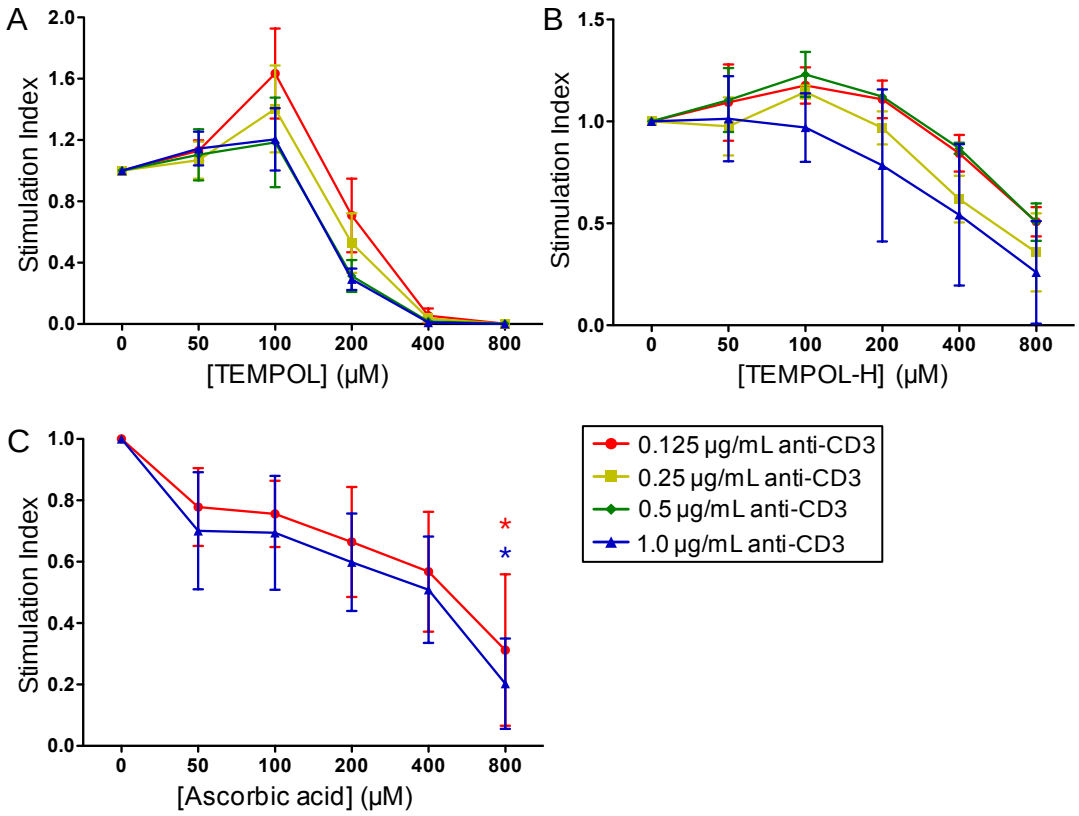

Figure 4.3: TEMPOL's influence on proliferation is similar to its reduced form, TEMPOL-H, but differs from the effect of ascorbic acid. Healthy murine spleen cells were treated for 48 hours with anti-CD3 as indicated and A) TEMPOL, B) TEMPOL-H, or C) ascorbic acid. Points represent the average results of 3 experiments, with bars ±SD. Data were normalized to obtain SI values by dividing the CCPM of each treatment by the CCPM of untreated (0 μM dose) samples. *Significant vs. 0 μM dose, $P < 0.05$. One-way ANOVA on ranks with Dunn's multiple comparison tests.

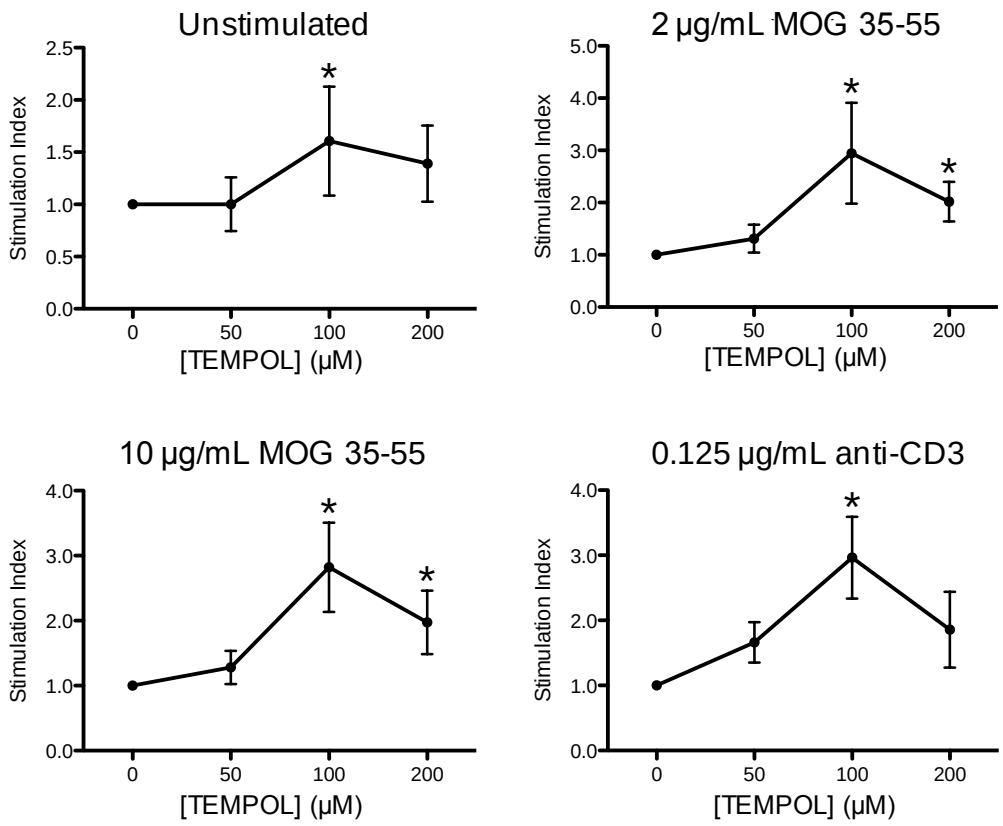

Figure 4.4: Lymph node cell proliferation is influenced by TEMPOL in culture. Lymph node cells from EAE mice were cultured in triplicate with the indicated stimulations and TEMPOL doses. Data were normalized to obtain SI values as described previously. Points represent the mean SI of lymph nodes from 6 mice, ±SD. *Significant vs. 0 µM TEMPOL, $P < 0.05$. One-way ANOVA on ranks with Dunn's multiple comparison tests.

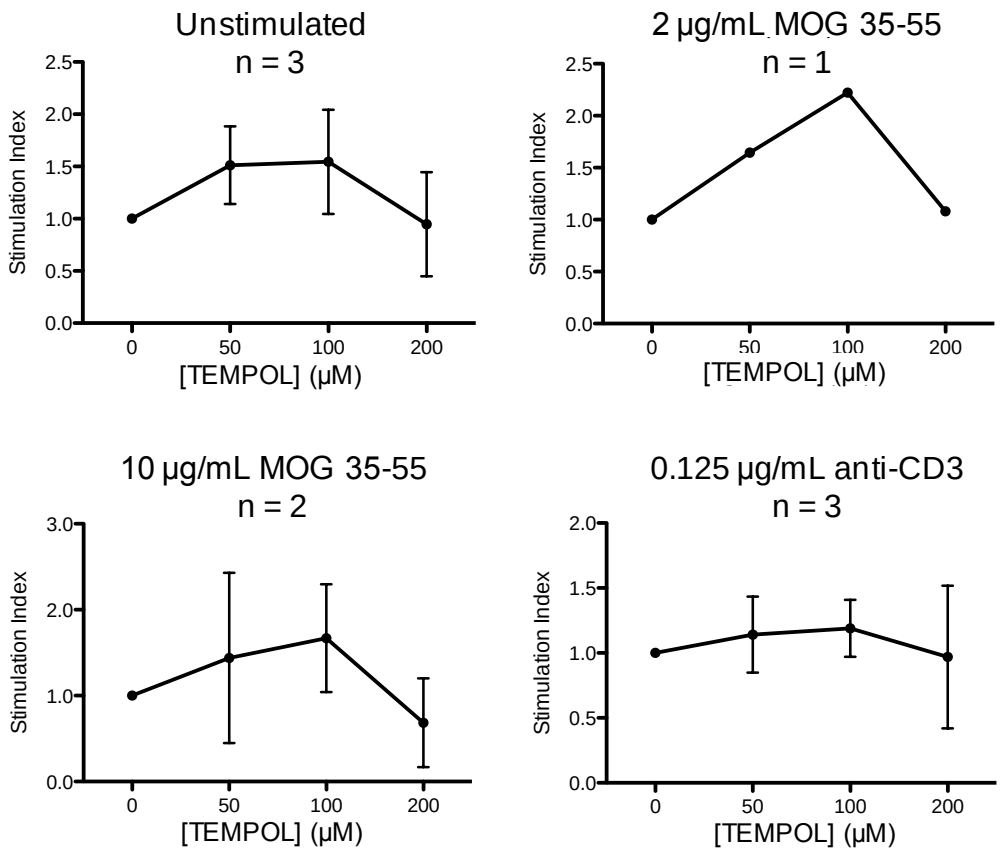

Figure 4.5: Spleen cell proliferation is influenced by TEMPOL in culture. Spleen cells from EAE mice were cultured in triplicate with the indicated stimulations and TEMPOL doses. Data were normalized to obtain SI values as described previously. Points represent the mean SI of spleens from n mice, ±SD.

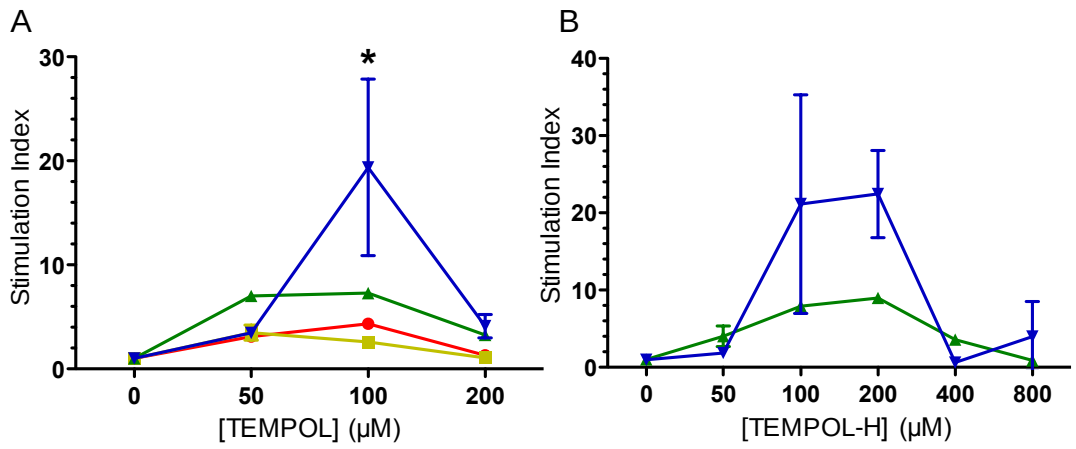

Figure 4.6: Mouse mixed lymphocyte reactions are enhanced by TEMPOL and TEMPOL-H. Background proliferation of the C57BL/6J cells alone as well as the response of FVB cells alone was negligible (not shown). Proliferation was measured by tritiated thymidine incorporation in the 16 hours following 72 hours of culture. Data were normalized to obtain SI values as described previously. Each line represents a unique mouse. Points represent the average SI of triplicate wells, with bars ±SD. Graphs illustrate A) n = 4 or B) n = 2 experiments. *Pooled results significant vs. 0 μM TEMPOL, $P < 0.05$. One-way ANOVA on ranks with Dunn's multiple comparison tests.

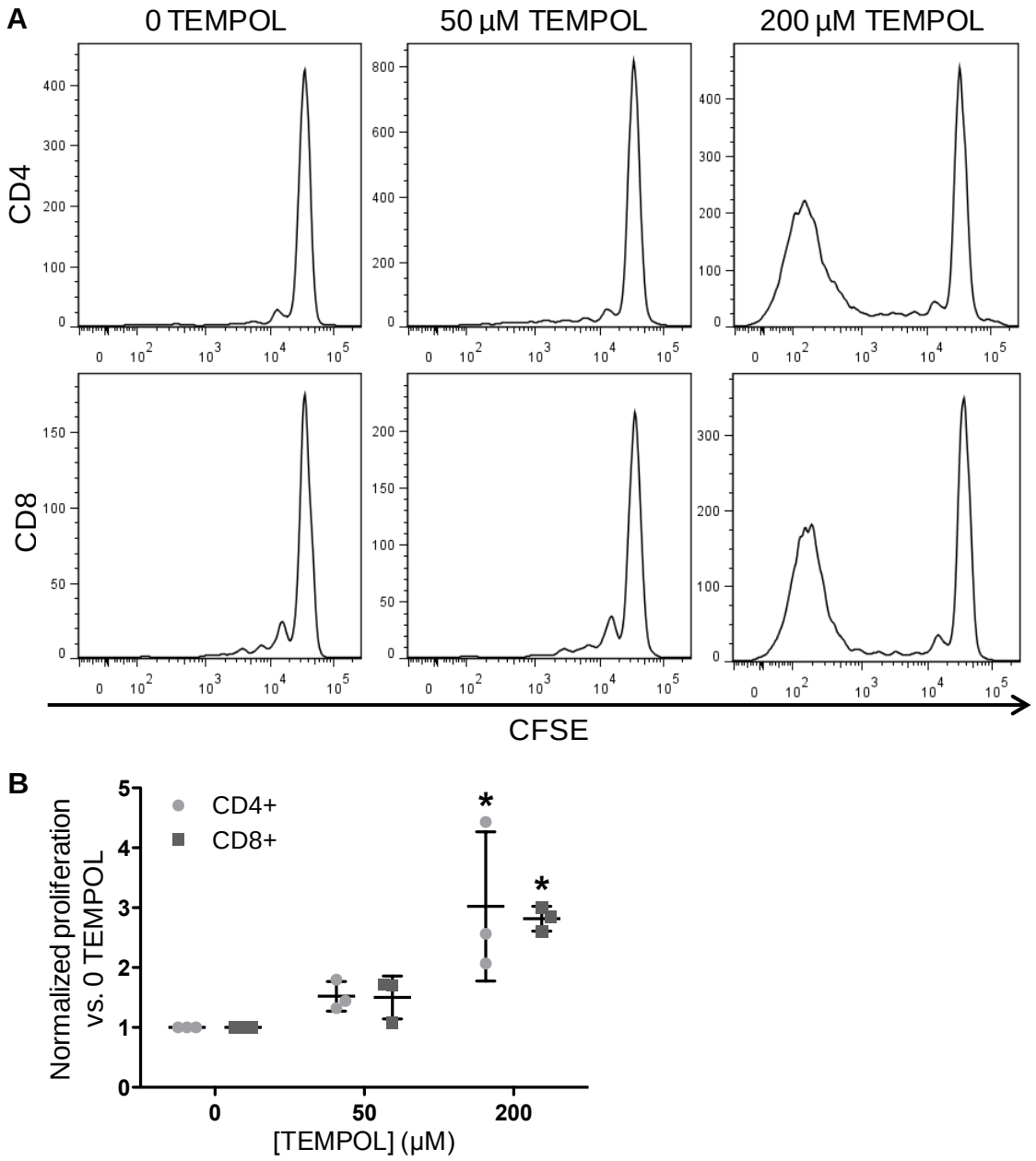

Figure 4.7: TEMPOL enhances T cell proliferation in human mixed lymphocyte reactions. Proliferation (measured by CFSE dilution) of both CD4+ and CD8+ T cells was significantly increased with 200 µM TEMPOL by Day 14 of the MLR. A) Representative histograms are shown from 1 of 3 experiments, showing CFSE levels in the CD4+ and CD8+ T cell populations. B) The graph shows the average results of 3 experiments performed in triplicate, with bars ±SD. Data were normalized by dividing the % of cells that proliferated at each dose by the % that proliferated with 0 µM TEMPOL. *Significant vs. 0 µM TEMPOL, $P < 0.05$. One-way ANOVA on ranks, Dunn's multiple comparison tests.

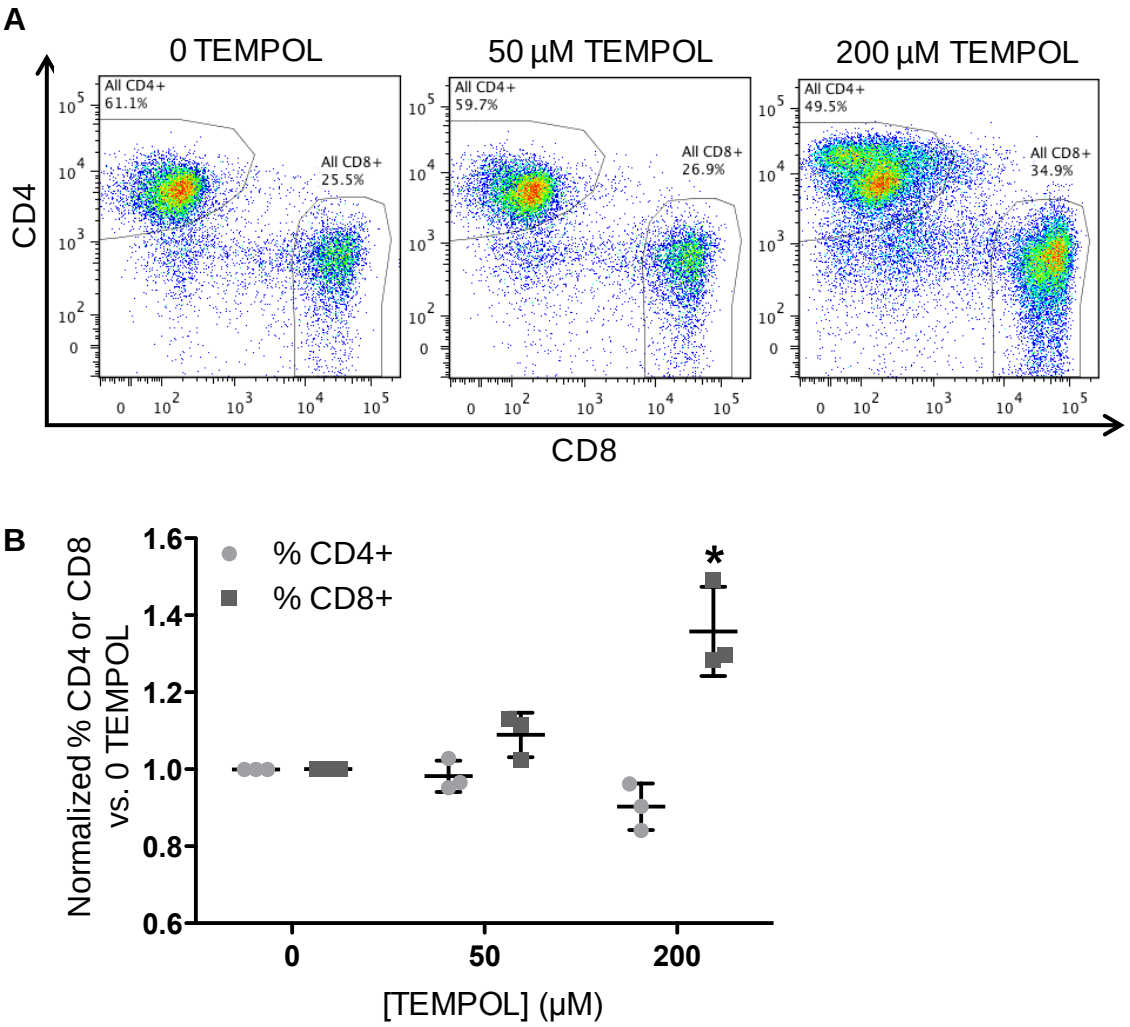

Figure 4.8: TEMPOL preferentially enriches CD8+ over CD4+ T cells in human mixed lymphocyte reactions. The CD8+ T cell population was significantly enriched with 200 µM TEMPOL by Day 14 of the MLR. A) Representative figures are shown from 1 of 3 experiments, indicating CD4+ and CD8+ T cells as percentages of the CD3+ T cell population. B) The graph shows average results of 3 experiments performed in triplicate. Data were normalized by dividing the % of CD3+ T cells that are CD4 or CD8+ at each dose by the % that are CD4 or CD8+ with 0 µM TEMPOL. *Significant vs. 0 µM TEMPOL, $P < 0.05$. One-way ANOVA on ranks, Dunn's multiple comparison tests.

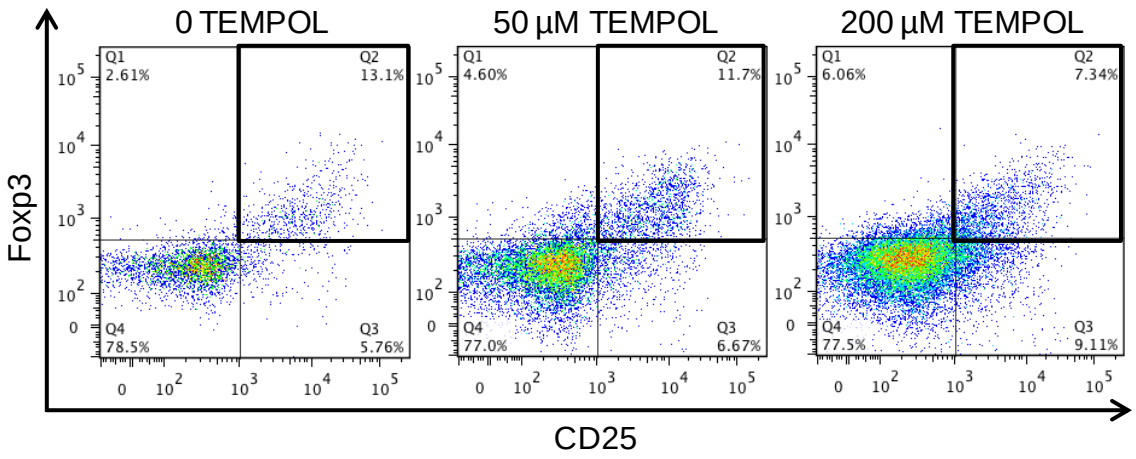

Figure 4.9: Regulatory T cells are decreased with TEMPOL in a human mixed lymphocyte reaction in a dose-dependent manner. Figures show Foxp3 versus CD25 expression within the CD4+ T cell population on Day 14 of the MLR. The highlighted upper right quadrant of each plot indicates the CD4+Foxp3+CD25+ T_{reg} cell population. Figures are from a single experiment performed in triplicate wells.

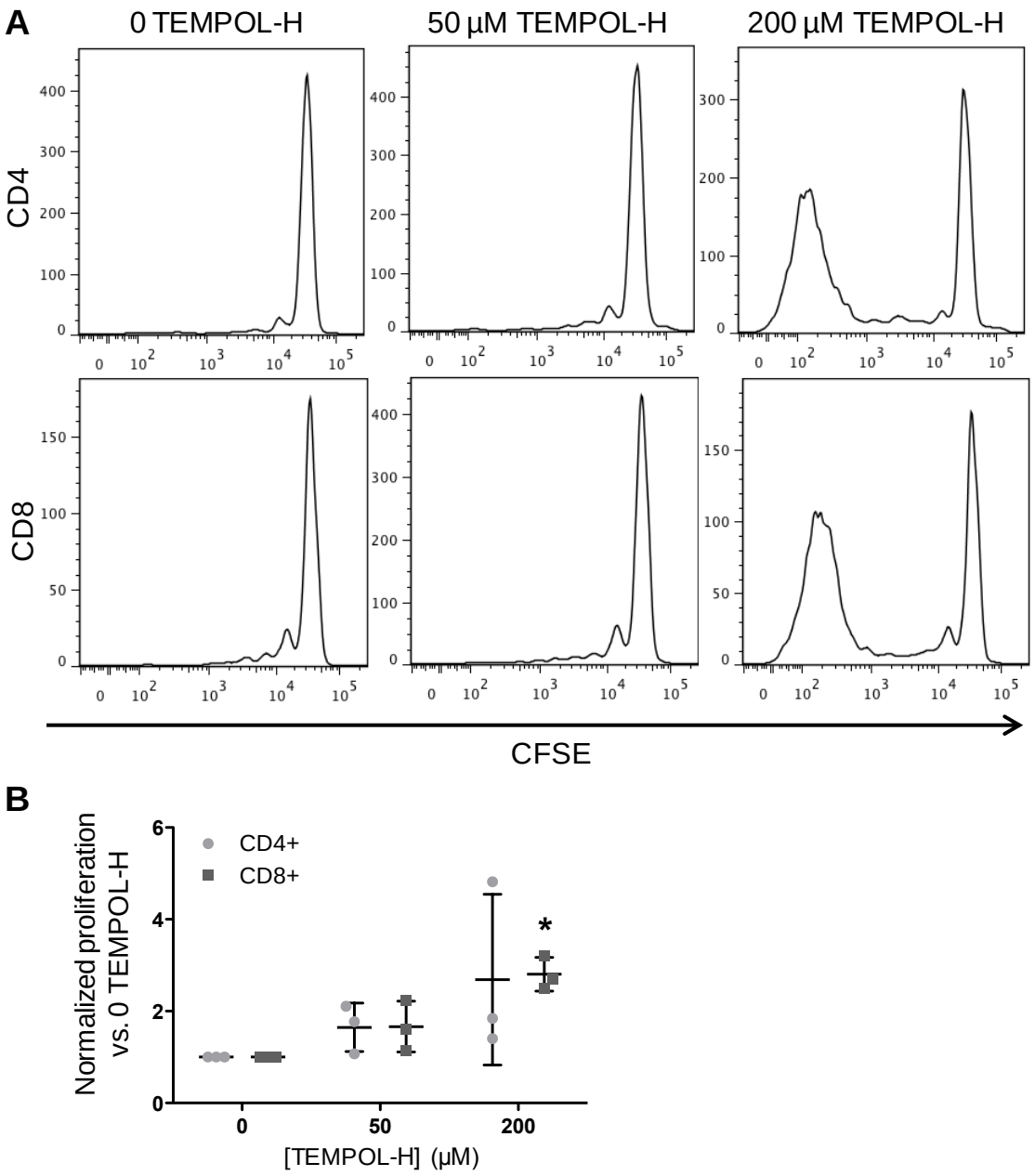

Figure 4.10: TEMPOL-H enhances T cell proliferation in human mixed lymphocyte reactions at Day 14. Proliferation (measured by CFSE dilution) of CD8+ T cells was significantly increased with 200 µM TEMPOL. A) Representative histograms are shown from 1 of 3 experiments. B) Graph shows the average results of 3 experiments performed in triplicate, with bars ±SD. Data were normalized by dividing the % of cells that proliferated at each dose by the % that proliferated with 0 µM TEMPOL-H. *Significant vs. 0 µM TEMPOL-H, $P < 0.05$. One-way ANOVA on ranks, Dunn's multiple comparison tests.

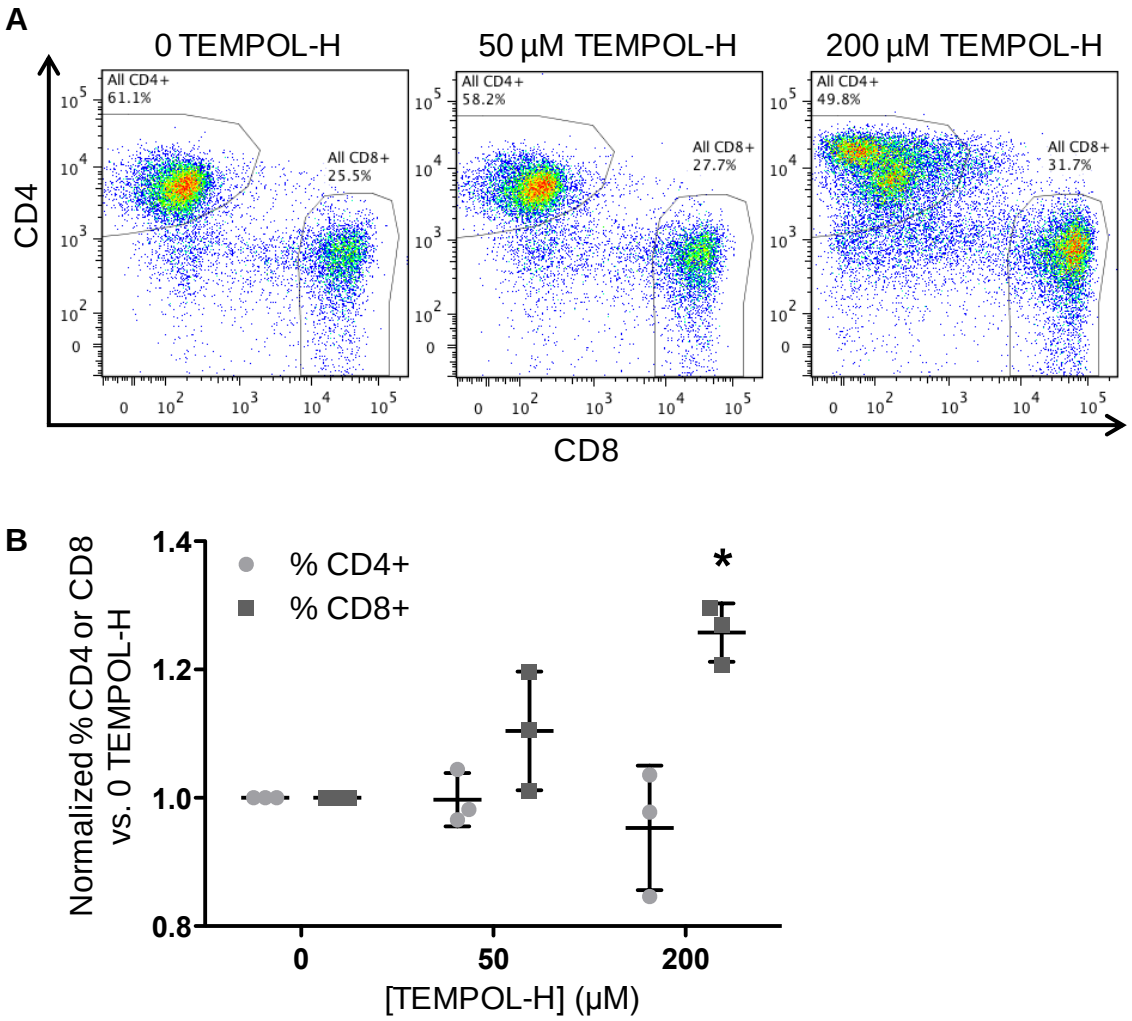

Figure 4.11: TEMPOL-H preferentially enriches CD8+ over CD4+ T cells in human mixed lymphocyte reactions. The CD8+ T cell population was significantly enriched with 200 µM TEMPOL-H by Day 14 of the MLR. A) Representative figures are shown from 1 of 3 experiments, indicating CD4+ and CD8+ T cells as percentages of the CD3+ T cell population. B) The graph shows average results of 3 experiments performed in triplicate. Data were normalized by dividing the % of CD3+ T cells that are CD4 or CD8+ at each dose by the % that are CD4 or CD8+ with 0 µM TEMPOL-H. *Significant vs. 0 µM TEMPOL-H, $P < 0.05$. One-way ANOVA on ranks, Dunn's multiple comparison tests.

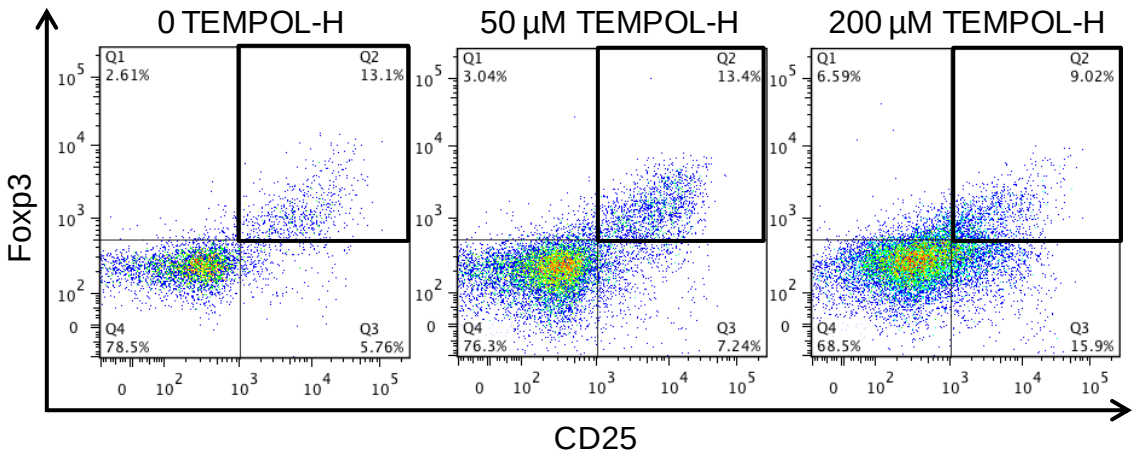

Figure 4.12: Regulatory T cells are decreased with TEMPOL-H in a human mixed lymphocyte reaction in a dose-dependent manner. Figures show Foxp3 versus CD25 expression within the CD4+ T cell population on Day 14 of the MLR. The highlighted upper right quadrant of each plot indicates the CD4+Foxp3+CD25+ T_{reg} cell population. Figures are from a single experiment performed in triplicate wells.

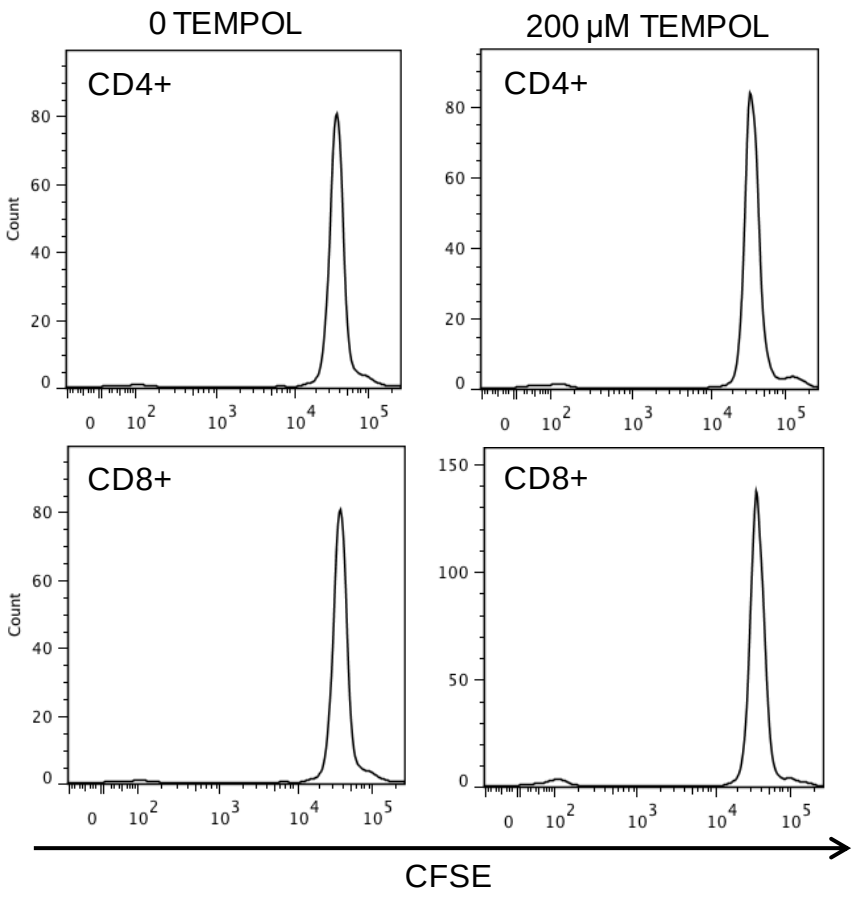

Figure 4.13: Unstimulated PBMCs show low proliferation that is not altered by TEMPOL. Figures show CFSE dilution of single-donor CD4+ and CD8+ T cells at Day 14 post-seed. The effect of TEMPOL-H on unstimulated PBMCs was not examined. Representative figures from 1 of 3 experiments are shown. One-way ANOVA on ranks, Dunn's multiple comparison tests.

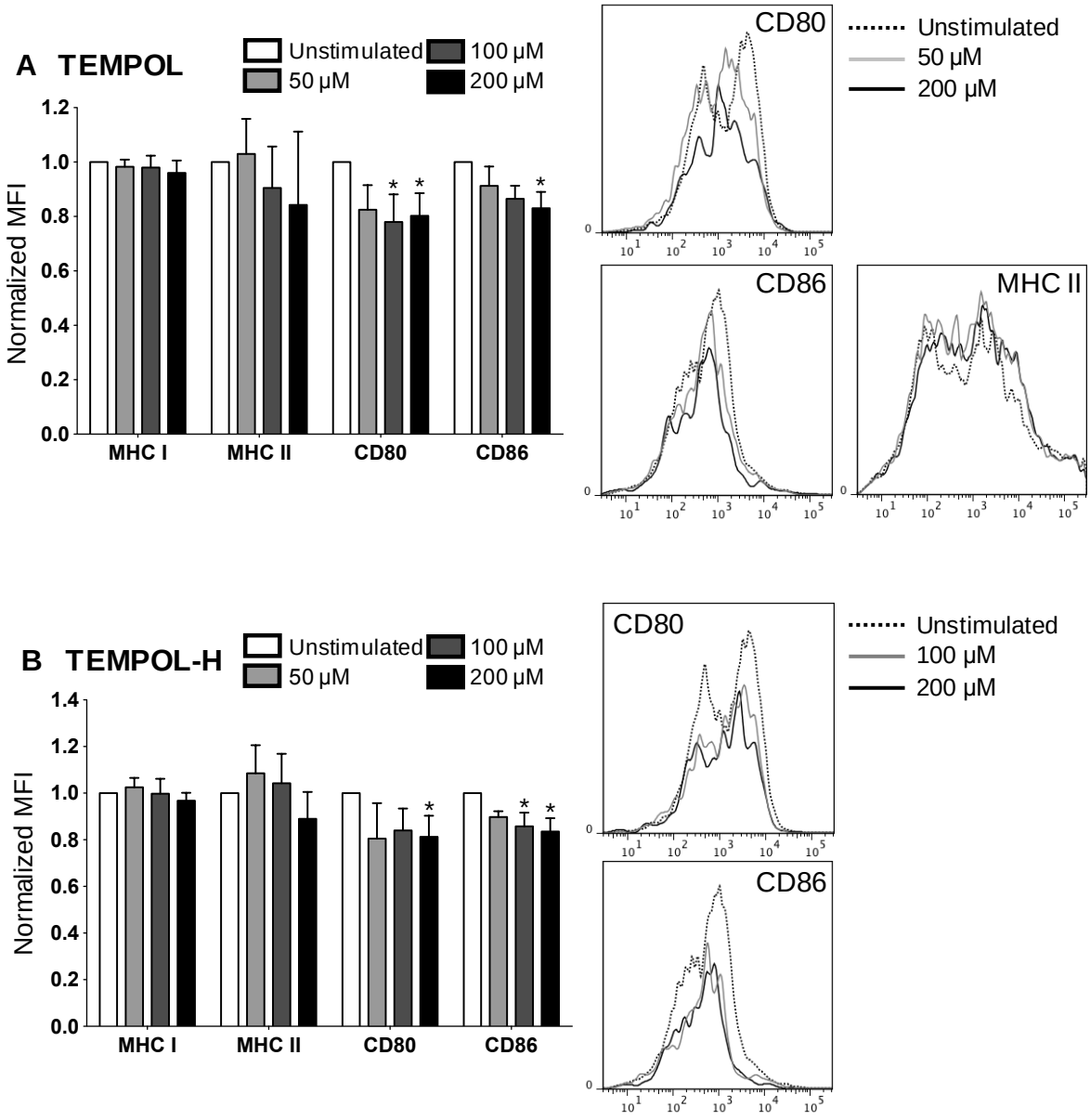

Figure 4.14: Expression of CD80 and CD86 is significantly reduced by TEMPOL and TEMPOL-H in splenic myeloid cells. A trend towards decreased MHC II expression was observed with TEMPOL, but was not significant. Healthy murine spleen cells were cultured for 48 hours with A) TEMPOL, or B) TEMPOL-H as indicated, then stained for flow cytometry. Analysis was performed by gating CD11b+CD11c- cells as a proportion of CD45+ leukocytes. MFI values for each surface marker were obtained, then normalized by dividing the MFI at each dose of TEMPOL or TEMPOL- H by the MFI value at the 0 µM dose. Bars represent pooled results of 4 experiments, ±SD. Representative histograms are shown. *Significant vs. 0 µM dose, $P < 0.05$. One-way ANOVA on ranks with Dunn's multiple comparison tests.

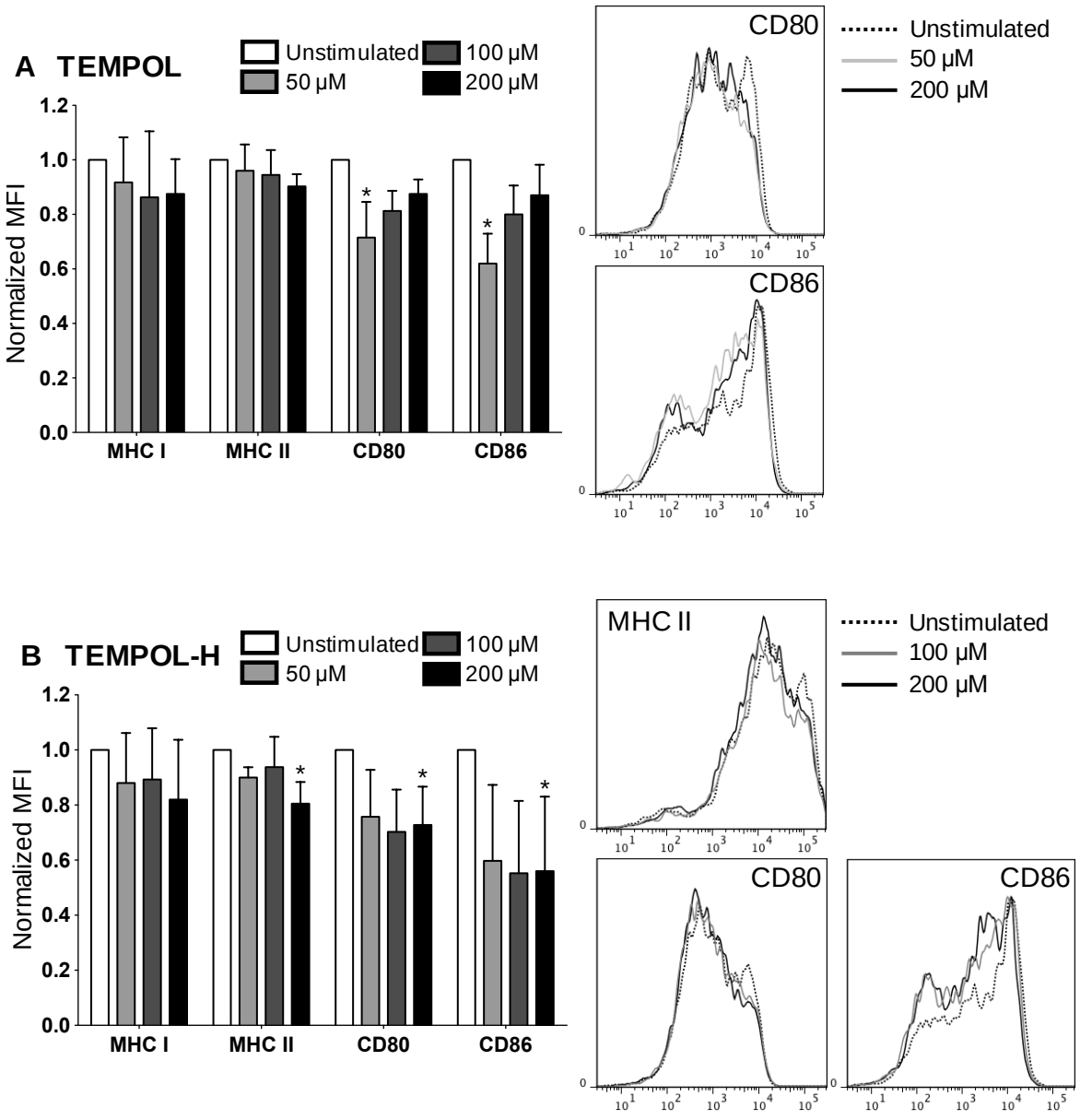

Figure 4.15: Expression of CD80 and CD86 is significantly reduced by TEMPOL and TEMPOL-H in splenic myeloid dendritic cells. MHC II expression was also significantly reduced by TEMPOL-H at 200 µM. Healthy murine spleen cells were cultured for 48 hours with A) TEMPOL, or B) TEMPOL-H as indicated, then stained for flow cytometry. Analysis was performed by gating CD11b+CD11c+ cells as a proportion of CD45+ leukocytes. MFI values for each surface marker were obtained, then normalized as described previously. Bars represent pooled results of 4 experiments, ±SD. Representative histograms are shown. *Significant vs. 0 µM dose, $P < 0.05$. One-way ANOVA on ranks with Dunn's multiple comparison tests.

Chapter 5: Discussion

5.1 Summary

Previous studies performed by Quandt *et al.* (unpublished data, manuscript in preparation) made it clear that the antioxidant TEMPOL effectively limits EAE disease symptoms in mice when given prophylactically. However, the exact mechanism of action by which TEMPOL affects disease remained unknown. Further, while previous studies with TEMPOL by other groups have demonstrated its anti-inflammatory and immunomodulatory effects, very few have investigated the means by which this occurs. The studies outlined in this thesis therefore endeavored to elucidate how TEMPOL might alter EAE pathogenesis, as well as how TEMPOL influences components of the immune system in healthy non-EAE animals, both *in vivo* and *in vitro*.

5.2 TEMPOL in EAE

The pathogenesis of our active EAE model can be roughly divided into four components, each of which may serve as a potential target for a modulator of inflammatory diseases such as TEMPOL [27]:

1. Self-reactive immune cells are activated in the periphery;
2. Altered BBB permeability facilitates entry of immune cells into the CNS;
3. Cells are reactivated when they encounter myelin, launching an immune response;

4. Other immune cells are recruited and mediators of inflammation are produced, leading to oxidative damage, demyelination, and neurodegeneration.

The studies described in this thesis have largely focused on the elements that are paramount to the initial steps of auto-reactive cell generation, development and differentiation of their phenotype. When EAE is induced, APCs presenting myelin fragments drain to the lymph nodes and travel to the spleen, and are thought to be representative of what occurs in the periphery. In the spleen, they encounter and activate naïve CD4+ T cells, causing them to differentiate into myelin-specific effector cells. These cells then cross the BBB into the CNS, where they are reactivated and can subsequently cause disease, by recruiting other immune cells and releasing cytotoxic cytokines such as IFNγ and TNFα [86, 87]. The initial T cell priming step is therefore an important component of disease development, where changes in the local microenvironment can alter the type of effector cells that are generated, potentially changing the phenotype of the immune response that is generated.

5.2.1 Contrast to immunosuppressive therapies

Immune-mediated diseases can often be effectively treated with immunosuppressive therapies, which function by globally limiting immune responses [88]. While effective, immunosuppression leaves a patient vulnerable to potentially life-threatening infections, so therapies with fewer adverse effects are generally preferred if they show efficacy. Mitoxantrone (Novantrone), for example, suppresses

proliferation of T cells, B cells, and macrophages [89]. It has been shown to effectively suppress EAE in mice, and has been approved as a DMT for MS. However, mitoxantrone has serious potential side effects, including cardiotoxicity, increased risk of infections, and cancer. As a result, it is indicated only for particularly aggressive forms of relapsing MS, when first-line therapies such as glatiramer acetate and interferon beta fail to be effective [90]. Teriflunomide (Aubagio) is a recently-approved oral MS therapy that inhibits T cell proliferation and activation [91]. Teriflunomide also ameliorates EAE, and it is relatively safe compared to mitoxantrone, but it still carries a risk of opportunistic infections [91]. In contrast, our results suggest that TEMPOL is not generally immunosuppressive – immune cells isolated from EAE mice on TEMPOL feed showed proliferative responses to antigen that were comparable to those of mice on control feed. This finding appears to be in opposition with studies performed in EAE using bilirubin, another potent antioxidant that ameliorates EAE [92]. In this study, T cell proliferation was found to be inhibited by bilirubin; however, this assay employed only CD4+ T cells, and this population was observed to be decreased in our *ex vivo* studies. Uric acid, which is also an antioxidant that is efficacious in EAE, does not limit *ex vivo* proliferative immune responses [93].

5.2.2 Production of pro-inflammatory cytokines

Rather than simply stopping an immune response, the studies described in this thesis suggest that TEMPOL is instead altering the nature/phenotype of the immune response that is generated/initiated. Analysis of the cytokines produced by

isolated lymphoid organ cells showed decreased levels of IFNγ, TNFα, and TGF-β1 production by cells isolated from TEMPOL-fed animals. IFNγ and TNFα are pro-inflammatory cytokines, promoting an inflammatory T_H1-type immune response that leads to ROS and RNS production, cytotoxicity, and tissue injury [94]. Both IFNγ and TNFα have been implicated in disease progression in MS, as well as in other immune-mediated diseases [95]. In the CNS, TNFα is observed within active lesions and in the CSF of people with MS, and is associated with BBB disruption [95]. *In vitro*, TNFα has been shown to mediate damage to myelin and oligodendrocytes [96]. IFNγ induces expression of MHC II, and has been shown to exacerbate MS when administered to patients [95]. The role of TGF-β1 is complex, paradoxically having both anti-inflammatory and pro-inflammatory effects [97]. However, studies show that TGF-β1 may be responsible for recruitment of neutrophils, monocytes, and macrophages during early stages of a localized inflammatory response [98]. Since our cells are taken during the early stages of EAE, a decrease in TGF-β1 during this time could be related to limited inflammation. TGF-β also plays a key role in the development of T_{reg} cells and T_H17 cells, though we did not observe any changes in IL-17 production by cells with TEMPOL [99].

Collectively, decreased production of these cytokines indicates a somewhat prototypical shift from a pro-inflammatory T_H1 response towards a more immunosuppressive or T_H2 type response. Driving such a shift has long been proposed to have beneficial effects in MS, and is the functional mechanism of the immunomodulator therapy glatiramer acetate [100]. Our cytokine data is supported by the observed differences in MOG-specific serum IgG antibodies: TEMPOL-fed

EAE mice had increased levels of IgG1, which is associated with a less inflammatory T_H2 immune response, and decreased levels of the IgG2c isotype that is associated with a pro-inflammatory T_H1 response [85].

GM-CSF production was generally found to be decreased with TEMPOL in EAE mice, though pooled results did not reach significance. Produced by activated T cells, GM-CSF is a pro-inflammatory cytokine that induces activation and differentiation of macrophages and DCs during an immune response [101]. A recent study by Codarri *et al*. showed that GM-CSF plays a vital role in the initiation of inflammation in EAE, with mice that are deficient in GM-CSF being completely resistant to EAE [101]. GM-CSF is brought into the CNS by T cells, where it activates resident microglia. As well, it has been shown that GM-CSF recruits myeloid cells to the CNS [101]. The mechanism by which TEMPOL might downregulate GM-CSF expression is unknown, but this effect may play a considerable role in explaining why mice on a TEMPOL diet do not develop severe EAE compared to controls.

Production of IL-2 was also decreased with TEMPOL in EAE mice, though this result is somewhat paradoxical. IL-2 is not pro-inflammatory, but does play a major role in the proliferation and differentiation of T cells into effector cells, where decreased IL-2 production leads to significantly reduced antigen-specific T cell expansion [102]. Theoretically, this could help to explain the amelioration of EAE with TEMPOL, though cytokine studies were performed on the same *ex vivo* cells that demonstrated no significant decrease in proliferative responses to antigen. As well, IL-2 has been shown to be important for differentiation of CD4+CD25+ T_{reg}

cells [103], but this T_{reg} population was in fact expanded with TEMPOL in our studies. However, IL-2 is mainly expressed by CD4+ T cells [102], the cell population that we found to be consistently reduced with TEMPOL both *ex vivo* and *in vitro*. Our observed decrease in IL-2 expression may therefore simply be in proportion to this reduction, with sufficient IL-2 being produced by remaining CD4+ and other cell types (CD8+ T cells, NK cells) to maintain normal immune function in this respect. Therefore, despite being significantly different, IL-2 may not be contributing to the effect of TEMPOL on disease.

In general, changes in cytokine production with TEMPOL tended to be most robust in cells stimulated with Anti-CD3 or ConA, with few differences observed in MOG-stimulated cells. This may be because MOG-reactive T cells are a small proportion of the population, meaning that alterations in cytokine levels may not be distinguishable, or that variability between animals is more pronounced with a small population. It is also worth noting that while anti-CD3 will activate all T cells, ConA preferentially activates suppressor cells, which may lead to a bias in cytokine production [104]. As well, while production of most cytokines tended to be decreased by TEMPOL, and trends between anti-CD3- and ConA-stimulated cells were generally similar, IL-10 stands out by being slightly increased with TEMPOL in anti-CD3-stimulated lymph node cells. In contrast, IL-10 production by ConA-stimulated cells was significantly decreased with TEMPOL. While the increase in IL-10 was not significant ($P = 0.087$), this cytokine may warrant further study as a potential mechanism for reducing disease, as it is associated with the less inflammatory and more suppressive T_H2-type response [50].

Once again, results of our TEMPOL studies showed similarities to those of experiments with bilirubin in EAE, though cytokine production with bilirubin was only assessed in antigen-specific T cells [92]. Nonetheless, similar decreases in production of IFNγ and IL-2 were observed.

5.2.3 Co-stimulatory molecule expression

The specific interaction between APCs and T cells during the initial priming stage of EAE is a crucial step in the initiation of an immune response. Altering expression of the surface markers involved in T cell activation can affect this interaction, and therefore the subsequent proliferation and differentiation of activated T cells [39]. While no changes were observed in lymphoid DCs with TEMPOL, both myeloid cell and myeloid DC populations in spleens and lymph nodes from TEMPOL-fed EAE mice exhibited decreased MHC II expression. Decreased MHC II expression by APCs could lead to decreased activation of CD4+ T cells, demonstrating an immunomodulatory role for TEMPOL. Decreased MHC II expression is characteristic of the interferon beta-1b drugs (Betaseron, Extavia) that are used in MS, which downregulate IFNγ-induced expression of MHC II on endothelial cells in the brain [105].

In contrast, a course of TEMPOL feed increased expression of CD80 and CD86 in these myeloid populations. While a number of research groups have shown that expression of CD80 (B7-1) by APC is linked to a T_H1 response while CD86 (B7-2) expression is associated with a T_H2 response, other studies have suggested that this may not be true [106]. Regardless, our studies did not suggest that upregulation

of B7 was biased towards either B7-1 or B7-2 molecules. While CD80 and CD86 can interact with CD28 to help activate T cells, they can also interact with CTLA-4, which inhibits T cells [107]. While CTLA-4 expression was not examined in this study, CD4+CD25+Foxp3+ T_{reg} cells express CTLA-4 as part of their suppressive function [107], and their population was increased with TEMPOL in lymph nodes. However, whether or not upregulation of CD80 and CD86 play a specific functional role in TEMPOL's function, or if it is simply associated with functional changes, remains to be elucidated.

5.2.4 Immune cell phenotype

The distribution of cell types within the lymphoid immune cell population was also examined in EAE mice, to determine if TEMPOL influences a change in the type of immune cells that are generated. Within the T cell compartment, a 15% increase in CD8+ T cells was observed in lymphoid organs from TEMPOL-fed animals, accompanied by a proportional decrease in CD4+ T cells. This resulted in a significantly decreased CD4/CD8 ratio, which was also observed in MLR experiments *in vitro*. In part, this shift may be explained by the observed decrease in MHC II expression by APCs in those same TEMPOL-fed animals, as decreased activation of CD4+ T cells could be expected if less MHC II is being expressed. However, the mechanism for an increased CD8+ T cell population is less clear, as no significant changes in MHC I expression were observed.

CD8+ cytotoxic T cells are "killer" cells that destroy other cells that are infected with intracellular pathogens [108]. CD8+ T cells are also thought to protect

against spontaneous malignant tumours, as they are able to detect abnormal cells [108]. In general, it would seem that an increase in CD8+ T cells could provide a "boost" to the immune system in the form of enhanced protection against pathogens. An increase in CD8+ T cells may therefore explain some of the observations made regarding mice on TEMPOL – they tend not to get sick as readily or develop tumours in comparison to controls [73].

Within the CD4+ T cell population, changes in the T_{reg} subset were also observed. In cells isolated from lymph nodes, a 30% increase in CD4+CD25+Foxp3+ T_{reg} cells was found with TEMPOL. Thus, even though the CD4+ population as a whole is shrinking, T_{reg} cells have become a significantly bigger proportion of the group. T_{reg} cells are known to be immunosuppressive, limiting T_H1 cell development and production of pro-inflammatory factors by secreting IL-10 and TGF-β1 [49]. A recent study demonstrated that a novel saline therapy upregulated CD4+CD25+Foxp3+ T_{reg} cells in *ex vivo* experiments by way of nitric oxide suppression, resulting in suppression of T_H1 and T_H17 cells and a shift towards a T_H2 response [109]. The saline therapy was also shown to ameliorate an adoptive transfer model of EAE. Overall, our observed relative increase in T_{reg} cells provides further support for our suggestion that TEMPOL influences a shift towards a less inflammatory immune response in EAE.

5.3 TEMPOL in a healthy immune system

Our studies in healthy animals confirm that TEMPOL is not merely globally suppressing the immune system, with isolated immune cells demonstrating

proliferative responses to antigen that are comparable to controls. Our observations in healthy animals on a TEMPOL diet were largely similar to those in EAE mice, though results were generally trends rather than significant differences. This suggests that TEMPOL has the greatest influence in a system were an immune response is occurring. However, a significant decrease in CD4/CD8 T cell ratios and an enrichment of lymph node T_{reg} cells were still observed, as were significant decreases in expression of co-stimulatory molecules in spleens. The fact that TEMPOL does affect elements of the immune system in a healthy animal supports our suggestion that it may set the stage for less pro-inflammatory or less destructive immune responses even before disease is reduced, in addition to playing a significant role in the initial T cell priming phase of EAE

While expression of surface markers was altered with TEMPOL in spleens of both healthy and EAE mice, some differences were observed. EAE mice showed no changes in surface marker expression in CD11b-CD11c+ lymphoid DC populations, while an increase in CD80 and a decrease in MHC I expression were seen with TEMPOL in spleens of healthy animals. However, overall trends were similar – expression of surface markers necessary for T cell activation tend to be decreased in all TEMPOL-fed animals, with MHC II expression consistently decreased in splenic myeloid cell and myeloid DC populations. It is of note that MHC I expression was decreased in all studied populations in spleens of healthy mice on TEMPOL, while CD8+ T cells were still observed to be enriched, suggesting that a mechanism other than a simple shift in MHC molecule expression may be at work in healthy animals.

5.4 Adding TEMPOL *in vitro*

In addition to feeding animals on a TEMPOL diet, experiments were also designed to test the effect of TEMPOL added to *in vitro* cell cultures. Because TEMPOL was added directly to isolated cells, this also afforded the opportunity to study the effects of varying TEMPOL doses on cell proliferation levels, proliferating cell populations, and surface marker expression. Experiments using cells isolated from lymphoid organs of EAE mice and healthy mice, stimulated with anti-CD3, both showed enhanced proliferation with TEMPOL up to a 100 μM dose. *In vivo*, our TEMPOL feed provides blood TEMPOL levels of 10 - 60 μM, so this indicates that TEMPOL is active at a dose that is biologically relevant.

Treating cells with anti-CD3 provides an artificial stimulation and expansion of T cells, but MLR experiments mimic a natural reaction to a non-self transplant, giving a more physiological view of how complex immune responses involving multiple cell types might be influenced by TEMPOL. Our studies in a human MLR model also showed increased proliferation with TEMPOL, as well as a decreased CD4+/CD8+ T cell ratio that echoes what was observed in experiments *in vivo*. In contrast, other researchers have shown that bilirubin does not alter T cell populations in MLR experiments [110]. Further, MLR experiments revealed that while both CD4+ and CD8+ T cells experience enhanced proliferation with TEMPOL, CD8+ T cells are specifically enriched. Interestingly, our results showed that while fewer CD8+ T cells proliferate compared to CD4+ T cells, they undergo extra divisions and therefore generate more daughter cells. The mechanism by which TEMPOL enhances proliferation *in vitro* was not specifically elucidated.

It has been shown that TEMPOL can limit apoptosis in some cell populations [111], though it may induce apoptosis in other cell types [112]. Other antioxidants have variable effects on apoptosis – bilirubin appears to induce it [92], while uric acid may protect against it [113]. If apoptosis was indeed limited by TEMPOL in our cultures, cells would be comparatively long-lived and therefore could proliferate to a greater extent than controls. Additionally, unlike studies *ex vivo*, the CD4+ T_{reg} cell population was decreased with TEMPOL in human MLR. This lack of suppressor cell activity may contribute to enhanced proliferation, while an enhanced T_{reg} population may limit proliferation *in vivo*.

Consistent with our comparison of lymphoid organ composition in control versus TEMPOL-fed animals, changes in surface marker expression were limited to CD11b+ myeloid cell and myeloid DC populations, and MHC II expression tended to be decreased. However, CD80 and CD86 expression were significantly decreased, in contrast to the upregulation of both B7 molecules that was observed *ex vivo*. Significant changes in surface marker expression were primarily observed with 200 μM doses of TEMPOL, which is somewhat higher than the levels reached in serum *in vivo*. The effect of TEMPOL on surface marker expression may therefore be dose-dependent, or the mechanism by which B7 expression is altered by TEMPOL is simply different *in vitro*.

Once ingested, TEMPOL largely exists in the body in its reduced form, TEMPOL-H [76]. Our *in vitro* studies with TEMPOL-H generally gave similar results to those of TEMPOL, though often not as robust. This may therefore explain some of the discrepancies between *in vitro* and *in vivo* studies – *in vivo*, TEMPOL is likely

reduced to a slightly less potent form prior to encountering immune cells, while *in vitro* cultures are (at least initially) able to directly interact with non-reduced TEMPOL.

Proliferation assays were also performed with ascorbic acid, to compare the effect of TEMPOL to that of a well-studied antioxidant. Ascorbic acid did not enhance proliferation compared to controls, therefore suggesting that its antioxidant properties are not as robust as those of TEMPOL. Accordingly, studies by other research groups have found that ascorbic acid does not protect against EAE [114]. However, studies have demonstrated that other antioxidants – including bilirubin and uric acid – are capable of suppressing various models of EAE [114] [115]. Mechanistic studies with these antioxidants have largely focused specifically on their role in protection against oxidative damage, suggesting that they limit disease by preventing oxidative stress-related permeability of the BBB and alleviate oxidative damage.

5.5 Conclusions and future directions

The studies described in this thesis suggest that TEMPOL has numerous anti-inflammatory properties that may explain its efficacy and potential to be a desirable MS therapy. It does not simply suppress immune responses, but instead may ameliorate disease by altering the pro-inflammatory phenotype of immune cells towards a less inflammatory response, with decreased production of the pro-inflammatory cytokines IFNγ, TGF-β1, and TNFα. In this regard, immune cells may be less likely to damage the target tissue or activate cells within the CNS that are

fundamental to inflammatory processes, such as microglia. In addition, TEMPOL promotes an enrichment of CD8+ T cells that may provide enhanced protection against pathogens and explain why animals on TEMPOL are generally healthier than controls. Studies by other groups have shown TEMPOL to be well-tolerated and orally efficacious in animals, with potential health benefits beyond the treatment of disease [73].

This research has been focused on TEMPOL's effect early in disease development, but other events in EAE pathogenesis may also be influenced by TEMPOL. After T cell priming in the periphery, immune cells must access the CNS, either by crossing the BBB or by other routes such as via the cerebrospinal fluid. Studies by Quandt *et al.* (unpublished data) have shown that EAE mice on TEMPOL feed have fewer immune cell infiltrates in the CNS compared to controls, suggesting that TEMPOL may play a role in altering leukocyte trafficking, or perhaps also influence BBB integrity or permeability. This may come in the form of alterations to endothelial cell tight junction proteins, changes in interactions between leukocytes and endothelial cells, or some combination of these two factors. To address this possibility, potential future *in vitro* studies have been designed using a mouse brain endothelial cell model (and could also be carried out *in vivo)* to determine if and how TEMPOL is capable of restoring BBB integrity in the presence of inflammatory cytokines.

While these studies have shown TEMPOL to be effective as a prophylactic, some may argue that this is of limited use in the treatment of an unpredictable disease such as MS. However, given the relapsing-remitting nature of MS and the

characterized initiation and resolution of immune responses over time in earlier stages of disease, a prophylactic regimen of TEMPOL could indeed be valuable. Furthermore, the well-characterized antioxidant and neuroprotective properties of TEMPOL not addressed in this study suggest that it may be particularly effective in limiting oxidative damage in the presence of inflammation, providing therapeutic benefits even after onset of disease. This is supported by experiments by Quandt *et al.* (unpublished data, manuscript in progress) that have shown that TEMPOL effectively ameliorates disease even when given 14 days after EAE induction, once symptoms have already appeared. By administering TEMPOL prior to EAE induction, and examining animals early in disease, we do not have the opportunity to assess TEMPOL's efficacy in neuroprotection and repair. Future studies with TEMPOL are expected to focus on these aspects, to determine how TEMPOL provides protection after onset of disease, specifically within the target tissue. Experiments have been proposed to study the effect on expression of oxidative damage markers, as well as changes in gene expression profiles.

While much remains to be studied, TEMPOL is nonetheless a promising potential therapeutic for the treatment of MS. The most desirable therapies for MS stop disease development at the earliest stages, limiting inflammation and the related axonal loss and neurodegeneration that are associated with disability. This may be done either by direct or indirect protection of neuronal populations, and perhaps even enhancing repair of damaged tissue. In these regards, the oral administration of TEMPOL provides a favourable alternative to current therapies,

and thus represents an important therapeutic agent for further evaluation and mechanistic studies.

References

1. Hemmer, B., et al., *Immunopathogenesis and immunotherapy of multiple sclerosis.* Nat Clin Pract Neurol, 2006. **2**(4): p. 201-11.

2. Conway, D. and J.A. Cohen, *Combination therapy in multiple sclerosis.* Lancet Neurol, 2010. **9**(3): p. 299-308.

3. Cook, S.D., *Multiple sclerosis.* Arch Neurol, 1998. **55**(3): p. 421-3.

4. Hickey, W.F., *The pathology of multiple sclerosis: a historical perspective.* J Neuroimmunol, 1999. **98**(1): p. 37-44.

5. Compston, A. and A. Coles, *Multiple sclerosis.* Lancet, 2008. **372**(9648): p. 1502-17.

6. Krupp, L.B., et al., *Fatigue in multiple sclerosis.* Arch Neurol, 1988. **45**(4): p. 435-7.

7. Dutta, R. and B.D. Trapp, *Pathogenesis of axonal and neuronal damage in multiple sclerosis.* Neurology, 2007. **68**(22 Suppl 3): p. S22-31; discussion S43-54.

8. Higginson, I.J., et al., *Is short-term palliative care cost-effective in multiple sclerosis? A randomized phase II trial.* J Pain Symptom Manage, 2009. **38**(6): p. 816-26.

9. *Who Gets MS?*, in *MS Explained*. 2009, Multiple Sclerosis Trust.

10. Beck, C.A., et al., *Regional variation of multiple sclerosis prevalence in Canada.* Mult Scler, 2005. **11**(5): p. 516-9.

11. Orton, S.M., et al., *Sex ratio of multiple sclerosis in Canada: a longitudinal study.* Lancet Neurol, 2006. **5**(11): p. 932-6.

12. Ebers, G.C., et al., *A full genome search in multiple sclerosis.* Nat Genet, 1996. **13**(4): p. 472-6.

13. Compston, A. and A. Coles, *Multiple sclerosis.* Lancet, 2002. **359**(9313): p. 1221-31.

14. Hafler, D.A., et al., *Risk alleles for multiple sclerosis identified by a genomewide study.* N Engl J Med, 2007. **357**(9): p. 851-62.

15. Healy, B.C., et al., *HLA B*44: protective effects in MS susceptibility and MRI outcome measures.* Neurology, 2010. **75**(7): p. 634-40.

16. Marrie, R.A., *Environmental risk factors in multiple sclerosis aetiology.* Lancet Neurol, 2004. **3**(12): p. 709-18.

17. van der Mei, I.A., et al., *Past exposure to sun, skin phenotype, and risk of multiple sclerosis: case-control study.* BMJ, 2003. **327**(7410): p. 316.

18. Sadovnick, A.D., et al., *A timing-of-birth effect on multiple sclerosis clinical phenotype.* Neurology, 2007. **69**(1): p. 60-2.

19. Deluca, H.F. and M.T. Cantorna, *Vitamin D: its role and uses in immunology.* FASEB J, 2001. **15**(14): p. 2579-85.

20. Ramagopalan, S.V., et al., *Expression of the multiple sclerosis-associated MHC class II Allele HLA-DRB1*1501 is regulated by vitamin D.* PLoS Genet, 2009. **5**(2): p. e1000369.

21. Munger, K.L., et al., *Vitamin D intake and incidence of multiple sclerosis.* Neurology, 2004. **62**(1): p. 60-5.

22. Munger, K.L., et al., *Serum 25-hydroxyvitamin D levels and risk of multiple sclerosis.* JAMA, 2006. **296**(23): p. 2832-8.

23. Ascherio, A., et al., *Epstein-Barr virus antibodies and risk of multiple sclerosis: a prospective study.* JAMA, 2001. **286**(24): p. 3083-8.

24. Lucas, R.M., et al., *Epstein-Barr virus and multiple sclerosis.* J Neurol Neurosurg Psychiatry, 2011. **82**(10): p. 1142-8.

25. Haahr, S. and P. Höllsberg, *Multiple sclerosis is linked to Epstein-Barr virus infection.* Rev Med Virol, 2006. **16**(5): p. 297-310.

26. Bar-Or, A., *The immunology of multiple sclerosis.* Semin Neurol, 2008. **28**(1): p. 29-45.

27. Ransohoff, R.M. and B. Engelhardt, *The anatomical and cellular basis of immune surveillance in the central nervous system.* Nat Rev Immunol, 2012. **12**(9): p. 623-35.

28. Ben-Nun, A., H. Wekerle, and I.R. Cohen, *The rapid isolation of clonable antigen-specific T lymphocyte lines capable of mediating autoimmune encephalomyelitis.* Eur J Immunol, 1981. **11**(3): p. 195-9.

29. Emerson, M.R., et al., *Enhancing the ability of experimental autoimmune encephalomyelitis to serve as a more rigorous model of multiple sclerosis through refinement of the experimental design.* Comp Med, 2009. **59**(2): p. 112-28.

30. Stromnes, I.M. and J.M. Goverman, *Passive induction of experimental allergic encephalomyelitis.* Nat Protoc, 2006. **1**(4): p. 1952-60.

31. Abromson-Leeman, S., et al., *T-cell properties determine disease site, clinical presentation, and cellular pathology of experimental autoimmune encephalomyelitis.* Am J Pathol, 2004. **165**(5): p. 1519-33.

32. Mannara, F., et al., *Passive experimental autoimmune encephalomyelitis in C57BL/6 with MOG: evidence of involvement of B cells.* PLoS One, 2012. **7**(12): p. e52361.

33. Mix, E., et al., *Animal models of multiple sclerosis--potentials and limitations.* Prog Neurobiol, 2010. **92**(3): p. 386-404.

34. Constantinescu, C.S., et al., *Experimental autoimmune encephalomyelitis (EAE) as a model for multiple sclerosis (MS).* Br J Pharmacol, 2011. **164**(4): p. 1079-106.

35. Pöllinger, B., et al., *Spontaneous relapsing-remitting EAE in the SJL/J mouse: MOG-reactive transgenic T cells recruit endogenous MOG-specific B cells.* J Exp Med, 2009. **206**(6): p. 1303-16.

36. Bettelli, E., et al., *Myelin oligodendrocyte glycoprotein-specific T and B cells cooperate to induce a Devic-like disease in mice.* J Clin Invest, 2006. **116**(9): p. 2393-402.

37. Quandt, J.A., et al., *Unique clinical and pathological features in HLA-DRB1*0401-restricted MBP 111-129-specific humanized TCR transgenic mice.* J Exp Med, 2004. **200**(2): p. 223-34.

38. Steinman, L. and S.S. Zamvil, *How to successfully apply animal studies in experimental allergic encephalomyelitis to research on multiple sclerosis.* Ann Neurol, 2006. **60**(1): p. 12-21.

39. Chitnis, T. and S.J. Khoury, *Role of costimulatory pathways in the pathogenesis of multiple sclerosis and experimental autoimmune encephalomyelitis.* J Allergy Clin Immunol, 2003. **112**(5): p. 837-49; quiz 850.

40. Bruck, W., et al., *Macrophages in multiple sclerosis.* Immunobiology, 1996. **195**(4-5): p. 588-600.

41. Weiss, N., et al., *The blood-brain barrier in brain homeostasis and neurological diseases.* Biochim Biophys Acta, 2009. **1788**(4): p. 842-57.

42. Benarroch, E.E., *Circumventricular organs: receptive and homeostatic functions and clinical implications.* Neurology, 2011. **77**(12): p. 1198-204.

43. Ganong, W.F., *Circumventricular organs: definition and role in the regulation of endocrine and autonomic function.* Clin Exp Pharmacol Physiol, 2000. **27**(5-6): p. 422-7.

44. Ligers, A., et al., *The CTLA-4 gene is associated with multiple sclerosis.* J Neuroimmunol, 1999. **97**(1-2): p. 182-90.

45. Laman, J.D., M. De Boer, and B.A. Hart, *CD40 in clinical inflammation: from multiple sclerosis to atherosclerosis.* Dev Immunol, 1998. **6**(3-4): p. 215-22.

46. Curtsinger, J.M. and M.F. Mescher, *Inflammatory cytokines as a third signal for T cell activation.* Curr Opin Immunol, 2010. **22**(3): p. 333-40.

47. Romagnani, S., *T-cell subsets (Th1 versus Th2).* Ann Allergy Asthma Immunol, 2000. **85**(1): p. 9-18; quiz 18, 21.

48. Wilson, N.J., et al., *Development, cytokine profile and function of human interleukin 17-producing helper T cells.* Nat Immunol, 2007. **8**(9): p. 950-7.

49. Marie, J.C., et al., *TGF-beta1 maintains suppressor function and Foxp3 expression in CD4+CD25+ regulatory T cells.* J Exp Med, 2005. **201**(7): p. 1061-7.

50. Gregori, S., K.S. Goudy, and M.G. Roncarolo, *The cellular and molecular mechanisms of immuno-suppression by human type 1 regulatory T cells.* Front Immunol, 2012. **3**: p. 30.

51. Haribhai, D., et al., *A requisite role for induced regulatory T cells in tolerance based on expanding antigen receptor diversity.* Immunity, 2011. **35**(1): p. 109-22.

52. Witherick, J., et al., *Mechanisms of oxidative damage in multiple sclerosis and a cell therapy approach to treatment.* Autoimmune Dis, 2010. **2011**: p. 164608.

53. Lobo, V., et al., *Free radicals, antioxidants and functional foods: Impact on human health.* Pharmacogn Rev, 2010. **4**(8): p. 118-26.

54. Lee, D.H., R. Gold, and R.A. Linker, *Mechanisms of Oxidative Damage in Multiple Sclerosis and Neurodegenerative Diseases: Therapeutic Modulation via Fumaric Acid Esters.* Int J Mol Sci, 2012. **13**(9): p. 11783-803.

55. Floyd, R.A., *Antioxidants, oxidative stress, and degenerative neurological disorders.* Proc Soc Exp Biol Med, 1999. **222**(3): p. 236-45.

56. Schreibelt, G., et al., *Lipoic acid affects cellular migration into the central nervous system and stabilizes blood-brain barrier integrity.* J Immunol, 2006. **177**(4): p. 2630-7.

57. van Meeteren, M.E., et al., *Dietary compounds prevent oxidative damage and nitric oxide production by cells involved in demyelinating disease.* Biochem Pharmacol, 2004. **67**(5): p. 967-75.

58. Smith, K.J., R. Kapoor, and P.A. Felts, *Demyelination: the role of reactive oxygen and nitrogen species.* Brain Pathol, 1999. **9**(1): p. 69-92.

59. Smith, K.J., et al., *Electrically active axons degenerate when exposed to nitric oxide.* Ann Neurol, 2001. **49**(4): p. 470-6.

60. van Horssen, J., et al., *Severe oxidative damage in multiple sclerosis lesions coincides with enhanced antioxidant enzyme expression.* Free Radic Biol Med, 2008. **45**(12): p. 1729-37.

61. van der Veen, C., et al., *Factors affecting events during oxidation of low density lipoprotein: correlation of multiple parameters of oxidation.* Free Radic Res, 1997. **27**(5): p. 459-76.

62. Han, M.H., et al., *Proteomic analysis of active multiple sclerosis lesions reveals therapeutic targets.* Nature, 2008. **451**(7182): p. 1076-81.

63. van Horssen, J., et al., *Nrf2 and DJ1 are consistently upregulated in inflammatory multiple sclerosis lesions.* Free Radic Biol Med, 2010. **49**(8): p. 1283-9.

64. Andrews, H.E., et al., *Mitochondrial dysfunction plays a key role in progressive axonal loss in Multiple Sclerosis.* Med Hypotheses, 2005. **64**(4): p. 669-77.

65. Lassmann, H., J. van Horssen, and D. Mahad, *Progressive multiple sclerosis: pathology and pathogenesis.* Nat Rev Neurol, 2012. **8**(11): p. 647-56.

66. Ali, R., R.S. Nicholas, and P.A. Muraro, *Drugs in development for relapsing multiple sclerosis.* Drugs, 2013. **73**(7): p. 625-50.

67. Tullman, M.J., *A review of current and emerging therapeutic strategies in multiple sclerosis.* Am J Manag Care, 2013. **19**(2 Suppl): p. S21-7.

68. Buck, D. and B. Hemmer, *Treatment of multiple sclerosis: current concepts and future perspectives.* J Neurol, 2011. **258**(10): p. 1747-62.

69. Hahn, S.M., et al., *Evaluation of tempol radioprotection in a murine tumor model.* Free Radic Biol Med, 1997. **22**(7): p. 1211-6.

70. Cuzzocrea, S., et al., *Tempol reduces the activation of nuclear factor-kappaB in acute inflammation.* Free Radic Res, 2004. **38**(8): p. 813-9.

71. Banday, A.A., et al., *Tempol reduces oxidative stress, improves insulin sensitivity, decreases renal dopamine D1 receptor hyperphosphorylation, and restores D1 receptor-G-protein coupling and function in obese Zucker rats.* Diabetes, 2005. **54**(7): p. 2219-26.

72. Deng-Bryant, Y., et al., *Neuroprotective effects of tempol, a catalytic scavenger of peroxynitrite-derived free radicals, in a mouse traumatic brain injury model.* J Cereb Blood Flow Metab, 2008. **28**(6): p. 1114-26.

73. Mitchell, J.B., et al., *A low molecular weight antioxidant decreases weight and lowers tumor incidence.* Free Radic Biol Med, 2003. **34**(1): p. 93-102.

74. Tsuhako, M.H., et al., *Tempol ameliorates murine viral encephalomyelitis by preserving the blood-brain barrier, reducing viral load, and lessening inflammation.* Free Radic Biol Med, 2010. **48**(5): p. 704-12.

75. Metz, J.M., et al., *A phase I study of topical Tempol for the prevention of alopecia induced by whole brain radiotherapy.* Clin Cancer Res, 2004. **10**(19): p. 6411-7.

76. Hahn, S.M., et al., *Evaluation of the hydroxylamine Tempol-H as an in vivo radioprotector.* Free Radic Biol Med, 2000. **28**(6): p. 953-8.

77. Soule, B.P., et al., *The chemistry and biology of nitroxide compounds.* Free Radic Biol Med, 2007. **42**(11): p. 1632-50.

78. Lublin, F.D. and S.C. Reingold, *Defining the clinical course of multiple sclerosis: results of an international survey. National Multiple Sclerosis Society (USA) Advisory Committee on Clinical Trials of New Agents in Multiple Sclerosis.* Neurology, 1996. **46**(4): p. 907-11.

79. Cassiani-Ingoni, R., et al., *Disease progression after bone marrow transplantation in a model of multiple sclerosis is associated with chronic microglial and glial progenitor response.* J Neuropathol Exp Neurol, 2007. **66**(7): p. 637-49.

80. Li, X., et al., *Intranasal delivery of E-selectin reduces atherosclerosis in ApoE-/- mice.* PLoS One, 2011. **6**(6): p. e20620.

81. Wang, D., et al., *Induction of immunotolerance via mPEG grafting to allogeneic leukocytes.* Biomaterials, 2011. **32**(35): p. 9494-503.

82. Palacios, R., *Concanavalin A triggers T lymphocytes by directly interacting with their receptors for activation.* J Immunol, 1982. **128**(1): p. 337-42.

83. Dittel, B.N., *Evidence that Fas and FasL contribute to the pathogenesis of experimental autoimmune encephalomyelitis.* Arch Immunol Ther Exp (Warsz), 2000. **48**(5): p. 381-8.

84. Reindl, M., et al., *Antibodies against the myelin oligodendrocyte glycoprotein and the myelin basic protein in multiple sclerosis and other neurological diseases: a comparative study.* Brain, 1999. **122 (Pt 11)**: p. 2047-56.

85. Stevens, T.L., et al., *Regulation of antibody isotype secretion by subsets of antigen-specific helper T cells.* Nature, 1988. **334**(6179): p. 255-8.

86. Liblau, R.S., et al., *Neurons as targets for T cells in the nervous system.* Trends Neurosci, 2013. **36**(6): p. 315-24.

87. Holmes, S., et al., *Multiple sclerosis: MHC associations and therapeutic implications.* Expert Rev Mol Med, 2005. **7**(3): p. 1-17.

88. Bach, J.F., *Immunosuppressive therapy of autoimmune diseases.* Trends Pharmacol Sci, 1993. **14**(5): p. 213-6.

89. Hartung, H.P., et al., *Mitoxantrone in progressive multiple sclerosis: a placebo-controlled, double-blind, randomised, multicentre trial.* Lancet, 2002. **360**(9350): p. 2018-25.

90. Edan, G., S. Morrissey, and E. Le Page, *Rationale for the use of mitoxantrone in multiple sclerosis.* J Neurol Sci, 2004. **223**(1): p. 35-9.

91. Warnke, C., et al., *Review of teriflunomide and its potential in the treatment of multiple sclerosis.* Neuropsychiatr Dis Treat, 2009. **5**: p. 333-40.

92. Liu, Y., et al., *Bilirubin possesses powerful immunomodulatory activity and suppresses experimental autoimmune encephalomyelitis.* J Immunol, 2008. **181**(3): p. 1887-97.

93. Kean, R.B., et al., *The peroxynitrite scavenger uric acid prevents inflammatory cell invasion into the central nervous system in experimental allergic encephalomyelitis through maintenance of blood-central nervous system barrier integrity.* J Immunol, 2000. **165**(11): p. 6511-8.

94. Kopf, M., M.F. Bachmann, and B.J. Marsland, *Averting inflammation by targeting the cytokine environment.* Nat Rev Drug Discov, 2010. **9**(9): p. 703-18.

95. Benveniste, E.N. and D.J. Benos, *TNF-alpha- and IFN-gamma-mediated signal transduction pathways: effects on glial cell gene expression and function.* FASEB J, 1995. **9**(15): p. 1577-84.

96. Selmaj, K.W. and C.S. Raine, *Tumor necrosis factor mediates myelin and oligodendrocyte damage in vitro.* Ann Neurol, 1988. **23**(4): p. 339-46.

97. Wahl, S.M., *Transforming growth factor beta: the good, the bad, and the ugly.* J Exp Med, 1994. **180**(5): p. 1587-90.

98. Wahl, S.M., et al., *Reversal of acute and chronic synovial inflammation by anti-transforming growth factor beta.* J Exp Med, 1993. **177**(1): p. 225-30.

99. Hatton, R.D., *TGF-β in Th17 cell development: the truth is out there.* Immunity, 2011. **34**(3): p. 288-90.

100. Oreja-Guevara, C., et al., *TH1/TH2 Cytokine profile in relapsing-remitting multiple sclerosis patients treated with Glatiramer acetate or Natalizumab.* BMC Neurol, 2012. **12**: p. 95.

101. Codarri, L., et al., *RORgammat drives production of the cytokine GM-CSF in helper T cells, which is essential for the effector phase of autoimmune neuroinflammation.* Nat Immunol, 2011. **12**(6): p. 560-7.

102. Boyman, O. and J. Sprent, *The role of interleukin-2 during homeostasis and activation of the immune system.* Nat Rev Immunol, 2012. **12**(3): p. 180-90.

103. Nelson, B.H., *IL-2, regulatory T cells, and tolerance.* J Immunol, 2004. **172**(7): p. 3983-8.

104. Dwyer, J.M. and C. Johnson, *The use of concanavalin A to study the immunoregulation of human T cells.* Clin Exp Immunol, 1981. **46**(2): p. 237-49.

105. Huynh, H.K., J. Oger, and K. Dorovini-Zis, *Interferon-beta downregulates interferon-gamma-induced class II MHC molecule expression and morphological changes in primary cultures of human brain microvessel endothelial cells.* J Neuroimmunol, 1995. **60**(1-2): p. 63-73.

106. MacPhee, I.A., et al., *CD80(B7.1) and CD86(B7.2) do not have distinct roles in setting the Th1/Th2 balance in autoimmunity in rats.* Scand J Immunol, 2001. **54**(5): p. 486-94.

107. Barnes, M.J., et al., *CTLA-4 promotes Foxp3 induction and regulatory T cell accumulation in the intestinal lamina propria.* Mucosal Immunol, 2013. **6**(2): p. 324-34.

108. Andersen, M.H., et al., *Cytotoxic T cells.* J Invest Dermatol, 2006. **126**(1): p. 32-41.

109. Mondal, S., et al., *Protection of Tregs, suppression of Th1 and Th17 cells, and amelioration of experimental allergic encephalomyelitis by a physically-modified saline.* PLoS One, 2012. **7**(12): p. e51869.

110. Haga, Y., M.A. Tempero, and R.K. Zetterman, *Unconjugated bilirubin inhibits in vitro cytotoxic T lymphocyte activity of human lymphocytes.* Biochim Biophys Acta, 1996. **1317**(1): p. 65-70.

111. Peixoto, E.B., et al., *Tempol reduces podocyte apoptosis via PARP signaling pathway in experimental diabetes mellitus.* Nephron Exp Nephrol, 2012. **120**(2): p. e81-90.

112. Monti, E., et al., *Nitroxide TEMPOL impairs mitochondrial function and induces apoptosis in HL60 cells.* J Cell Biochem, 2001. **82**(2): p. 271-6.

113. Mattson, M.P., et al., *Activation of NF-kappaB protects hippocampal neurons against oxidative stress-induced apoptosis: evidence for induction of manganese superoxide dismutase and suppression of peroxynitrite production and protein tyrosine nitration.* J Neurosci Res, 1997. **49**(6): p. 681-97.

114. Spitsin, S.V., et al., *Comparison of uric acid and ascorbic acid in protection against EAE.* Free Radic Biol Med, 2002. **33**(10): p. 1363-71.

115. Liu, Y., et al., *Bilirubin as a potent antioxidant suppresses experimental autoimmune encephalomyelitis: implications for the role of oxidative stress in the development of multiple sclerosis.* J Neuroimmunol, 2003. **139**(1-2): p. 27-35.